Work Order No. 582-15-53990-09
Contract # 582-15-50417
Project #FY15-46
Task 5

Final Report
Simulation of the Stratospheric Contribution to Surface Ozone

PREPARED UNDER A CONTRACT FROM THE
TEXAS COMMISSION ON ENVIRONMENTAL QUALITY

The preparation of this report was financed through a contract from the State of Texas through the Texas Commission on Environmental Quality.
The content, findings, opinions and conclusions are the work of the author(s) and do not necessarily represent findings, opinions or conclusions of the TCEQ.

Prepared for:
Jim Smith
Texas Commission on Environmental Quality
121 Park 35 Circle MC 164
Austin, TX 78753

Prepared by:
Sue Kemball-Cook, Jaegun Jung, Thomas Pavlovic, Wei-Chun Hsieh, Jeremiah Johnson and Greg Yarwood
Ramboll Environ
773 San Marin Drive, Suite 2115
Novato, California, 94998
www.environcorp.com
P-415-899-0700
F-415-899-0707

August 2015

RAMBOLL ENVIRON

CONTENTS

APPENDIX A

Model Performance Evaluation for Initial CAMx Runs

TABLES

FIGURES

LIST OF ACRONYMS AND ABBREVIATIONS

AEIC	Aviation Emission Inventory Code
CAMx	Comprehensive Air Quality Model with Extensions
CB6r2	Carbon Bond 6 Revision 2 Chemical Mechanism
CFCs	Chlorofluorocarbons
ClOx	Cl+ClO
Cly	Sum of ClOx and its reservoirs
COSMIC	Constellation Observing System for Meteorology, Ionosphere and Climate
EDGAR	Emission Database for Global Atmospheric Research
GC	GEOS-Chem
GEOS	Goddard Earth Observing System
GMI	Global Modeling Initiative
EPA	Environmental Protection Agency
FINN	Fire Inventory from NCAR
GFED	Global Fire Emissions Database
HCFCs	Hydro-chlorofluorocarbons
HEMCO	Harvard-NASA Emissions Component
HOx	Hydrogen oxide radicals
HNO_3	Nitric acid
hPa	Hectopascals
hr	Hour
HYSPLIT	HYbrid Single-Particle Lagrangian Integrated Trajectory
INTEX-A	Intercontinental Chemical Transport Experiment - North America
IVOCS	Intermediate volatility organic compounds
JPL	Jet Propulsion Laboratory
Kg	Kilogram
LBS	Liquid binary sulfate
LINOZ	Linearized Stratospheric Ozone Model
MEGAN	Model of Gases and Aerosols from Nature
N_2O	Nitrous Oxide
NAAQS	National Ambient Air Quality Standard
NCAR	National Center for Atmospheric Research
NCEP	National Center for Environmental Prediction
NEI	National Emission Inventory
NetCDF	Network Common Data Form
NMB	Normalized mean bias
NME	Normalized mean error
NO	Nitric oxide
NOx	Oxides of nitrogen
NOy	Total oxidized nitrogen
OCS	Carbonyl sulfide
Ox	Odd oxygen $O+O_3$
PAN	Peroxyacetyl nitrate
PM	Particulate matter

POA	Primary organic aerosol
ppb	parts per billion
PSC	Polar stratospheric cloud
SAGE II	Stratospheric Aerosol and Gas Experiment II
SIP	State Implementation Plan
SOA	Secondary organic aerosol
STE	Stratosphere-troposphere exchange
SYNOZ	Synthetic Stratospheric Ozone Algorithm
TCEQ	Texas Commission on Environmental Quality
UCX	Unified Chemistry Extension
VOC	Volatile organic compound
yr	Year

EXECUTIVE SUMMARY

In this report, we describe the development of lateral and top boundary conditions for the Texas Commission on Environmental Quality's (TCEQ's) 2012 ozone modeling. Ramboll Environ ran both the standard and Unified Tropospheric-Stratospheric Chemistry Extension (UCX; Eastham et al., 2014) versions of the GEOS-Chem global model version 10-01 (Bey et al., 2001; Yantosca et al., 2014) for the 2012 ozone season. Then, we extracted lateral and model top boundary conditions from both GEOS-Chem simulations for use in modeling of June 2012 with the Comprehensive Air Quality Model with Extensions (CAMx; Ramboll Environ, 2015). GEOS-Chem UCX explicitly simulates chemistry in both the stratosphere and troposphere while the standard version of GEOS-Chem focuses on the troposphere and has a simplified treatment of stratospheric chemistry. We evaluated the performance of the standard and UCX versions of the GEOS-Chem model in simulating ozonesonde observations at U.S. sites during June 2012. The two GEOS-Chem simulations were very similar in the lower and middle troposphere, but the UCX simulation of ozone in the lower stratosphere was consistently closer to the observed ozone profiles than the simulation using the standard version of GEOS-Chem.

Next, we ran CAMx for the TCEQ's June 2012 episode using the two sets of GEOS-Chem boundary conditions. We evaluated CAMx model performance in these two runs against surface ozone observations, aloft aircraft measurements of ozone and NOy[1], and ozonesonde profiles. The model performance evaluation against observed surface and aloft ozone and aloft NOy indicated that the GEOS-Chem model was functioning correctly in both the standard and UCX configurations and provides reasonable model top boundary conditions to the CAMx model. CAMx boundary conditions developed using the UCX and standard versions of GEOS-Chem produce nearly identical CAMx ground level ozone simulations in East Texas. Small and intermittent differences in hourly surface ozone on the order of 3 ppb or less occurred at higher elevation sites such as Big Bend in Texas and sites in the Rocky Mountains. Comparison of the two CAMx simulations of ozone and NOy in the upper troposphere and lower stratosphere showed that differences were small between the two CAMx runs using boundary conditions developed with the UCX and standard versions of GEOS-Chem. Both CAMx runs had a high bias with respect to ozonesonde observations in the lower stratosphere.

The CAMx model performance evaluation using surface and aloft measurements indicates that for air quality planning applications focused on ground level ozone during typical summer conditions, either the standard or UCX version of GEOS-Chem could be used to develop top and lateral boundary conditions. The UCX version of GEOS-Chem has a more complete representation of the chemistry of the stratosphere than the simplified chemistry of the standard version of GEOS-Chem and produces a more realistic simulation of stratospheric ozone, but is more resource–intensive. The model run time for a GEOS-Chem UCX simulation is

[1] NOy is the sum of NOx and other oxidized nitrogen compounds that result from atmospheric reactions of NOx, such as nitric acid (HNO3), peroxyacetyl nitrate (PAN), organic nitrates, etc.

twice that of the standard version of GEOS-Chem. The UCX version of GEOS-Chem requires a 5-year spinup period, while the standard version requires a 1-year spinup period. The difference in spinup is due to the slower time scale of dynamical processes in the stratosphere relative to the troposphere, which is the main focus of the standard version of GEOS-Chem. The UCX version, which explicitly simulates both the stratosphere and the troposphere, requires a longer period of time to remove the influence of the initial conditions from the simulation of the stratosphere. The developers of UCX are considering providing UCX initial conditions files for a range of simulation years so that users of the model would not be required to perform a 5-year spinup. This would significantly reduce the computational burden of using the UCX version of GEOS-Chem for development of boundary conditions for CAMx.

The June 2012 CAMx modeling database developed by the TCEQ has its model top at an altitude of approximately 15 km above ground level. Depending on latitude, season and weather conditions the model top can be located within either the troposphere or the stratosphere. The CB6r2 chemical mechanism (Yarwood et al., 2012) used in CAMx was developed for use in the troposphere. We evaluated whether the chemistry in CAMx should be extended to represent lower stratosphere conditions using a scheme similar to that of the GEOS-Chem UCX.

The horizontal component of the wind speed in the upper troposphere and lower stratosphere over North America is fast enough that the residence time of air in the TCEQ continental-scale 36 km modeling domain within the upper layers of CAMx is typically 3-5 days. Therefore, the CAMx lateral and top boundary conditions are the most important influence on chemical species concentrations in the highest model layers unless there are chemical reactions occurring within the CAMx modeling domain that significantly affect species concentrations on a time scale shorter than 3-5 days.

The question of whether it is appropriate to use a UCX-like stratospheric chemistry mechanism for the lower stratosphere in CAMx depends on whether UCX and CAMx CB6r2 chemical mechanisms produce significantly different concentrations of species in air parcels during the parcels' 5-day residence time in the modeling domain. One method for investigating this question would be to run the UCX and CB6r2 mechanisms in a box model for a 5-day period with initial concentrations representative of the lower stratosphere and compare species concentrations. Box modeling was outside the scope of this project, so we addressed this question by examining the chemistry of key chemical species and their lifetimes in the lower stratosphere.

We focused on ozone and NOx because these are the species whose concentrations in the upper model layers are most likely to be relevant to the TCEQ's SIP modeling. The simulation of ozone in the lower stratosphere is relevant for modeling intrusions of ozone-rich stratospheric air that can affect near-surface ozone levels in Texas or upwind states, while simulation of NO_2 and its reservoir species is relevant for comparison with satellite NO_2 column data. There are no photochemical sources or sinks of odd oxygen ($Ox=O+O_3$) or NOx that act to change the concentrations of these species on the time scale of a few days in the lower stratosphere. The

model solution in the lower stratosphere should therefore be largely controlled by the boundary conditions. Therefore, we believe it is unlikely that the use of UCX-like stratospheric chemistry would produce a significantly different simulation of ozone or NOx in the highest model layers than the CB6r2 chemical mechanism.

To test the sensitivity of the model to CB6r2 chemistry in the lower stratosphere, we ran CAMx with chemistry turned off in the lower stratosphere. Turning off the chemistry in the stratosphere had very little effect on the modeled ozone and NOy. Modeled vertical profiles of NOy and ozone in the stratosphere with chemistry turned on and off were nearly indistinguishable, with differences in the lower stratospheric ozone concentrations of 0.1 ppb or less. We conclude that the boundary conditions are far more important than chemistry for simulation of ozone and NOx in the upper troposphere and lower stratosphere in CAMx.

1.1 Recommendations

Below, we summarize recommendations arising from this study:

- For air quality planning applications focused on ground level ozone during typical summer conditions, either the standard or UCX version of GEOS-Chem could be used
  - UCX has an explicit representation of the stratosphere and provides a better simulation of stratospheric ozone, but is currently more resource-intensive to use
- The UCX version of GEOS-Chem should be used to develop CAMx boundary conditions for applications where simulation of the upper troposphere and lower stratosphere is critical, such as:
  - Simulation of stratospheric ozone intrusions
  - Comparison with column-integrated satellite data
- For applications where simulation of the upper troposphere and lower stratosphere is critical, we recommend evaluating whether moving the CAMx top boundary to 20 km permits CAMx with GEOS-Chem UCX-derived boundary conditions to perform better in the upper troposphere/lower stratosphere than CAMx boundary conditions developed with the standard version of GEOS-Chem
- Incorporation of UCX-like stratospheric chemistry in CAMx is not necessary because the CAMx lateral and top boundary conditions are far more important than chemistry in determining concentrations of ozone and NOx in the upper troposphere and lower stratosphere

2.0 INTRODUCTION

2.1 Background and Purpose

As the National Ambient Air Quality Standard (NAAQS) for ozone becomes more stringent, understanding ozone transport into Texas becomes increasingly important. Because their lifetimes are relatively long in the upper troposphere, ozone and a substantial fraction of total oxidized nitrogen (NOy[2]) can be transported for long distances and potentially mixed downward into the planetary boundary layer, where they can influence surface ozone concentrations (Cooper et al., 2015). It is therefore desirable that regional air quality models used for ozone air quality planning accurately simulate the transport and fate of ozone and NOy in the upper troposphere and lower stratosphere. The Texas Commission on Environmental Quality (TCEQ) uses the Comprehensive Atmosphere Model with Extensions (CAMx; Ramboll Environ, 2015) for ozone State Implementation Plan (SIP) modeling.

In Project FY13-10, CAMx was updated to improve the simulation of NOy in the upper troposphere (Kemball-Cook et al., 2013). ENVIRON evaluated a series of model changes designed to address the CAMx low bias for upper tropospheric NOy noted in Project FY12-08 (Kemball-Cook et al., 2012). The results of Project FY13-10 showed stratosphere-to-troposphere transport to be an important source of upper troposphere NOy and ozone that must be represented correctly in order to accurately model their respective mass budgets. In Project FY14-15, ENVIRON implemented in CAMx spatially and temporally varying top boundary conditions from the Goddard Earth Orbiting System model with Chemistry (GEOS-Chem; Bey et al., 2001, Yantosca et al., 2014) global model; this improved CAMx performance for ozone and NOy in the upper troposphere and lower stratosphere in the TCEQ's June 2006 episode (Kemball-Cook et al., 2014).

The TCEQ is in the process of developing and testing a new ozone modeling platform for June 2012 using CAMx[3]. Like the TCEQ's 2006 ozone model, the 2012 modeling platform uses a nested 36/12/4 km grid system covering the continental United States and requires lateral and model top boundary conditions that can be derived from global models such as GEOS-Chem. The standard version of GEOS-Chem, which was used to derive the boundary conditions currently in use in TCEQ's modeling, uses a simplified treatment of stratospheric chemistry. The vertical ozone profiles of ozone concentrations simulated by this version of GEOS-Chem can differ markedly from observed ozone profiles in the lower stratosphere/upper troposphere (e.g. Kemball-Cook et al., 2014).

The purpose of this project was to assess possible improvements to TCEQ's 2012 CAMx modeling platform through use of alternative boundary conditions derived with a new version of GEOS-Chem which incorporates the Unified Tropospheric–Stratospheric Chemistry Extension

[2] NOy is the sum of NOx and other oxidized nitrogen compounds that result from atmospheric reactions of NOx, such as nitric acid (HNO3), peroxyacetyl nitrate (PAN), organic nitrates, etc.
[3] http://www.tceq.texas.gov/airquality/airmod/data/tx2012

(UCX; Eastham et al., 2014). The UCX explicitly simulates chemistry in the stratosphere and may provide more realistic boundary conditions for TCEQ's modeling than the standard version of GEOS-Chem, which has a simplified treatment of stratospheric chemistry.

2.2 Project Objectives

The objectives of this Project (FY15-46) were to:

(1) Develop lateral and model top boundary conditions for the TCEQ's 2012 ozone modeling; and to

(2) Evaluate whether chemistry in CAMx should be extended to represent lower stratosphere conditions using a UCX-like scheme.

In this report, we summarize efforts to accomplish these two objectives. Section 3 of this report contains description of the standard version of the GEOS-Chem model as well as the extended UCX version. In Section 4, we present the results of the model performance evaluation for both GEOS-Chem and CAMx at the surface and aloft. In Section 5, we give an overview of the CAMx layer structure and its relationship to the mean structure of the atmosphere in the vicinity of the tropopause. We examine the chemistry of SIP-relevant species in the lower stratosphere and the time-scales on which they vary. We use this analysis together with an estimate of the residence time of lower stratospheric air in the modeling domain to infer the relative importance of boundary conditions and CAMx chemistry in the lower stratosphere. We then discuss the potential impact of incorporating UCX-like chemistry into CAMx. Finally, in Section 6, we summarize the results of this study and make recommendations for development of boundary conditions in future modeling efforts.

3.0 MODEL DESCRIPTION

Two chemical transport models were used in this project. In this section, we give a brief introduction to the models and describe how they were used.

3.1 GEOS-Chem Model

GEOS-Chem is a global chemistry-transport model originally developed at Harvard University and now developed and run by users around the world for a variety of applications. It is an Eulerian photochemical grid model. GEOS-Chem is driven by off-line meteorological fields from the Goddard Earth Observing System (GEOS).

3.1.1 GEOS-Chem Version 10-01

GEOS-Chem version 10-01 was released in May, 2015, and has a different structure from the previous GEOS-Chem version, 9-01-03, which was used to develop boundary conditions for the TCEQ's June 2006 ozone model. There have been many updates to the model science and structure and bug fixes. Below are important science and structural updates[4]:

- Emissions
    - HEMCO (the Harvard-NASA Emissions Component) - New emission processing program and NetCDF emissions database
    - Update of biomass burning emissions from GFED3 to GFED4[5] (or FINN)
    - Update of MEGAN biogenic emissions[6]
    - Update of EDGAR global anthropogenic emissions
    - Update of Asian emissions from Street to MIX
    - Update of US NEI emissions from 2005 to 2011
    - Update of aircraft emissions from Wang et al. (1998) and Park et al. (2004) to AEIC (Aviation Emissions Inventory Code) v. 2.0
- Chemistry
    - Addition of UCX stratospheric chemistry extension (described in Section 3.1.3)
    - Incorporation of updated isoprene chemistry in the standard mechanism[7]
    - Update of photolysis mechanism from FAST-J to FAST-JX
    - Inorganic chemistry updates from JPL 06 to JPL 11
    - Update of RO_2+HO_2 Reaction Rate
    - Increase of NO_3 aerosol reactive uptake coefficient (gamma) from $1.0x10^{-4}$ to 0.1

[4] http://acmg.seas.harvard.edu/geos/doc/man/appendix_10.html
[5] http://onlinelibrary.wiley.com/doi/10.1002/jgrg.20042/abstract
[6] http://wiki.geos-chem.org/MEGAN_v2.1_plus_Guenther_2012_biogenic_emissions
[7] http://wiki.seas.harvard.edu/geos-chem/index.php/New_isoprene_scheme#New_reactions

- SOA simulation with semi-volatile POA
- Improved SOA chemistry and can include aerosol from intermediate volatile organic compounds (IVOCs).

GEOS-Chem is a tropospheric chemistry-transport model; however, because radiative transfer in the stratosphere and stratosphere-troposphere exchange (STE) of chemical species can have a significant impact on the troposphere, GEOS-Chem may be run with either of two methods of accounting for stratospheric chemistry. These two options are described below. (A previous option, a flux-based boundary condition algorithm known as Synoz, has been replaced by the LINOZ algorithm described in Section 3.1.2)

3.1.2 GEOS-Chem Standard Version Stratospheric Chemistry

The first method for accounting for the effects of stratospheric chemistry in GEOS-Chem is to use a simple, linearized treatment of stratospheric chemistry that is applied to each grid cell that lies above the troposphere (Murray, 2012). For key species other than ozone, GEOS-Chem uses a simple mass balance (equation 1) and a three-dimensional lookup table of monthly mean production rates (P) and loss frequencies (k) that were generated by a previous multi-year integration of the NASA Global Modeling Initiative (GMI) "combo" model (e.g. Considine et al.,2008). The GMI model has a detailed simulation of both stratospheric and tropospheric chemistry. At the beginning of each month, GEOS-Chem looks up monthly mean GMI modeled production rates and loss frequencies and marches the species concentration, *m*, forward in time according to:

$$\frac{dm}{dt} = P - km. \quad (1)$$

For *k*>0, equation (1) becomes

$$m(t) = m(0)e^{-kt} + \frac{P}{k}(1 - e^{-kt}), \quad (2)$$

otherwise,

$$m(t) = m(0) + Pt. \quad (3)$$

GEOS-Chem species (m) with linearized stratospheric chemistry include: NOx, Ox, PAN, CO, HNO_3, and CH_4. The full list of GEOS-Chem species may be found at http://wiki.seas.harvard.edu/geos-chem/index.php/Stratospheric_chemistry.

Ozone is treated with a linearized ozone model called LINOZ (McLinden et al., 2000), in which the change in ozone with time is assumed to depend linearly on the amount of ozone present, the temperature, and the ozone column overhead. The ozone tendency, dO_3/dt, is linearized around climatological values of these three quantities. In LINOZ, it is assumed that the effects of variations in other chemical species (e.g. NOy, methane, Cly) on ozone are small and that specifying the mean distributions of these other species provides sufficient accuracy in the ozone calculation. LINOZ employs a first-order Taylor expansion of stratospheric chemical rates

in which the ozone tendency ($OT \equiv$ Production - Loss) is linearized about the ozone mixing ratio (O_3), temperature (T), and the overhead ozone column density (C_{O3}) for each grid cell:

$$\frac{dO_3}{dt} = OT\left(O_3, T, C_{O_3}\right) \quad (3)$$

Using superscripts (X^0) to represent climatological values for each quantity that vary by location and time of year,

$$\frac{dO_3}{dt} \cong OT^0 + \left.\frac{\partial OT}{\partial O_3}\right|_0 (O_3 - O_3^0) + \left.\frac{\partial OT}{\partial T}\right|_0 (T - T^0) + \left.\frac{\partial OT}{\partial C_{O_3}}\right|_0 \left(C_{O_3} - C_{O_3}^0\right) \quad (4)$$

As for the other stratospheric species, the production and loss terms are drawn from the GMI model simulation. This simple simulation of ozone and other chemical species in the stratosphere reflects GEOS-Chem's focus on tropospheric chemistry, and aims to simulate the essential features of STE without incurring the computational costs of running a full chemistry model of the stratosphere.

3.1.3 GEOS-Chem UCX Stratospheric Chemistry

The second method for simulating stratospheric chemistry in GEOS-Chem is a new module, the Unified Tropospheric–Stratospheric Chemistry Extension (UCX; Eastham et al., 2014). This module is only available in GEOS-Chem version 10-01 or later. The UCX version of GEOS-Chem uses the model's existing gas-phase chemistry in the troposphere, but extends the model to use an adapted version of the stratospheric chemistry of NASA's GMI model above the troposphere and below 0.1 hPa, the approximate pressure of the stratopause. The UCX version of the GMI stratospheric chemical mechanism was updated by Eastham et al. to be consistent with the 2011 JPL Chemical Kinetics and Photochemical Data Evaluation (JPL-10-06; Sander et al., 2011). Eastham et al. added 28 species and 104 kinetic reactions beyond what is in the standard GEOS-Chem model's tropospheric chemistry mechanism (Eastham et al., 2013). There are eight additional heterogeneous reactions and 34 additional photolytic decompositions. The UCX stratospheric chemistry includes full ozone chemistry of NOx, ClOx, BrOx, HOx and is outlined in Figure 3-1.

There are a number of enhancements in the UCX relative to the standard GEOS-Chem chemistry that reflect differences in stratospheric and tropospheric chemistry:

- The UCX contains an extension (FAST-JX[8] v7.0a) of the Fast-J photolysis scheme used in the standard version of GEOS-Chem. Fast-JX treats photolysis at shorter wavelengths than Fast-J so that wavelengths relevant to stratospheric photolysis are included in the model.

[8] http://wiki.seas.harvard.edu/geos-chem/index.php/FAST-JX_v7.0_photolysis_mechanism

- The standard version of GEOS-Chem does not model atomic oxygen species explicitly because their lifetimes are very short; they are treated as intermediate species only. Because atomic oxygen species are important in stratospheric chemistry, the UCX treats oxygen atoms in two electronic states, $O(^3P)$ and $O(^1D)$, as explicit species. Ground state atomic hydrogen (H) and nitrogen (N) are also modeled explicitly.

- Eastham et al. updated GEOS-Chem's gas phase chemistry mechanism to include more detailed treatments of bromine and chlorine chemistry and also added heterogeneous halogen chemistry.

- The UCX can simulate polar stratospheric clouds (PSCs) and background liquid binary sulfate (LBS) aerosols that are not modeled in the standard version of GEOS-Chem.

- With the new stratospheric chemistry implemented in the UCX, additional emissions and boundary conditions were required. In the UCX, a single surface layer mixing ratio boundary condition is used for N_2O, chlorofluorocarbons (CFCs), hydro chlorofluorocarbons (HCFCs), halons, carbonyl sulfide (OCS) and long-lived organic chlorine species. The standard version of GEOS-Chem simulates emissions of biogenic bromine species, and this treatment is carried through to the UCX.

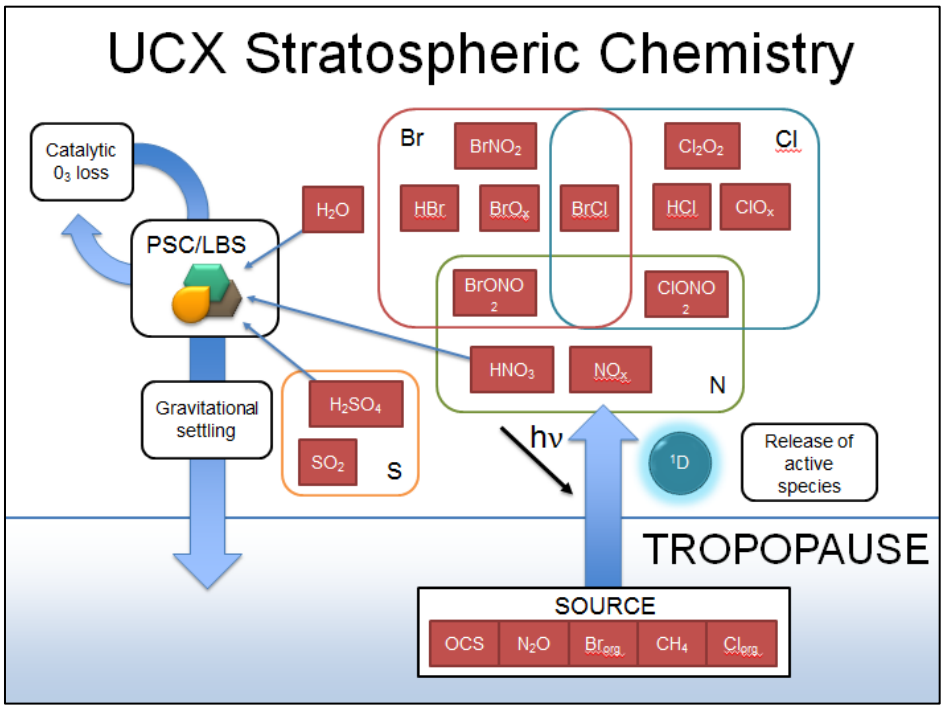

Figure 3-1. Illustration of the UCX scheme for stratospheric ozone available in GEOS-Chem (figure from Weisenstein et al., 2013).[9]

Because the UCX is not applied higher in the atmosphere than 0.1 hPa, the chemistry of the mesosphere is not simulated explicitly. Instead, a relaxation to climatology similar to the scheme used for the stratosphere in the standard version of GEOS-Chem (See Section 3.1.2) is used above 0.1 hPa. This prevents the spurious accumulation in the stratosphere of species that have sinks above the stratopause.

While UCX allows for a more detailed representation of stratospheric chemistry in GEOS-Chem, the additional complexity on the model slows down the GEOS-Chem model run time by approximately a factor of 2^{10}. In Project FY15-46, we applied version 10-01 of the GEOS-Chem model that allows the use of UCX. We used GEOS-5 meteorology and ran GEOS-Chem at 2°x2.5° grid resolution. A summary of the differences between the standard and UCX GEOS-Chem runs is given in Table 3-1.

For the chemistry solver, the standard version stratospheric chemistry run uses its default option, SMVGEAR II, while the UCX stratospheric chemistry run uses the Kinetic PreProcessor (KPP11) as the KPP is the UCX run's default option. The SMVGEAR II takes chemical reactions

[9] Abbreviations used in Figure 2-1 are: PSC, polar stratospheric clouds; LBS, liquid binary sulfate aerosols; O(^{1}D), oxygen atoms in the singlet D excited electronic state

[10] http://acmg.seas.harvard.edu/geos/word_pdf_docs/steering_cmte/gc_sc_minutes_05Jun2014.pdf

[11] http://wiki.seas.harvard.edu/geos-chem/index.php/KPP_solvers_FAQ

and uses sparse matrix and vectorization techniques to solve the reaction equations. On the other hand, KPP preprocesses the chemical reactions for specific chemistry mechanism and creates FORTRAN source codes, and these source codes are used to solve the chemical reaction equations. KPP provides several Runge-Kutta, LSODE, and several Rosenbrock solver options. The default option is Rosenbrock Rodas-3. The KPP Rosenbrock Rodas-3 solver is faster than SMVGEAR II by up to 10% and gives a slightly more accurate solution; therefore, KPP Rosenbrock Rodas-3 was used for the UCX run.

The GEOS-Chem developers provided GEOS-Chem UCX stratospheric initial conditions from an AER 2D zonal chemistry-transport model (Weisenstein et al., 1997) simulation. The GEOS-Chem UCX developers recommend a 5-year spinup period before beginning a UCX model run. This is due to the slow rate of circulation in the stratosphere relative to the troposphere. Unlike the troposphere, the stratosphere is stably stratified so that vertical motions are very slow. The stratospheric circulation is characterized by a slow meridional overturning known as the Brewer-Dobson circulation, which is shown in Figure 3-2. In this circulation, air enters the stratosphere via upward motion across the tropical troposphere. The Brewer-Dobson circulation, which is driven by planetary-scale waves, brings air from the tropical stratosphere poleward and downward. This moves ozone poleward from the tropics, where ozone production is favored by the presence of strong sunlight, and creates the polar ozone maxima seen in Figure 3-2. The transport time from the tropics to the polar regions can be as long as several years. In order for GEOS-Chem UCX to spin up all species, including the NOx, HOx, BrOx and ClOx species which play an important role in ozone destruction, the model must be run for several years. The UCX developers note that stratospheric NOx and HNO_3 require less time (~1 year of spinup) to come into equilibrium.

For this project, time constraints precluded running GEOS-Chem UCX for five years before beginning the simulation of June 2012. For both the standard and UCX GEOS-Chem runs, a one-year model spinup was performed for the year 2011 and the simulation extended from January 1 to December 31, 2012. Our analysis focused on June 1-30, 2012, which means that GEOS-Chem had a 17 month spinup period before the beginning of the simulation period that was used to develop June 2012 boundary conditions for CAMx. A year of spinup is sufficient for the standard version of GEOS-Chem (e.g. Yantosca et al., 2014). For the GEOS-Chem UCX, the 17 month spinup is shorter than the recommended 5-year spinup, and this introduces uncertainty into the comparison of the UCX and standard versions of GEOS-Chem because of the possibility that the UCX run may still be influenced by the initial conditions.

Table 3-1. GEOS-Chem run configuration for the standard and UCX model runs.

Science Options	GEOS-Chem Version 10-01 Model Configuration	
	Standard Version Stratospheric Chemistry	**UCX Stratospheric Chemistry**
Version	Version 10-01	
Output Vertical Grid Mesh	47 Layers	72 Layers
Horizontal Grids	2x2.5 degree (Nx, Ny = 144, 91)	
Initial Conditions	1 year full spin-up	
Meteorology	Year-specific GEOS-5 meteorology	
Chemistry		
Chemistry mechanism	GEOS-Chem standard chemistry with secondary organic aerosols (SOA)	UCX
Photolysis mechanism	FAST-JX	
Horizontal and Vertical Transport		
Advection Scheme	TPCORE	
Other Transport		
Cloud convection scheme	On / Relaxed Arakawa-Schubert	
Stratosphere-troposphere exchange	LINOZ	UCX
Planetary Boundary Layer (PBL) mixing	On / Full mixing in the PBL	
Dry deposition scheme	Wesely	
Numerics		
Chemistry Solver	SMVGEAR II	KPP - Rosenbrock Rodas-3
Parallelization	OMP	

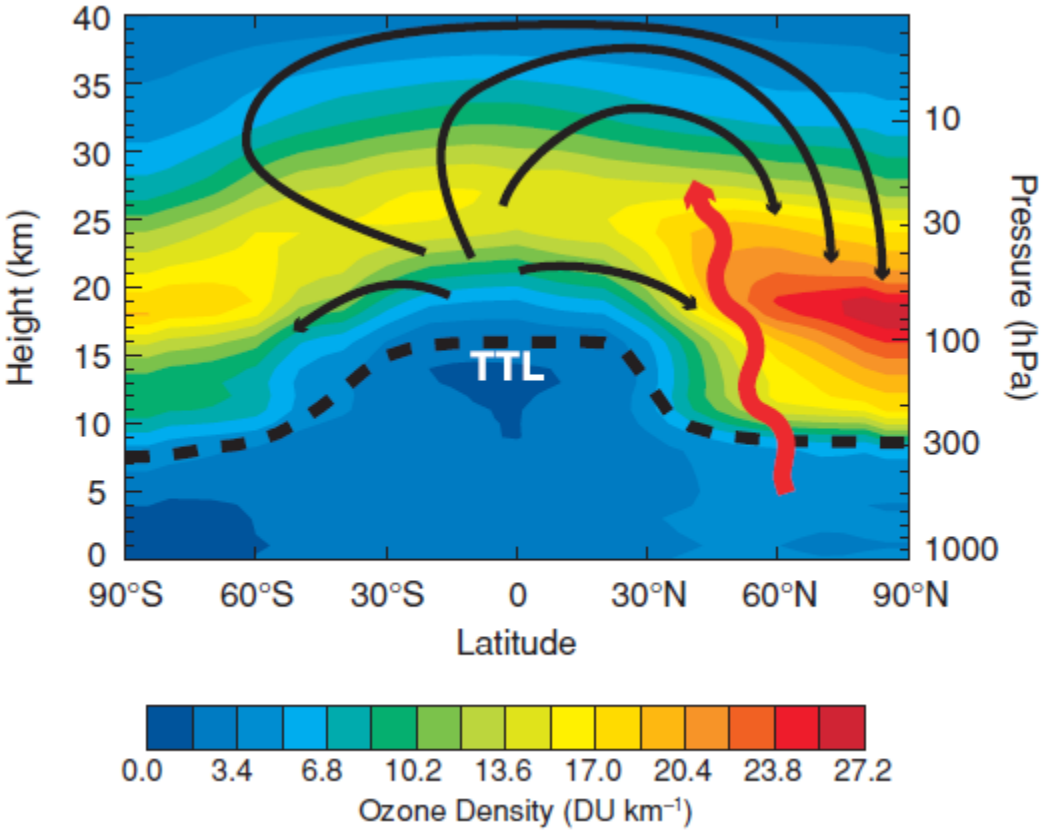

Figure 3-2. Schematic of the Brewer-Dobson circulation. Meridional cross-section of the atmosphere showing ozone density (colour contours; in Dobson units (DU) per km) during Northern Hemisphere (NH) winter (January to March), from the climatology of Fortuin and Kelder (1998). The dashed line denotes the tropopause, and TTL stands for tropical tropopause layer. The black arrows indicate the Brewer-Dobson circulation during NH winter, and the wiggly red arrow represents planetary waves that propagate from the troposphere into the winter stratosphere. Figure and caption text: IPCC report: https://www.ipcc.ch/pdf/special-reports/sroc/Boxes/b0102.pdf

3.2 Modification of GEOS2CAMx Boundary Condition Pre-Processor

The CAMx boundary condition processor GEOS2CAMx[12] is used to develop initial conditions and lateral boundary condition input files for CAMx from GEOS-Chem output data. GEOS2CAMx performs the vertical and horizontal interpolation needed to map the GEOS-Chem output to the CAMx grid and also performs the mapping between the GEOS-Chem species and the CAMx chemical mechanism specified by the user. In Project FY14-15, the GEOS2CAMx processor was modified to extract top boundary conditions as well as lateral boundary conditions from GEOS-Chem output. CAMx was then modified to read the resulting top boundary conditions.

[12] Available at http://www.camx.com/download/support-software.aspx.

Since Project 14-15, GEOS-Chem model chemistry has been revised and the GEOS2CAMx preprocessor was updated to account for new GEOS-Chem output species as well as to supply halogen species to CAMx. For example, following updates in GEOS-Chem isoprene chemistry (i.e. incorporation of Paulot et al. [2009] scheme)[13] isoprene nitrates, propanone nitrate, hydroxyacetone, glycoaldehyde, nitrate from methacrolein and methyl vinyl ketone, and peroxyacetic acid as well as other species can now be written out by the GEOS2CAMx preprocessor. Halogen species added to GEOS2CAMx include bromine and species such as Br_2, Br, BrO, HOBr, HBr, $BrNO_2$, $BrNO_3$, $CHBr_3$, CH_2Br_2, and CH_3Br which were not previously accounted for in the GEOS2CAMx species mapping. Additionally, ozone and NO_2 are now explicit tracer species since GEOS-Chem version 9-02, while they were estimated from Ox and NOx in GEOS-Chem version 9-01-03 or earlier. The updated GEOS2CAMx program considers isoprene products and related species and bromine and related compounds. For ozone and NO_2, GEOS2CAMx takes the GEOS-Chem species directly as a 1:1 match instead of deriving them from Ox and NOx.

GEOS-Chem uses two different vertical structures when it simulates and when it writes model output. Within the model, GEOS-Chem uses the full vertical layer structure from its meteorology data. However, when it writes output, it uses a reduced layer structure above ~80 hPa (~17 km) to reduce disk space usage. In GEOS-5 meteorology, the total number of the full vertical layers is 72 while the reduced layers consist of 47. The current GEOS-Chem UCX run, however, uses the full vertical layer in writing output. The existing GEOS2CAMx program was updated to account for the new species mapping and for reading the GEOS-Chem vertical layer structure. All these updates are implemented in GEOS2CAMx version 2.3.

3.3 CAMx Model

The CAMx regional air quality model is an Eulerian photochemical grid model that can be applied over spatial scales ranging from sub-urban to continental. CAMx simulates the emission, dispersion, chemical reaction, and removal of pollutants in the troposphere by solving the pollutant continuity equation for each chemical species on a system of nested three-dimensional grids. The Eulerian continuity equation describes the time dependence of the average species concentration within each grid cell volume as a sum of all of the physical and chemical processes operating on that volume.

CAMx is the model used by the TCEQ for their SIP modeling. The rationale for the TCEQ's selection of CAMx for SIP modeling is described in TCEQ SIP modeling protocols[14,15]. In this project, CAMx was applied for a 2012 high ozone episode using modeling inputs developed by

[13] http://wiki.geos-chem.org/New_isoprene_scheme
[14] http://www.tceq.texas.gov/assets/public/implementation/air/sip/dfw/ad_2011/AppE_Protocol_ado.pdf
[15] https://www.tceq.texas.gov/assets/public/implementation/air/am/modeling/hgb8h2/doc/HGB8H2_Protocol_20090715.pdf

the TCEQ[16] including meteorology and emission inventory inputs. The modeled episode extends from June 1-30, 2012 with a CAMx spinup period that extends from May 16-31, 2012. The nested 36/12/4 km modeling domain is shown in Figure 3-3.

The purpose of the high resolution 4 km modeling grid (shown in green in Figure 3-3.) is to accurately simulate local and regional ozone production and transport within east Texas. The 12 km grid (shown in blue in Figure 3-3.) includes a substantial area that would typically be upwind of Texas during an ozone episode with easterly or northeasterly winds. This is necessary to accurately represent any influence of ozone transport since ozone formation is modeled more accurately by a 12 km grid than a 36 km grid.

In accordance with EPA draft modeling guidance (EPA, 2014), the outer 36 km domain shown in black in Figure 3-3 was designed to be large enough to encompass all important upwind sources of emissions and to allow use of clean or relatively clean boundary conditions. CAMx is a regional model and is designed to simulate a limited area of the earth's atmosphere. It therefore requires boundary conditions at the lateral edges of the 36 km modeling grid as well as at the CAMx model's top boundary. CAMx lateral boundary conditions are generally supplied by a global chemistry-transport model. In this project, CAMx lateral boundary conditions were supplied by the GEOS-Chem model.

Figure 3-3. CAMx nested 36/12/4 km modeling domains for the 2012 episode.

[16] http://www.tceq.texas.gov/airquality/airmod/data/tx2012

In the TCEQ's modeling, the CAMx top boundary is located at approximately 15 km, which is within or near the stratosphere. The vertical structure of the CAMx modeling domain is illustrated in Figure 3-4 and Figure 3-5.

To improve computational efficiency, the number of model layers simulated by CAMx in the middle and upper troposphere is reduced relative to the Weather Research and Forecasting (WRF; Skamarock et al., 2005) model used to supply meteorological data to CAMx. This degradation of CAMx vertical resolution is known as layer collapsing because multiple meteorological model layers are collapsed into a single CAMx layer.

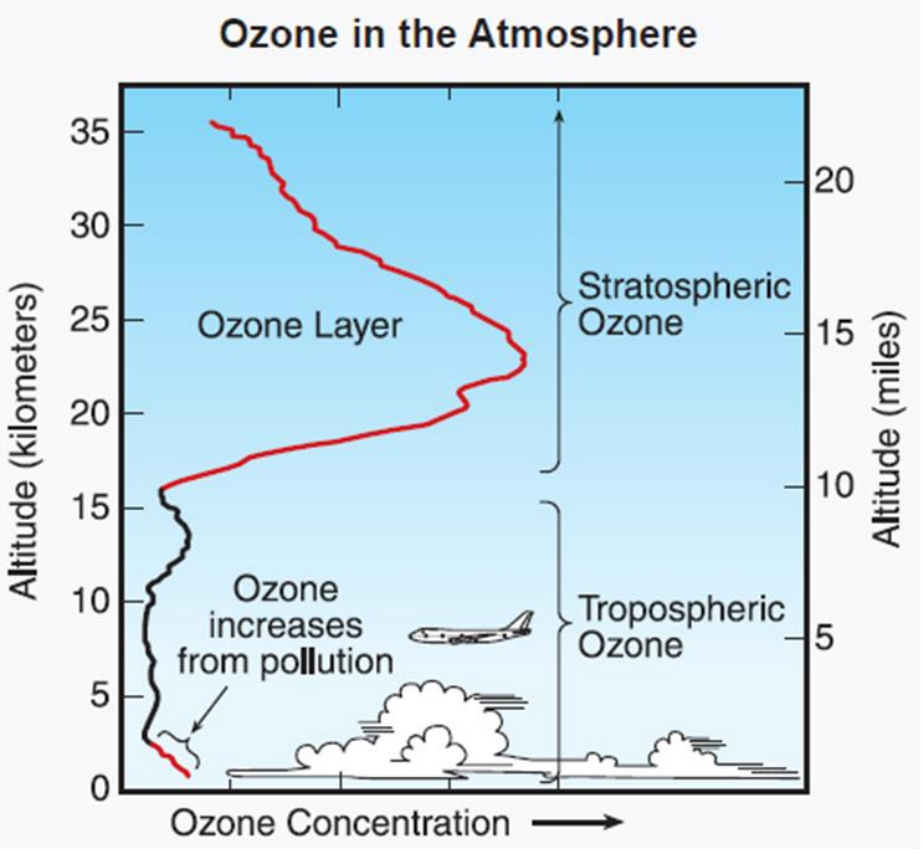

Figure: http://esrl.noaa.gov/csd/assessments/ozone/2006/chapters/Q1.pdf

Figure 3-4. TCEQ 2012 model vertical structure and extent and climatological profile of mid-latitude ozone. Left panel is EPA figure[17]. Right panel is TCEQ figure excerpted from image shown in Figure 3-5.

[17] http://esrl.noaa.gov/csd/assessments/ozone/2006/chapters/Q1.pdf

Vertical Layer Structure

Corresponding WRF Layer	Layer Top (m AGL)	CAMx Layer	Layer Center (m AGL)	Thickness (m)
38	15179.1	28	13637.9	3082.5
36	12096.6	27	10631.6	2930.0
32	9166.6	26	8063.8	2205.7
29	6960.9	25	6398.4	1125.0
27	5835.9	24	5367.0	937.9
25	4898.0	23	4502.2	791.6
23	4106.4	22	3739.9	733.0
21	3373.5	21	3199.9	347.2
20	3026.3	20	2858.3	335.9
19	2690.4	19	2528.3	324.3
18	2366.1	18	2234.7	262.8
17	2103.3	17	1975.2	256.2
16	1847.2	16	1722.2	249.9
15	1597.3	15	1475.3	243.9
14	1353.4	14	1281.6	143.6
13	1209.8	13	1139.0	141.6
12	1068.2	12	998.3	139.7
11	928.5	11	859.5	137.8
10	790.6	10	745.2	90.9
9	699.7	9	654.7	90.1
8	609.7	8	565.0	89.3
7	520.3	7	476.1	88.5
6	431.8	6	387.9	87.8
5	344.0	5	300.5	87.1
4	256.9	4	213.8	86.3
3	170.6	3	127.8	85.6
2	85.0	2	59.4	51.0
1	33.9	1	17.0	33.9

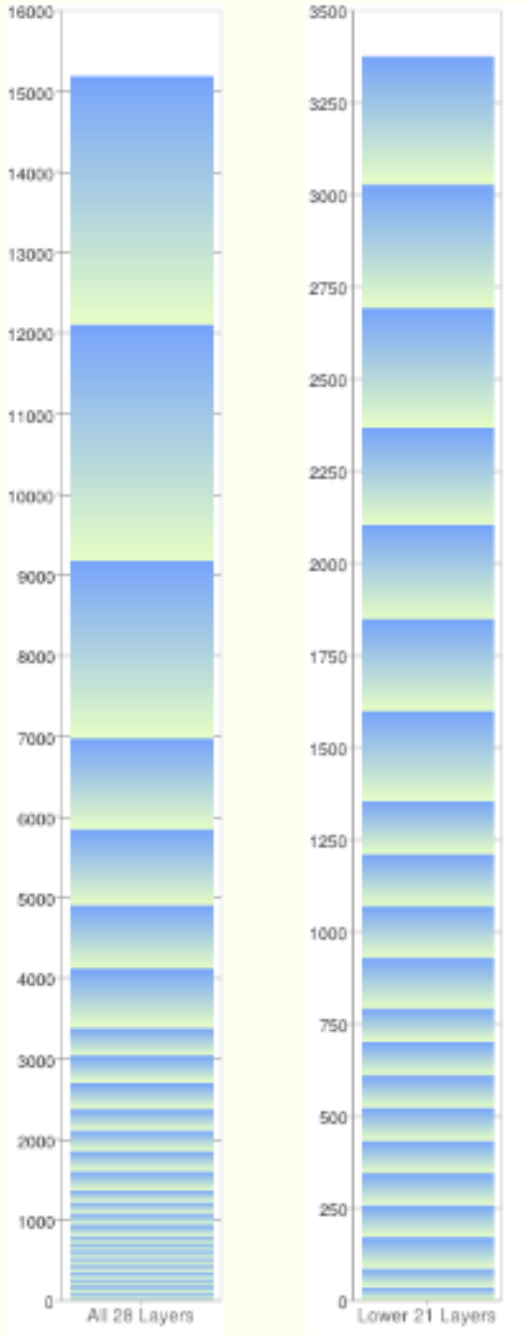

AGL - Above Ground Level.

Figure 3-5. June 2012 model WRF and CAMx layer structure. TCEQ figure from http://www.tceq.texas.gov/airquality/airmod/rider8/modeling/domain.

Initially, three CAMx simulations of the June 2012 episode were conducted. All were performed using the TCEQ modeling platform model settings. The three CAMx simulations were identical except for the specification of the model boundary conditions and are named accordingly (Table 3-2). The Zero Gradient run used the original internally-defined zero-gradient mixing ratio assumption at the CAMx model top. The purpose of the Zero Gradient run was to determine whether the use of GEOS-Chem-derived top boundary conditions improved model performance relative to the CAMx default Zero Gradient assumption used in the TCEQ June 2012 modeling platform. Project FY14-15 performed this comparison for the TCEQ's June 2006 episode, but a similar evaluation had not yet been done for the June 2012 episode.

The G-C Std CAMx run used boundary conditions derived using the GEOS-Chem standard version 10-01 model with LINOZ used for stratospheric ozone. The G-C UCX CAMx run used boundary conditions derived using GEOS-Chem version 10-01 with the UCX extension.

Table 3-2. Top and lateral boundary condition (BC) for the three initial 28-layer CAMx runs.

CAMx Run Name	Lateral BC	Top BC
Zero Gradient	Rider 8 dataset – bc patched[18]	N/A – zero gradient mixing ratio topcon
G-C Std	GEOS-Chem v.10-01 standard – bc patched[18]	GEOS-Chem v.10-01 standard
G-C UCX	GEOS-Chem v.10-01 UCX standard – bc patched[18]	GEOS-Chem v.10-01 UCX standard

Lateral and top boundary conditions for the outer 36 km grid were extracted from the GEOS-Chem simulations for all three runs using GEOS2CAMx v2.3. Modifications were made to the GEOS-Chem lateral boundary conditions to increase unrealistically low CO concentrations and reduce impacts from 2012 wildfires in northern Manitoba. Based on evaluation of the TCEQ Near-Real Time Ozone Model platform, Johnson et al. (2013) determined that ozone is overestimated in the GEOS-Chem model output. Therefore, we performed a flat 10 ppb ozone reduction and applied various caps to ozone precursors over the Gulf of Mexico and Atlantic Ocean in order to deplete the ozone coming onshore. The lateral boundary condition caps are summarized in Table 3-3 and this process is referred to as a "bc patch" in Table 3-2.

[18] O3 concentrations are reduced by 5 ppb, and for the Caribbean and the Gulf of Mexico, additional 10 ppb of O3 is reduced to offset the overestimation of GEOS-Chem O3. For O3 precursor species such as NOx, VOC, and CO, specific ranges are applied to be comparable to measurement range. Similar patches were applied in the TCEQ forecasting project.

Table 3-3. Maximum concentration limits for ozone precursors applied to the 36 km lateral boundary condition grid cells across the Gulf of Mexico, Caribbean Sea, and Atlantic Ocean south of Cape Hatteras.

Species	Description	Max. Concentration (ppb)
NO2	Nitrogen dioxide	0.05
CO	Carbon monoxide	150.0
N2O5	Dinitrogen pentoxide	0.001
HNO3	Nitric acid	0.25
PNA	Peroxynitric acid	0.001
H2O2	Hydrogen peroxide	0.5
NTR	Organic nitrates	0.01
FORM	Formaldehyde	0.25
ALD2	Acetaldehyde	0.05
ALDX	Propionaldehyde and higher aldehydes	0.02
PAR	Paraffin carbon bond (C-C)	1.0
OLE	Terminal olefin carbon bond (R-C=C)	0.01
ETHA	Ethane	1.0
MEPX	Methylhydroperoxide	0.1
PAN	Peroxyacetyl Nitrate	0.01
PANX	C3 and higher peroxyacyl nitrate	0.001
INTR	Organic nitrates from ISO2 reaction with NO	0.001
ISOP	Isoprene	0.1
ISPD	Isoprene product (lumped methacrolein, methyl vinyl ketone, etc.)	0.1
TERP	Monoterpenes	0.05
ISP	Isoprene (SOA chemistry)	0.1
TRP	Monoterpenes (SOA chemistry)	0.05
TOL	Toluene and other monoalkyl aromatics	0.02
XYL	Xylene and other polyalkyl aromatics	0.01
SO2	Sulfur dioxide	0.1
PRPA	Propane	0.5
ACET	Acetone	0.25
KET	Ketone carbon bond (C=O)	0.05
BENZ	Benzene	0.1

3.4 Initial CAMx Modeling

We ran CAMx for the TCEQ's June 2012 episode using the three methods of specifying top boundary conditions described in Table 3-2. These three initial runs used the layer collapsing scheme shown in Figure 3-5 and the default TCEQ 2012 emission inventory. We evaluated CAMx model performance in these three runs against surface ozone observations, aloft aircraft measurements of ozone and NOy, and ozonesonde profiles. This evaluation is described in detail in the Interim Report on Tasks 2 and 3 (Jung et al., 2015) and is reproduced in part in Appendix A of this report. We summarize the results of the evaluation below.

The model performance evaluation against observed surface and aloft ozone and aloft NOy indicated that the GEOS-Chem model was functioning correctly in both the standard and UCX

configuration and was providing reasonable lateral and model top boundary conditions to CAMx. However, the evaluation of the vertical profiles of NO_2 against aircraft data indicated that it was necessary to refine the modeling platform in order to compare observed and modeled ozone and NOy in the upper troposphere. Following the evaluation, we made the following revisions to the CAMx modeling platform:

1. Added upper tropospheric NOx emissions that are currently not present in the TCEQ 2012 model:
    a. Aircraft cruise emissions
    b. Lightning NOx emissions

2. Reprocessed the CAMx meteorological inputs so that CAMx can be run without layer collapsing that diminishes the model's vertical resolution in the region of strong ozone and NOy gradients near the tropopause.

The additions to the TCEQ 2012 emission inventory are described in Section 3.4.1 and 3.4.2. We note that the TCEQ is currently developing both aircraft emissions and lightning NOx emissions for the 2012 episode, but these inventories were not yet available at the time the modeling for this project was performed.

3.4.1 TCEQ Aircraft Emission Inventory

The TCEQ developed a single-day aircraft emission inventory for use in the June 2006 modeling episode (Doug Boyer, TCEQ, personal communication, 2013). Although the year does not match the June 2012 modeling episode, this was the best immediately available source of aircraft cruise emissions for the TCEQ modeling domain. The 2006 single day aircraft emission inventory was developed using the Advanced Emission Model (AEM3) developed at the EUROCONTROL Experimental Centre (http://www.eurocontrol.int/services/advanced-emission-model). For climb, cruise and descent phases of flight at altitudes greater than 3,000 feet, AEM3 estimates fuel burn and aircraft emissions based on user-specified aircraft and engine types and aircraft flight profiles (the aircraft's path in time and space). AEM3 calculates emissions for a set of pollutants, including NOx, for each flight segment for each aircraft, and uses an updated version of the Boeing Method 2 (EEC-BM2). Boeing Method 2 is used to compute emission factors, fuel flow and emissions with consideration for atmospheric and flight conditions. For altitudes less than 3,000 feet, AEM3 does not use flight trajectory data to calculate fuel burn and emissions with Boeing Method 2, but instead uses the landing and take-off (LTO) cycle defined by the International Civil Aviation Organization (ICAO). The LTO cycle consists of four modes of aircraft operation (takeoff, climb, approach, and taxi) with specific thrust settings and time in flight mode defined for each part of the cycle. Emissions from AEM3 for altitudes < 3,000 feet were not used because these emissions are accounted for in the airport emission inventories in the TCEQ's June 2012 SIP modeling inventory.

The TCEQ used NASA's Flight Track Database (http://www-angler.larc.nasa.gov/flighttracks/) to supply the flight profile data required for input to AEM3. This database contains detailed flight information for every commercial flight in the U.S. on the June, 2006 day for which the

inventory was developed. AEM3 was then used to calculate the emissions for all flights and flight segments. The TCEQ then ran the EPS3 emissions model for each unique flight segment for each hour using the PRESHP/PSTSHP link-based module to preserve the spatial detail inherent in the inventory (Doug Boyer, TCEQ, personal communication, 2013). The spatial distribution of the single-day emission inventory for the eastern U.S. is shown in Figure 3-6.

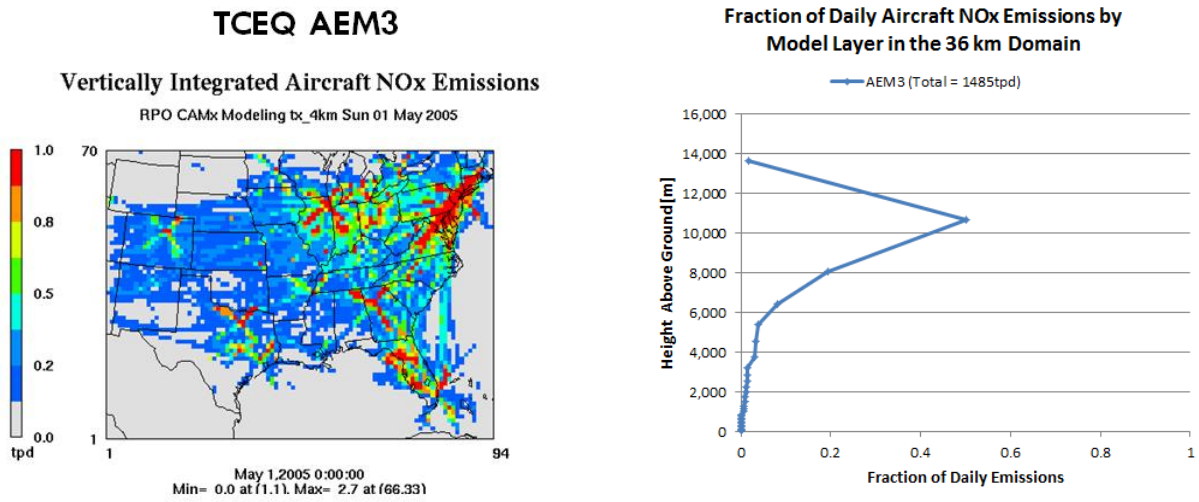

Figure 3-6.TCEQ aircraft emission inventory. Left panel: vertically integrated aircraft NOx emissions for a subset of the TCEQ 36 km modeling domain. Right panel: Vertical distribution of aircraft NOx emissions for the TCEQ AEM3 aircraft inventory averaged across the 36 km domain.

3.4.2 Lightning NOx Emission Inventory

NOx is formed in lightning channels as the heat released by the electrical discharge causes the conversion of N_2 and O_2 to NO. Lightning NOx can be important in determining the tropospheric NOx budget and in understanding its effect on upper tropospheric ozone and OH; therefore, lightning NOx is typically incorporated in global modeling (e.g. Tost et al. 2007, Sauvage et al. 2007; Emmons et al., 2010), and has also been integrated into regional modeling studies (e.g. Allen et al. 2012).

Lightning NOx emissions (LNOx) can be estimated directly based on the number of lightning flashes, the intensity of each flash, the lightning type (cloud-to-ground vs. cloud-to-cloud), and the amount of NOx emitted per flash. While the number of lightning flashes and flash intensity can be determined from data gathered by the National Lightning Detection Network (NLDN), there is uncertainty in the estimates of emissions of NOx per flash. As a result, there is a large variation in reported global lightning NOx emissions, with values ranging from 1-20 Tg N $year^{-1}$ (Schumann and Huntrieser, 2007; Zhang et al., 2003a, b; Lee et al., 1997).

Because formation of lightning NOx is associated with deep convection in the atmosphere, LNOx production is typically parameterized in terms of the modeled convective activity. LNOx production is often assumed to be related to cloud top height or convective rainfall. One

shortcoming of this approach is that convective clouds where lightning typically occurs are difficult for atmospheric models to simulate accurately. Errors in the modeled amount and intensity of cumulus convection can degrade the simulation of LNOx production. It is possible to estimate lightning emissions based on observations of lightning flashes. There are surface networks that observe lightning flash activity (such as the NLDN) as well as satellite observations of lightning from the Lightning Imaging Sensor (LIS) and the Optical Transient Detector (OTD) instruments. While it is possible to construct an LNOx emission inventory based on observed flash counts, this type of emission inventory will not provide a self-consistent simulation of the vertical transport of LNOx due to modeled convection. For example, if lightning flashes are observed in a region where no convective activity is predicted by the model, emissions of LNOx may be allowed to remain near the surface, whereas the actual atmosphere would be undergoing intense vertical mixing due to convection, causing some of the emitted LNOx to be transported rapidly into the upper troposphere by convective updrafts.

Recent efforts to model LNOx production have taken a hybrid approach that preserves the consistency of the modeled convection and the location of LNOx emissions, but also attempts to constrain the LNOx emissions to match observed distributions of lightning or an estimate of total emissions. A number of such schemes are available (e.g. Allen et al. 2010; Murray et al. 2012). We selected the scheme of Koo et al. (2010) because this scheme is consistent with the approach outlined above and has already been implemented as a CAMx preprocessor; development of a new LNOx preprocessor was not possible within the time frame of this project.

Koo et al. (2010) estimated annual total LNOx emissions for North America using NLDN flash data from Orville et al. (2002) and (Boccippio et al., 2001). The NO emissions factor that determines the amount of NO generated per flash of lightning is taken from the EULINOX study (Holler and Schumann, 2000) and is 9.3 kg N per flash. Using these data, Koo et al. estimate the total LNOx emissions for North America to be 1.06 Tg N year^{-1}. Lightning emissions are then allocated to grid cells where modeled convection occurs using convective precipitation as a proxy for lightning activity. The hourly and gridded 3-D lightning NO emissions are calculated as follows:

$$E(x,t) = R_{NO} P_C(x,t) D(x,t) p(x,t)$$

where E(x,t) is the NO emission rate (mol hr^{-1}) at time t and grid location x; R_{NO} is the NO emission factor; P_C is the convective precipitation (m hr^{-1}) at time t and grid location x; D(x,t) is the convective cloud depth (m) at time t and grid location x; and p(x,t) is the pressure (Pa) at time t and grid location x. Constraining the total emissions within North America to 1.06 Tg N year^{-1} requires that R_{NO} be equal to 3.9x10^{-12}.

This parameterization was used to generate emissions for the June 2012 episode. Because the TCEQ 4 km WRF simulation for this episode did not employ a cumulus parameterization, the results from the 12 km grid, which did use a cumulus scheme, were used on the 4 km grid. Comparison of the vertical distribution of LNOx emissions produced by the Koo et al.

parameterization with observed lightning activity data presented in Allen et al., (2012) and Hansen et al. (2010) suggests that the Koo scheme produces a distribution of LNOx that is too strongly peaked in the lower atmosphere. Therefore, we used the vertical profiles of Ott et al. (2010) to distribute the LNOx emissions in the vertical.

Ott et al. (2010) used a three-dimensional cloud resolving model (CRM) to simulate six mid-latitude and subtropical thunderstorms that were the subject of intensive field studies. Lightning within the thunderstorms was monitored by ground-based observing systems and research aircraft measured the chemical properties (including NOx) of the atmosphere in the clouds. Ott et al. modeled NOx within the clouds and then compared the modeled NOx distribution with in-cloud aircraft data. They developed vertical profiles for allocating LNOx in regional or global models that are specific to the type of thunderstorm that was modeled. They developed subtropical, mid-latitude and tropical profiles, which are shown in Figure 3-7. The Ott scheme is currently used to distribute LNOx in the vertical in the GEOS-Chem model (Murray et al., 2012).

Ott et al. (2010) recommend that in the northern hemisphere warm season, the subtropical profile be used south of 40°N and the mid-latitude profile be used northward of 40°N; this guidance was followed in the present study. They suggest that the profile be scaled to the modeled cloud top height in each grid cell and that when the cloud top height is less than 16 km, the fraction of LNOx be taken from those layers and redistributed evenly to the layers from surface to cloud top, and this recommendation was followed, as well. The LNOx emissions were modeled as point sources injected into each model grid cell with zero plume rise.

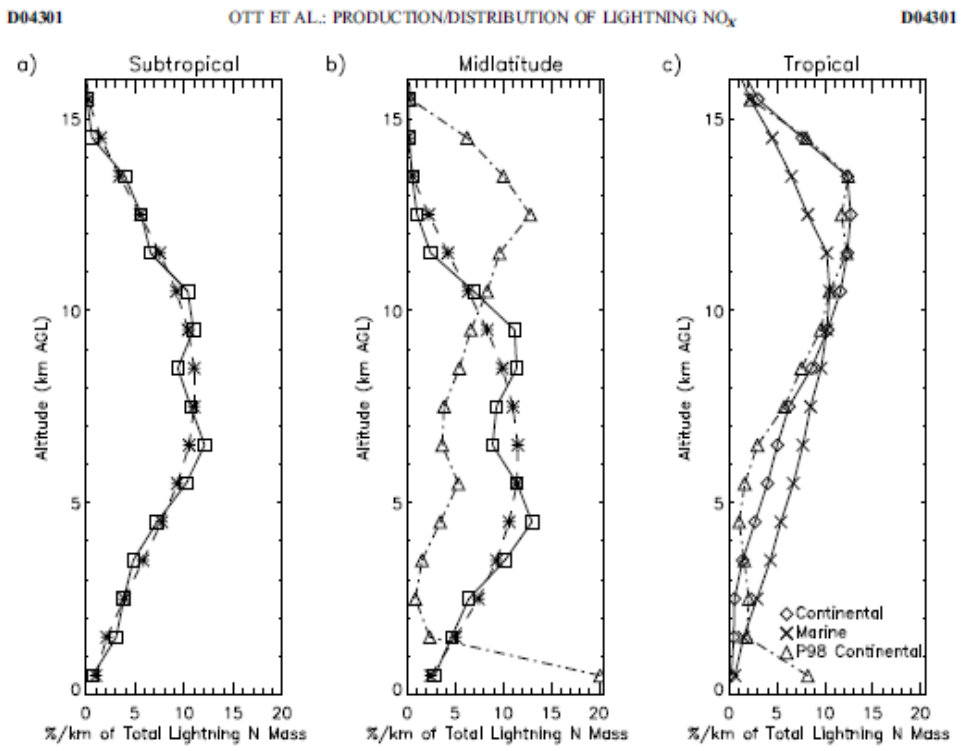

Figure 12. Average vertical distribution of percentage of LNO_x mass per kilometer following convection (solid) for the (a) subtropical and (b) midlatitude continental regimes. Dashed line shows polynomial fit. Midlatitude continental profile from *Pickering et al.* [1998] (dash-dot) is also shown in Figure 12b. The hypothetical tropical marine profile (c) was created by extrapolating the subtropical average profile to a higher tropopause regime while the tropical continental profile was constructed using the *Pickering et al.* [1998] profile with the boundary layer maximum removed and that mass redistributed into layers from 4 to 11 km.

Figure 3-7. Vertical Profiles from Ott et al. (2010) used for vertical distribution of LNOX emissions.

3.5 Final CAMx Modeling

We re-ran the CAMx simulations for the G-C Std and G-C UCX configurations shown in Table 3-1 using the updated inventory with aircraft and LNOx emissions and using the full 38-layer resolution of the WRF model (i.e. no layer collapsing). Based on the surface and aloft ozone performance evaluation shown in Appendix A, we did not re-run the Zero Gradient case. The Zero Gradient case showed vertical profiles of ozone that differed in shape from the observed ozone profiles due to the constraint imposed by the zero gradient mixing ratio top boundary condition, and surface ozone performance was slightly worse than in the two CAMx runs that used GEOS-Chem output data for the top boundary conditions. These results were similar to those obtained in Project FY14-15 for the June 2006 modeling episode (Kemball-Cook et al., 2014). Therefore, we did not perform a final CAMx run for the Zero Gradient case.

4.0 FINAL CAMX RUN MODEL PERFORMANCE EVALUATION

In Section 4, we present the results of the model performance evaluation at the surface and aloft for the final CAMx runs using GEOS-Chem output data for the top and lateral boundary conditions.

4.1 Surface Performance Evaluation for Ozone

The performance of the GEOS-Chem Std and UCX CAMx runs in simulating surface layer ozone was evaluated at rural sites within the 36 km CAMx modeling grid and at sites in Texas in the 4 km modeling grid. We evaluated CAMx against ground level observations from Clean Air Status and Trends Network (CASTNET) sites within the 36 km grid (right panel of Figure 4-1). The CASTNET monitors are located in rural areas and were used in this study because regions outside of Texas and surrounding states were modeled using a 36 km grid, which cannot be expected to accurately simulate variations in ozone within an urban area.

We also evaluated ozone at monitors within Texas using the modeling output from the 4 km grid. Within the 4 km grid centered on East Texas (Figure 3-3), ozone data from the TCEQ's Continuous Air Monitoring Station (CAMS) sites were used for the model performance evaluation (left panel of Figure 4-1). The goal of the evaluation was to determine the effect of the different CAMx top boundary conditions on modeled ground level ozone at sites within Texas. When selecting sites for display in this section, we included sites that had the largest differences in surface ozone between the two CAMx runs. These CAMS sites tended to be in rural and near-coastal locations, where the boundary conditions make a larger relative contribution to the total ozone than at inland urban sites, which are more heavily influenced by local emissions. We also included sites that showed minimal differences. Inland urban sites such as those in the Dallas-Fort Worth Area, where local ozone production is more important, tended to show only very small differences between the two CAMx runs.

Consistent with EPA Modeling Guidance (EPA, 2014), we used multiple statistical metrics in the model performance evaluation. We evaluated the root mean square error (RMSE), normalized mean bias (NMB), normalized mean error (NME), and the coefficient of determination (r^2). These metrics are defined in Table 4-1.

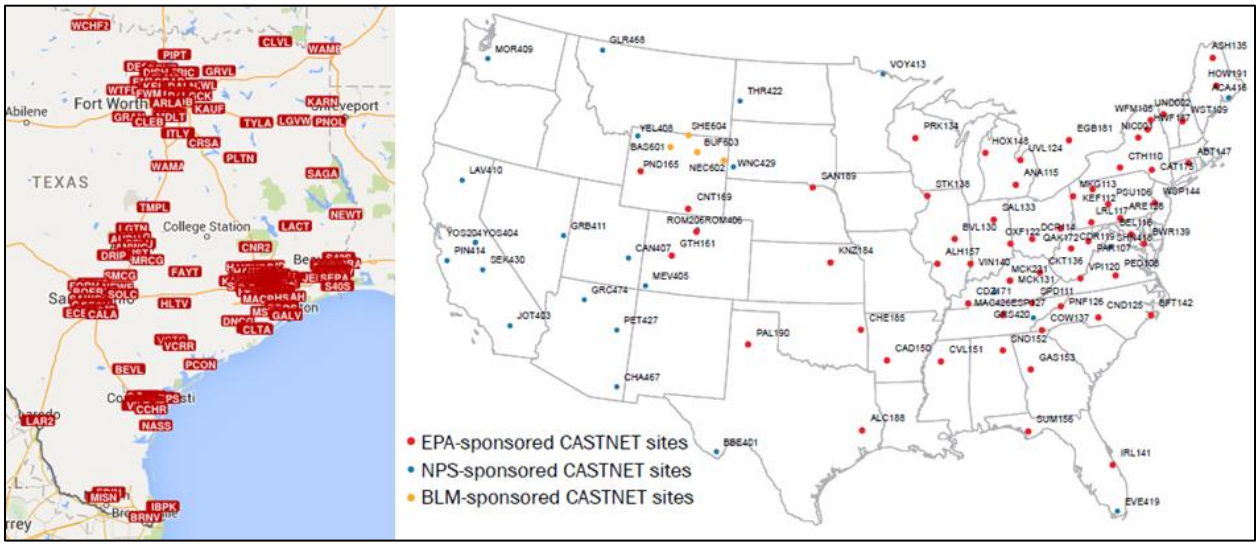

Figure 4-1. Surface model performance evaluation sites. Left: TCEQ CAMS sites in the 4 km domain. TCEQ figure[19]. Right: location of CASTNet Sites. EPA figure.[20]

Table 4-1. Definition of statistical performance metrics for CAMx and GEOS-Chem modeling.

Metric	Definition[1]
Mean Bias (MB)	$\frac{1}{N}\sum_{i=1}^{N}(P_i - O_i)$
Mean Error (ME)	$\frac{1}{N}\sum_{i=1}^{N}\lvert P_i - O_i\rvert$
Root Mean Squared Error (RMSE)	$\sqrt{\frac{\sum_{i=1}^{N}(P_i - O_i)^2}{N}}$
Normalized Mean Bias (NMB) (-100% to +∞)	$\frac{\sum_{i=1}^{N}(P_i - O_i)}{\sum_{i=1}^{N} O_i}$
Normalized Mean Error (NME) (0% to +∞)	$\frac{\sum_{i=1}^{N}\lvert P_i - O_i\rvert}{\sum_{i=1}^{N} O_i}$
Coefficient of Determination (r^2) (0 to 1)	$\left(\frac{\sum_{i=1}^{N}(P_i - \overline{P})(O_i - \overline{O})}{\sqrt{\sum_{i=1}^{N}(P_i - \overline{P})^2 \sum_{i=1}^{N}(O_i - \overline{O})^2}}\right)^2$

[1]Pi and Oi are the predicted and observed values (Oi,Pi) at the i[th] site paired in space and time and N is the number of observed/modeled data pairs.

[19] https://www.tceq.texas.gov/airquality/airmod/data/site

[20] http://epa.gov/castnet/javaweb/docs/CASTNET_Factsheet_2013.pdf

4.1.1 Evaluation on 4 km Grid

Below, we summarize the main findings of the model performance evaluation for surface ozone on the 4 km grid.

- The CAMx model has an overall high bias for ozone. The normalized mean bas (NMB) plots in Figure 4-2 through Figure 4-7 frequently show positive values of the NMB for days with 8-hour average ozone exceeding the 40 ppb threshold.

- For periods where modeled ozone was higher (lower) than observed ozone, bias was generally larger (smaller) in the G-C UCX CAMx run and smaller (larger) in the G-C std CAMx run. Surface ozone was generally slightly higher in the G-C UCX CAMx run than in the G-C std CAMx run.

- The two CAMx runs agree well for surface ozone throughout most of the June 2012 episode.

- The largest differences in surface layer ozone between the two runs occurred during June 10-15, a period of relatively low observed ozone at most East Texas CAMS sites.

- During the last week of June, East Texas experienced a period of widespread high ozone, and differences between the two CAMx runs were very small. At most sites, the time series for the two runs are nearly indistinguishable during June 24-29.

- At the coastal sites Aransas Pass (Figure 4-3) and Galveston (Figure 4-4), differences between the two CAMx runs were among the largest and most sustained of all East Texas monitors and these differences reached their largest values during the low ozone period June 10-15. Even for these coastal sites, the period with high ozone at end of June showed very little difference in ozone between the two runs.

- The largest difference during the two runs at any monitor during the June 2012 episode was 1.9 ppb and occurred on June 4 at the Danciger (CAMS 618) monitor. Observed 1-hour ozone for this hour was 36 ppb (i.e. not a high ozone period).

In general, the differences in surface ozone between the two CAMx runs are small (1.9 ppb or less), which indicates that the influence of the top boundary condition is generally small at the surface, especially during periods of high ozone in East Texas during June 2012.

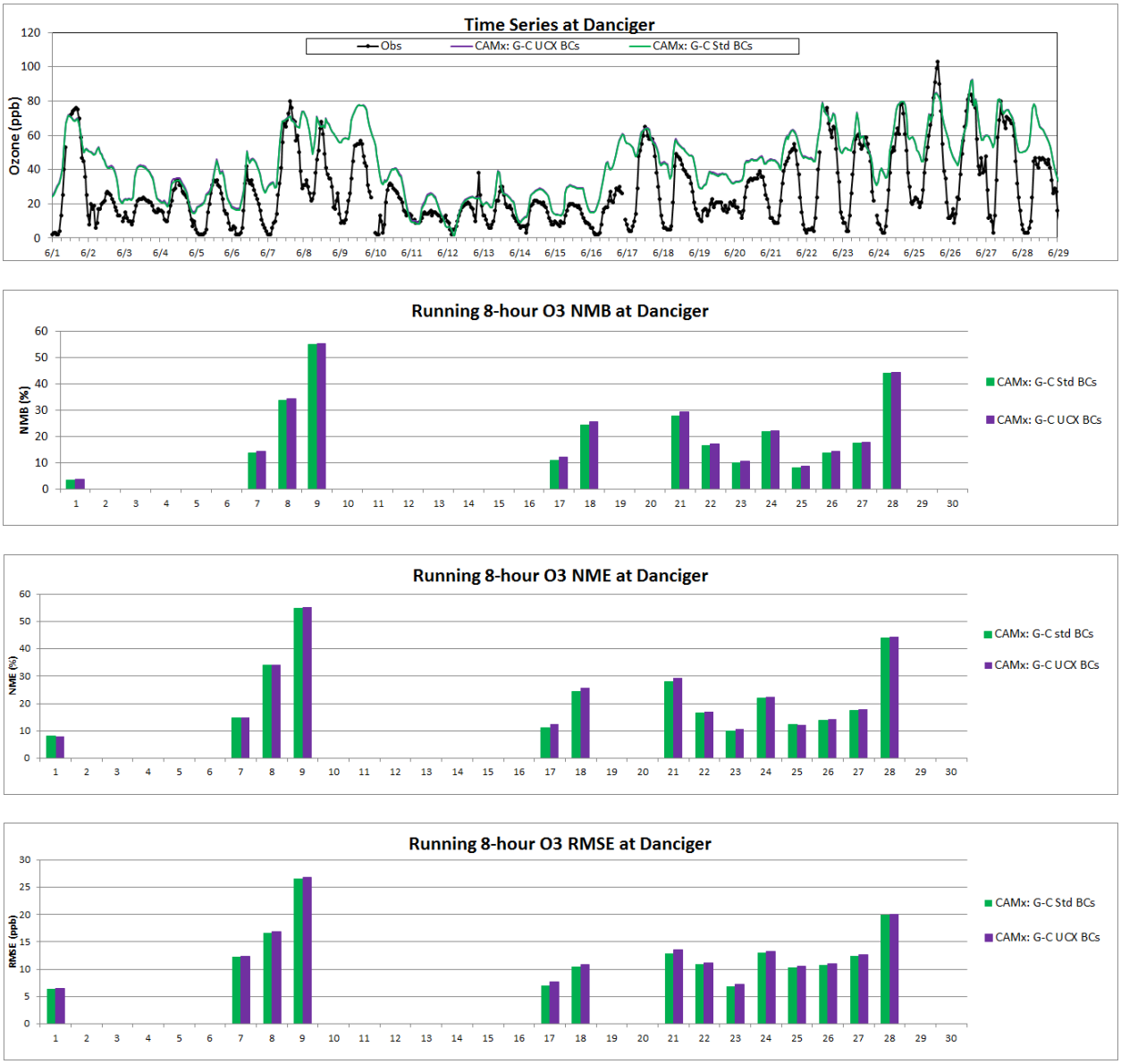

Figure 4-2. Upper panel: observed 1-hour ozone (black) at the Danciger (CAMS 618) monitor versus modeled 1-hour average surface layer ozone during the June 1-30, 2012 period for the GEOS-Chem (G-C) Std BC CAMx run (green) and G-C UCX BC CAMx Run (purple). 2nd panel from top: normalized mean bias (NMB) for 8-hour average ozone. 3rd panel from top: normalized mean error (NME) for 8-hour average ozone. 4th panel from top: root mean square error (RMSE) for 8-hour average ozone.

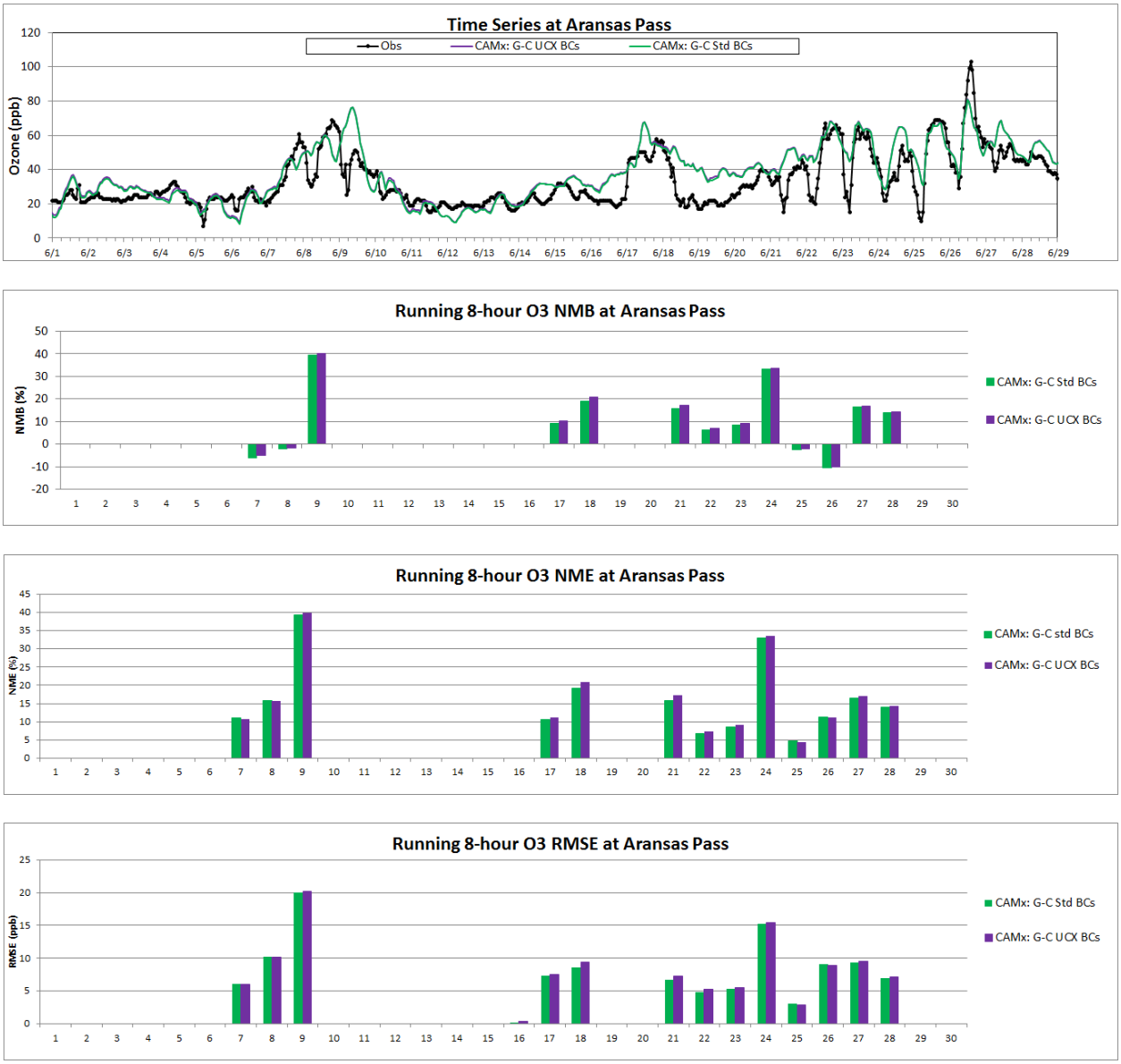

Figure 4-3. Upper panel: observed 1-hour ozone (black) at the Aransas Pass (CAMS 659) monitor versus modeled 1-hour average surface layer ozone during the June 1-30, 2012 period for the G-C Std BC CAMx run (green) and G-C UCX BC CAMx Run (purple). 2nd panel from top: normalized mean bias (NMB) for 8-hour average ozone. 3rd panel from top: normalized mean error (NME) for 8-hour average ozone. 4th panel from top: root mean square error (RMSE) for 8-hour average ozone.

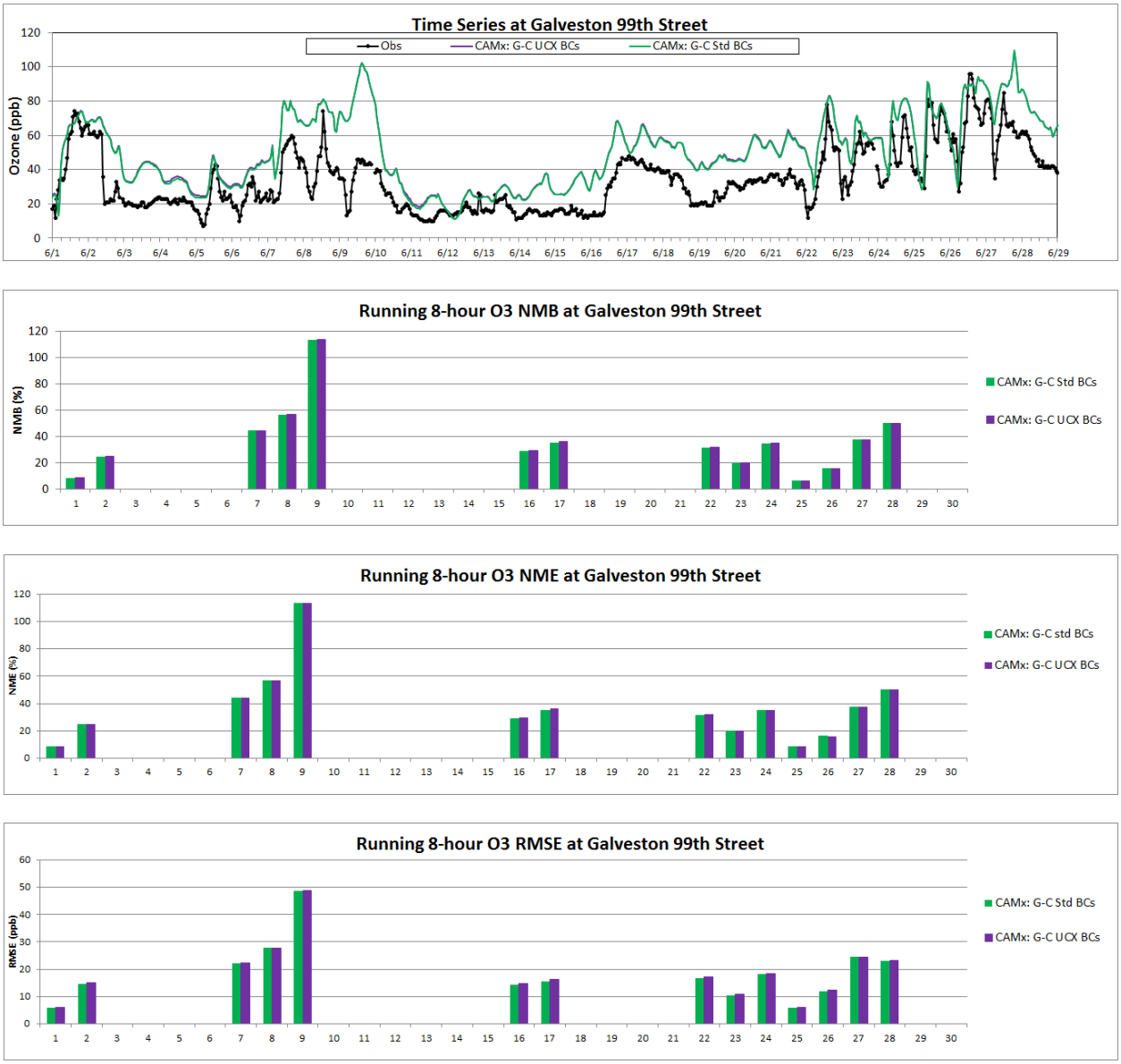

Figure 4-4. Upper panel: observed 1-hour ozone (black) at the Galveston 99th St. (CAMS 1034) monitor versus modeled 1-hour average surface layer ozone during the June 1-30, 2012 period for the G-C Std BC CAMx run (green) and G-C UCX BC CAMx Run (purple). 2nd panel from top: normalized mean bias (NMB) for 8-hour average ozone. 3rd panel from top: normalized mean error (NME) for 8-hour average ozone. 4th panel from top: root mean square error (RMSE) for 8-hour average ozone.

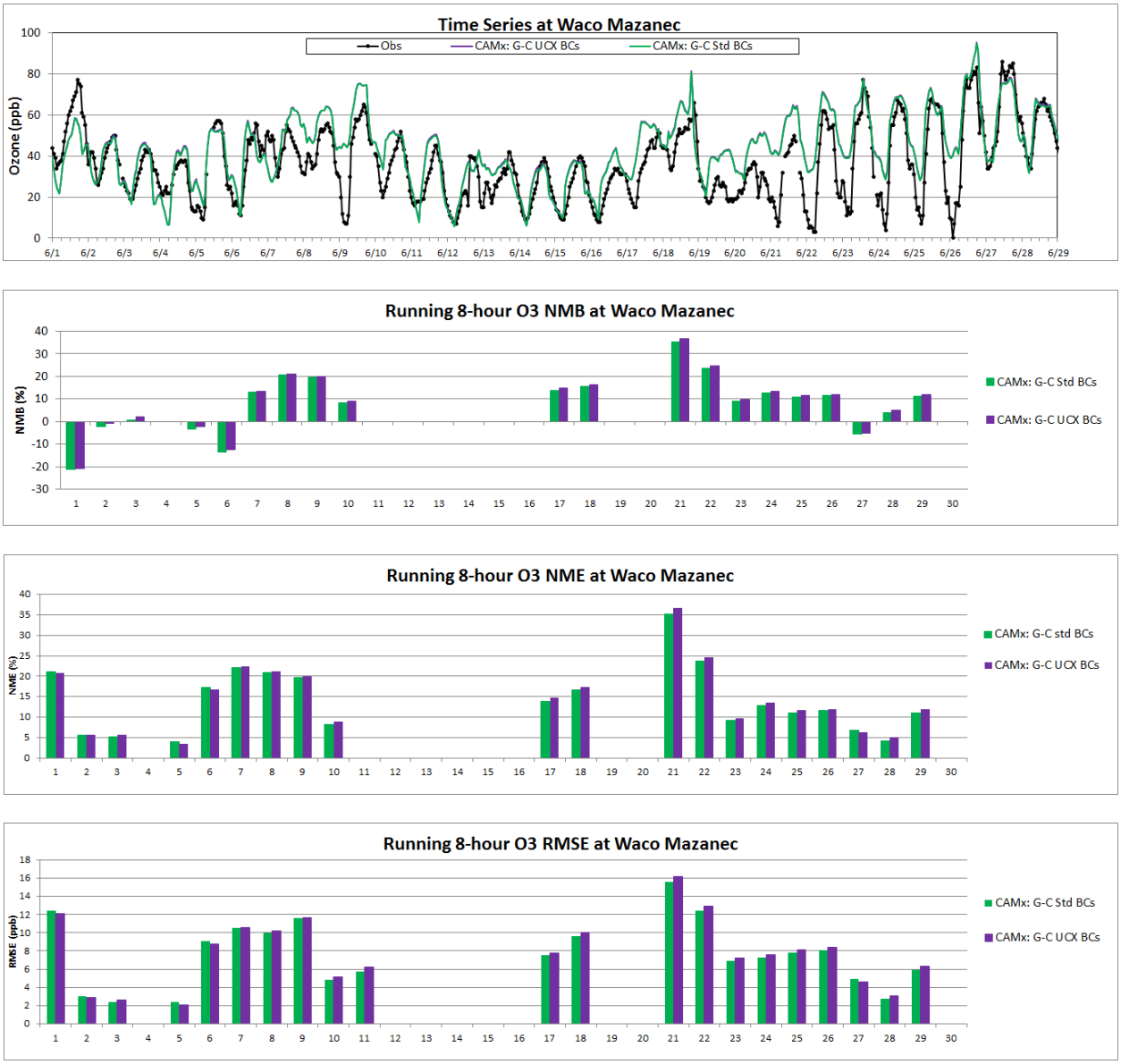

Figure 4-5. Upper panel: observed 1-hour ozone (black) at the Waco Mazanec (CAMS 1037) monitor versus modeled 1-hour average surface layer ozone during the June 1-30, 2012 period for the G-C Std BC CAMx run (green) and G-C UCX BC CAMx Run (purple). 2nd panel from top: normalized mean bias (NMB) for 8-hour average ozone. 3rd panel from top: normalized mean error (NME) for 8-hour average ozone. 4th panel from top: root mean square error (RMSE) for 8-hour average ozone.

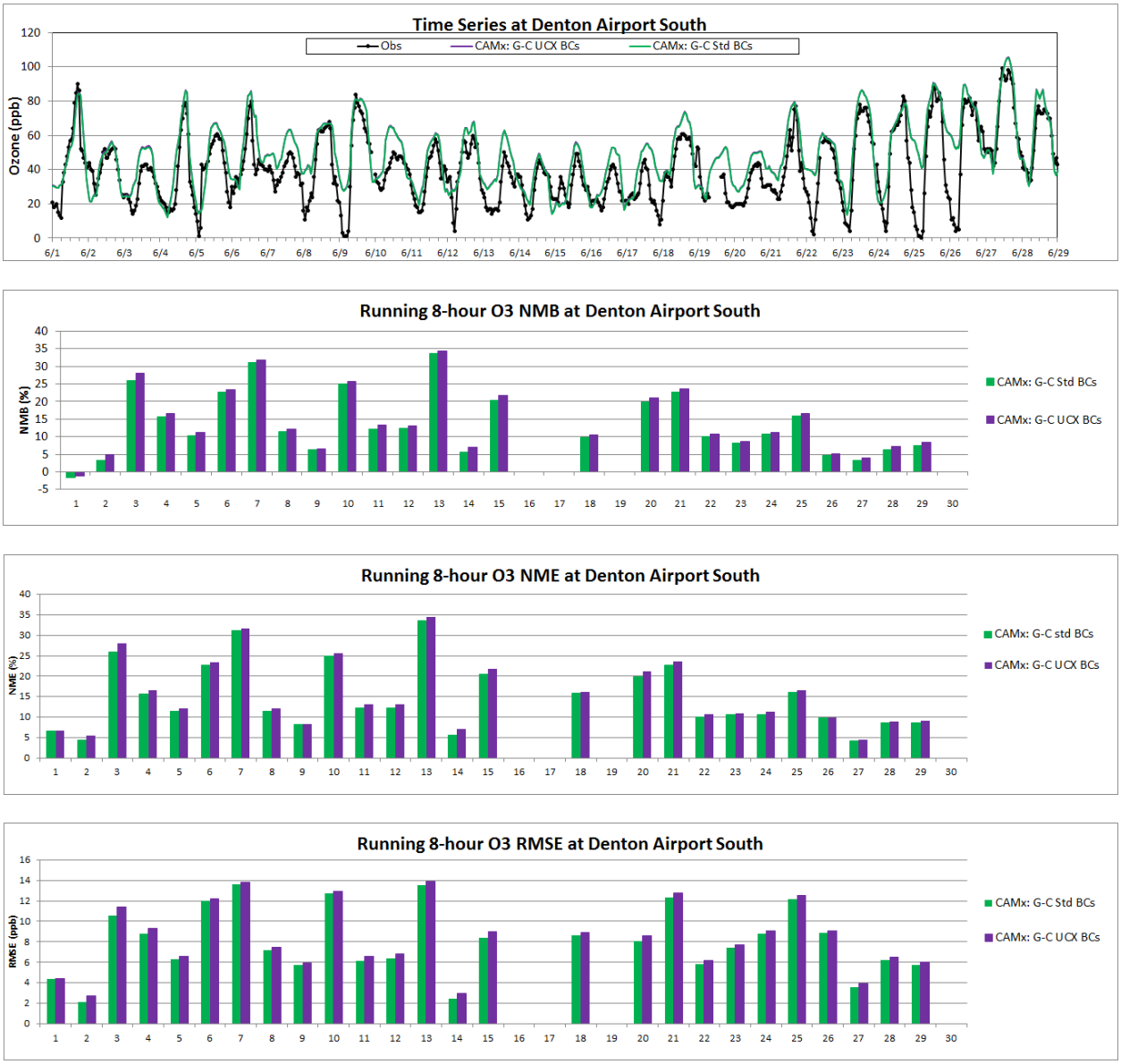

Figure 4-6. Upper panel: observed 1-hour ozone (black) at the Denton Airport South (CAMS 56) monitor versus modeled 1-hour average surface layer ozone during the June 1-30, 2012 period for the G-C Std BC CAMx run (green) and G-C UCX BC CAMx Run (purple). 2nd panel from top: normalized mean bias (NMB) for 8-hour average ozone. 3rd panel from top: normalized mean error (NME) for 8-hour average ozone. 4th panel from top: root mean square error (RMSE) for 8-hour average ozone.

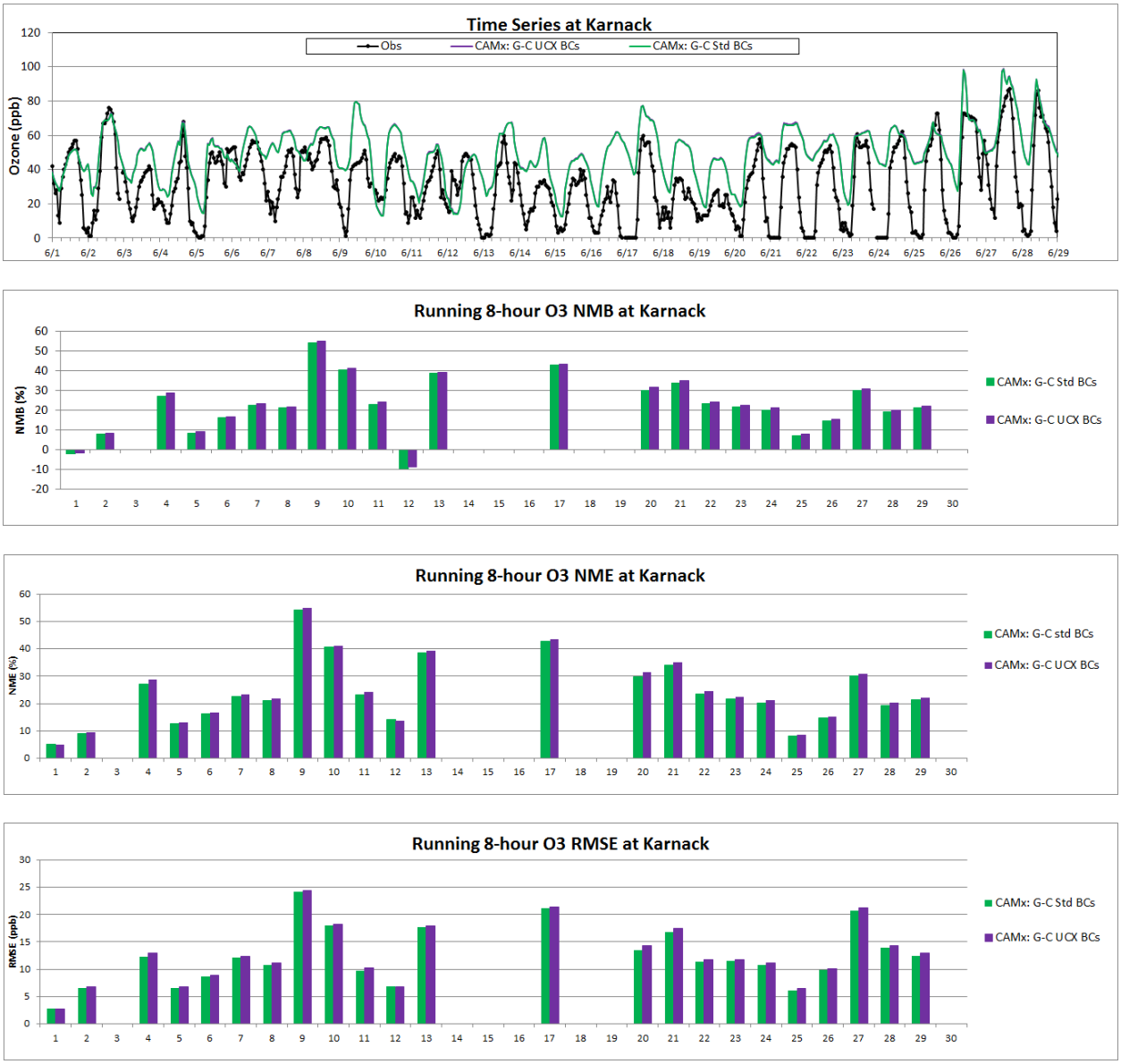

Figure 4-7. Upper panel: observed 1-hour ozone (black) at the Karnack (CAMS 85) monitor versus modeled 1-hour average surface layer ozone during the June 1-30, 2012 period for the G-C Std BC CAMx run (green) and G-C UCX BC CAMx Run (purple). 2nd panel from top: normalized mean bias (NMB) for 8-hour average ozone. 3rd panel from top: normalized mean error (NME) for 8-hour average ozone. 4th panel from top: root mean square error (RMSE) for 8-hour average ozone.

4.1.2 Evaluation on 36 km Grid

In Figure 4-8 through Figure 4-22, we summarize the surface model performance evaluation on the continental-scale 36 km grid. Figure 4-8 through Figure 4-21 show observed and modeled 1-hour ozone time series for a subset of sites shown in the right panel of Figure 4-1. Figure 4-22 shows the episode average MNB for 8-hour ozone for the June 1-30, 2012 period. Both runs have a pronounced high bias over the eastern U.S. and minimal or low bias over the western U.S. The tendency of ozone models to overestimate ozone in the southeastern U.S. and Ohio River Valley has been noted previously in TCEQ's CAMx modeling (e.g. ENVIRON, 2010, 2011) as well as by other groups using other regional air quality models (e.g. Herwehe et al., 2011). Because the episode average differences between the two CAMx runs are small for most sites, we focus on time series of observed ground layer ozone and modeled surface layer ozone for both runs.

The results of the time series comparison are summarized below:

- Sites that are in the eastern U.S. (Abington, CT) and/or are at relatively low elevation (Ann Arbor, MN) tended to have smaller and less frequent differences between the two CAMx model runs. Sites that are at higher elevation or are otherwise influenced by the presence of nearby high terrain showed more frequent and larger differences between the runs.

- At the Texas CASTNET sites, Big Bend (Figure 4-11), Alabama-Coushatta (Figure 4-10) and Palo Duro (Figure 4-12), differences between the two runs were small.

- Where differences were apparent between the CAMx runs with GEOS-Chem top boundary conditions, the G-C UCX CAMx run generally had higher ozone than the G-C Std CAMx run.

- Sites at higher elevations (Figure 4-14, Figure 4-15, and Figure 4-16) tended to have larger differences between the runs, while eastern sites (Figure 4-21, Figure 4-21) and sites in the Midwest (Figure 4-18) and Southeast (Figure 4-19) tended to have smaller differences between the CAMx runs.

- Where the two CAMx runs had a positive bias, agreement with observations was generally better for the CAMx G-C Std run than the CAMx G-C UCX run because the CAMx UCX run generally had slightly higher ozone. This is consistent with the 4 km grid evaluation. The NMB for 8-hour average ozone shows a similar pattern (Figure 4-22).

- Where the two CAMx runs had a negative bias, agreement with observations was generally better for the CAMx G-C UCX run than the CAMx G-C Std run because the CAMx G-C UCX run generally had higher ozone. The NMB for 8-hour average ozone shows a similar pattern (Figure 4-22).

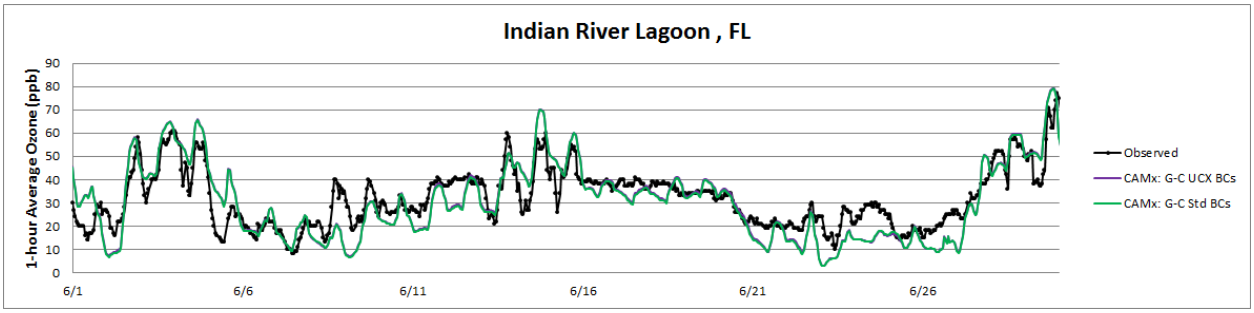

Figure 4-8. Indian River Lagoon, FL. Elevation 2 m.

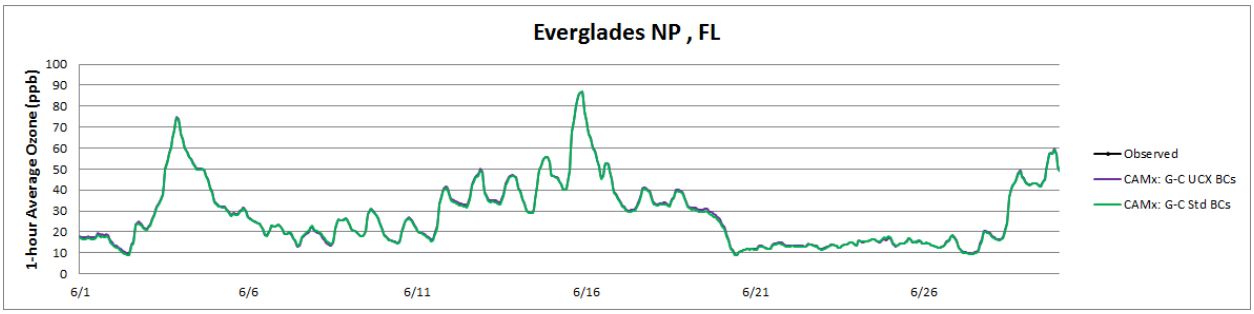

Figure 4-9. Everglades NP, FL. Elevation 2 m. (Note: no observations available).

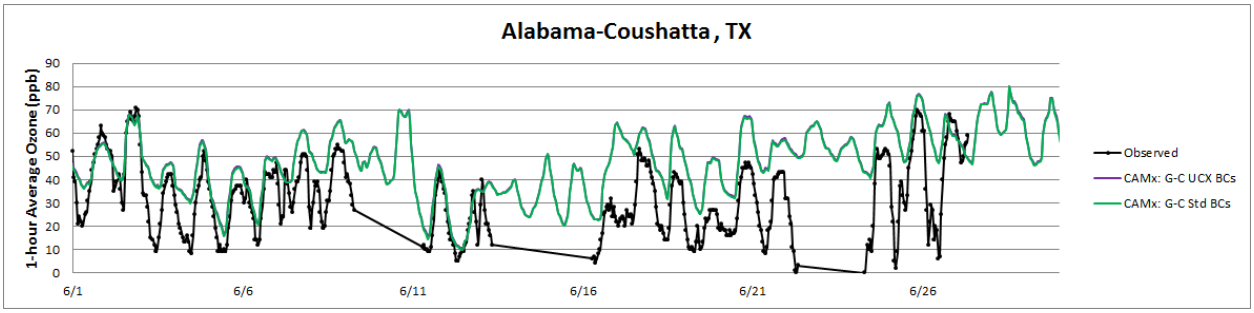

Figure 4-10. Alabama-Coushatta, TX. Elevation 105 m.

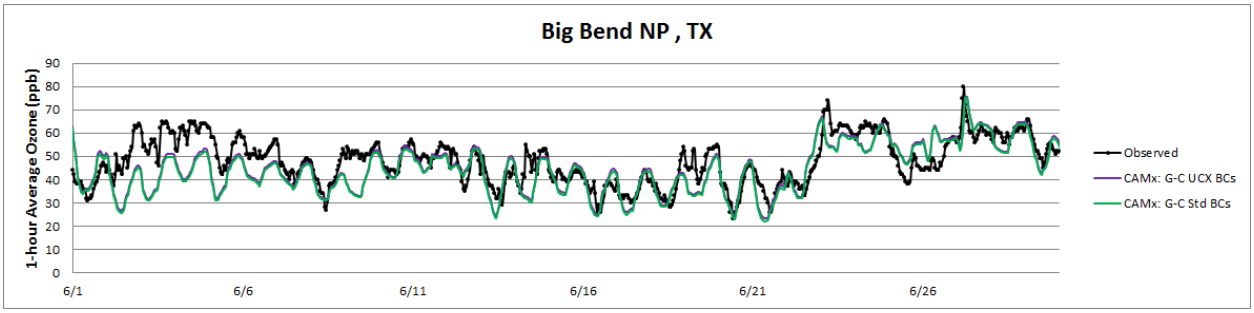

Figure 4-11. Big Bend NP, TX. Elevation 1,052 m.

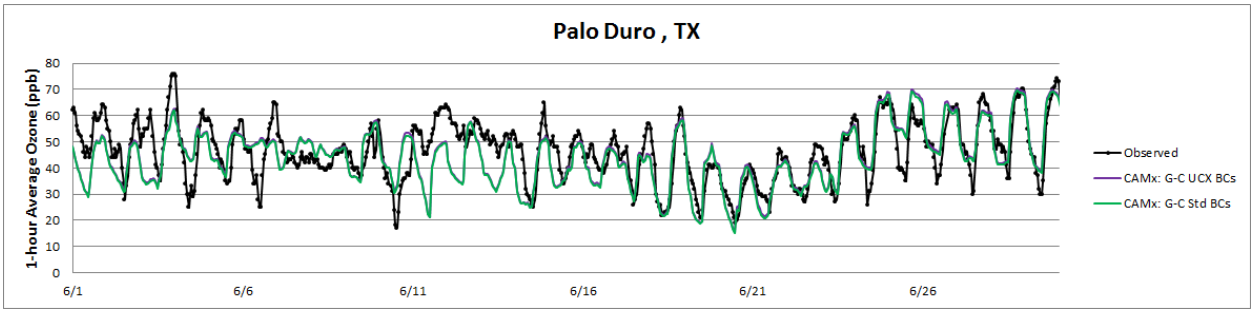

Figure 4-12. Palo Duro, TX. Elevation 1,053 m.

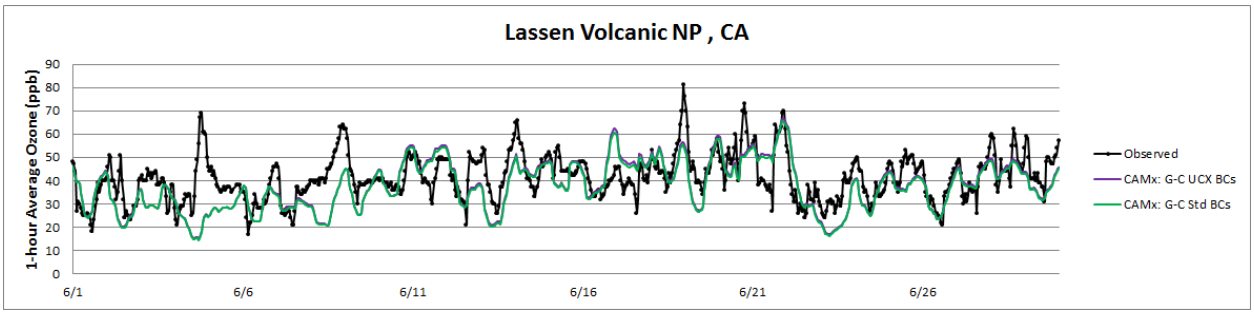

Figure 4-13. Lassen Volcanic NP, CA. Elevation 1,756 m.

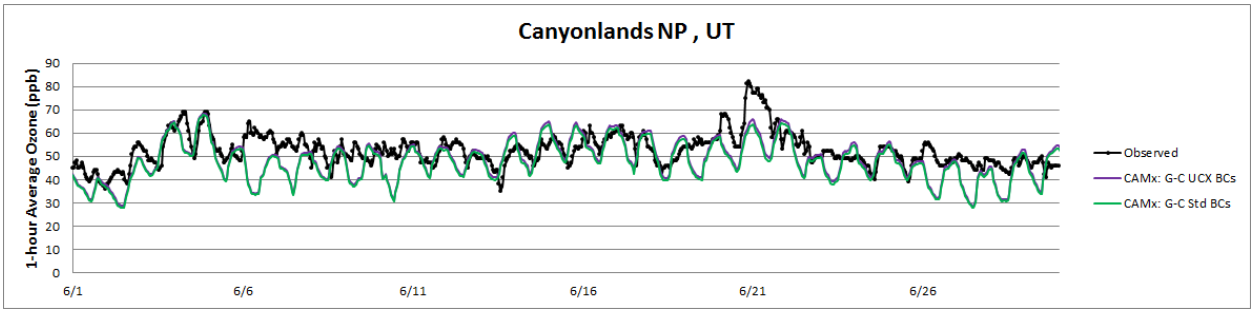

Figure 4-14. Canyonlands NP, UT. Elevation 1,809 m.

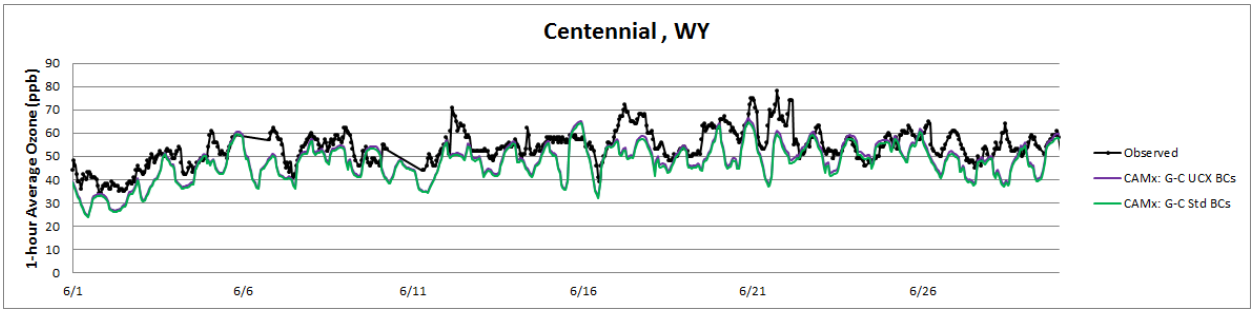

Figure 4-15. Centennial, WY. Elevation 3,175 m.

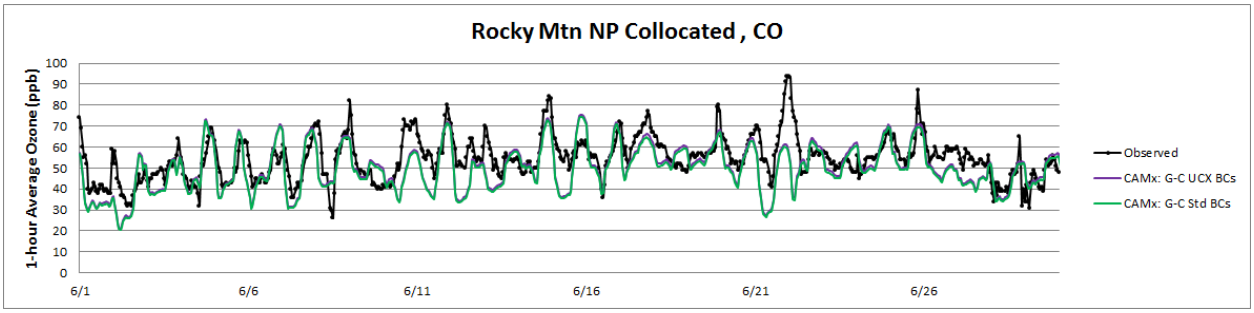

Figure 4-16. Rocky Mountain National Park, Collocated. Elevation 2,742 m.

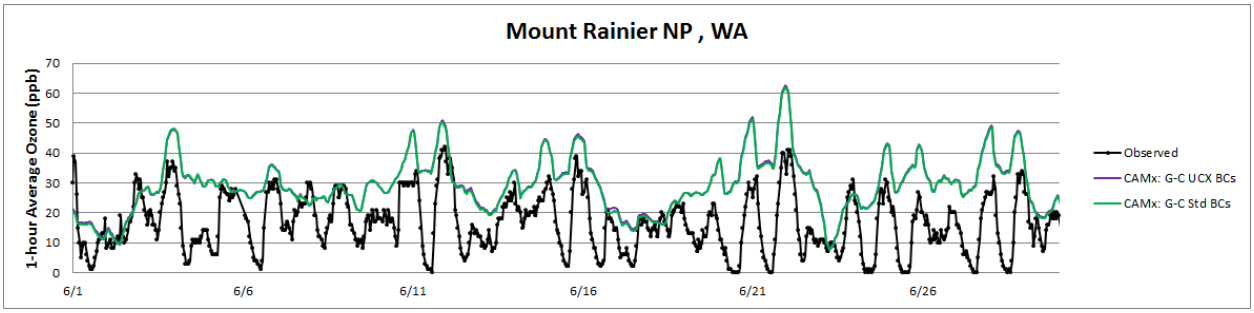

Figure 4-17. Mount Rainier, WA. Elevation 415 m.

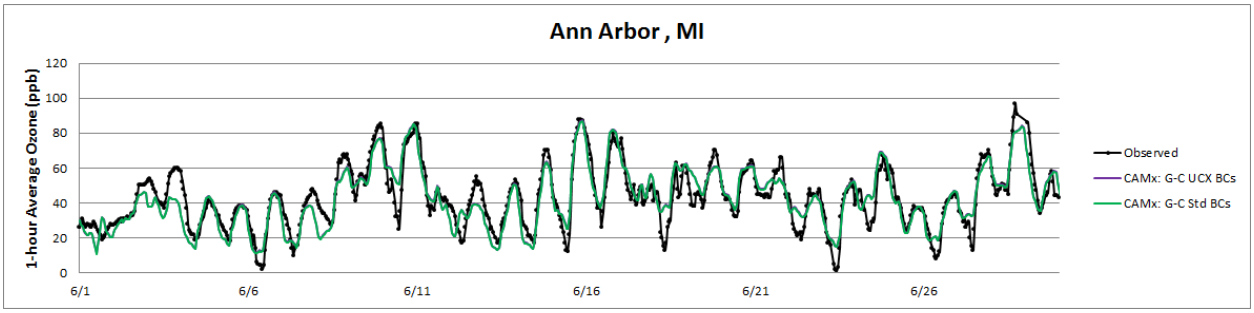

Figure 4-18. Ann Arbor, MI. Elevation 266 m.

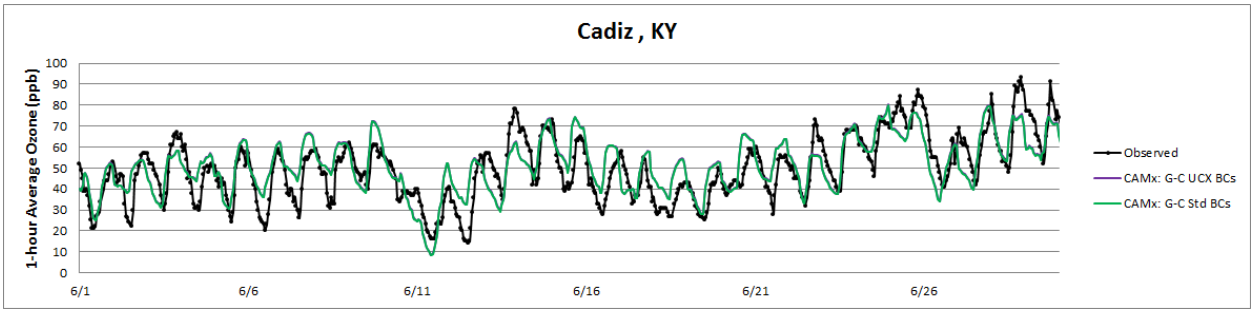

Figure 4-19. Cadiz, KY. Elevation 190 m.

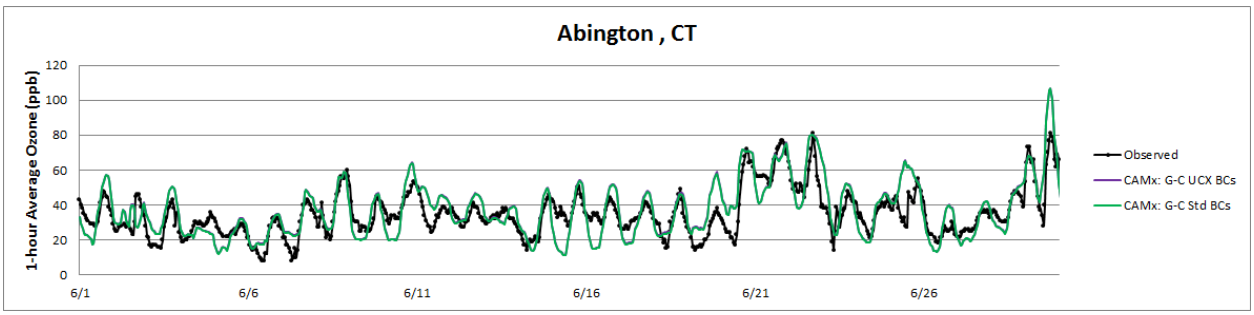

Figure 4-20. Abington, CT. Elevation 202 m.

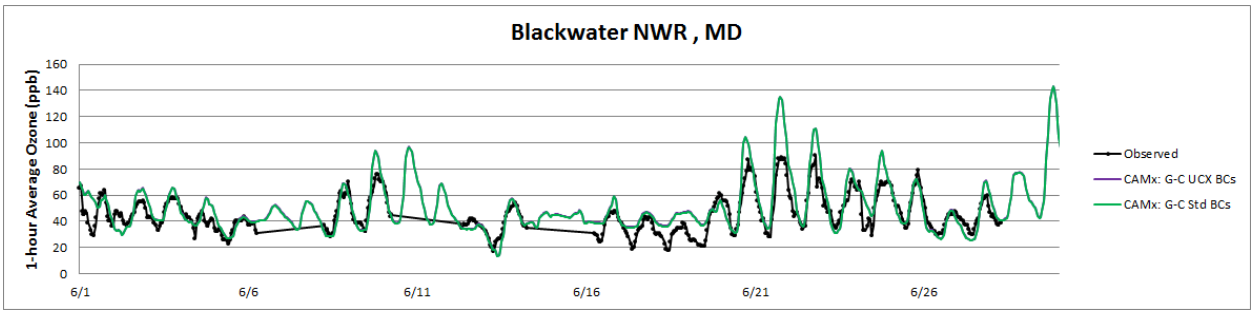

Figure 4-21. Blackwater NWR, MD. Elevation 1 m.

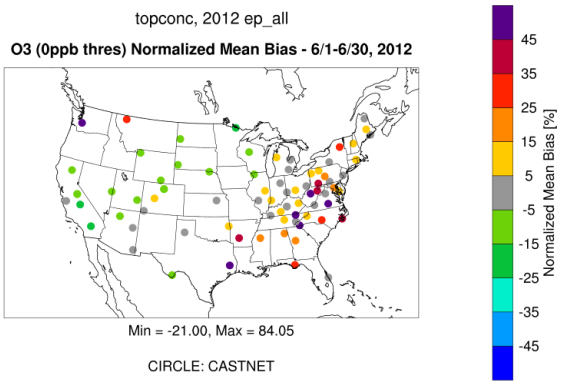
topconc, 2012 ep_all
O3 (0ppb thres) Normalized Mean Bias - 6/1-6/30, 2012
Min = -21.00, Max = 84.05
CIRCLE: CASTNET

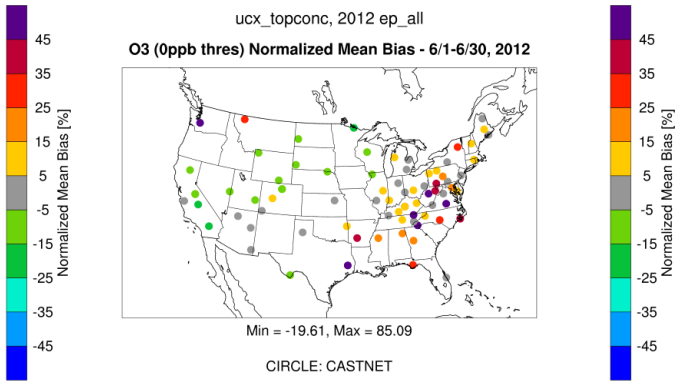
ucx_topconc, 2012 ep_all
O3 (0ppb thres) Normalized Mean Bias - 6/1-6/30, 2012
Min = -19.61, Max = 85.09
CIRCLE: CASTNET

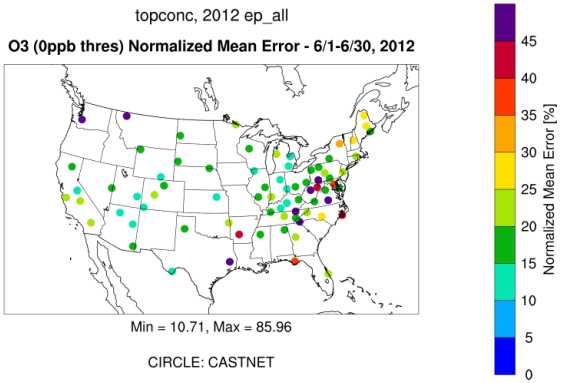
topconc, 2012 ep_all
O3 (0ppb thres) Normalized Mean Error - 6/1-6/30, 2012
Min = 10.71, Max = 85.96
CIRCLE: CASTNET

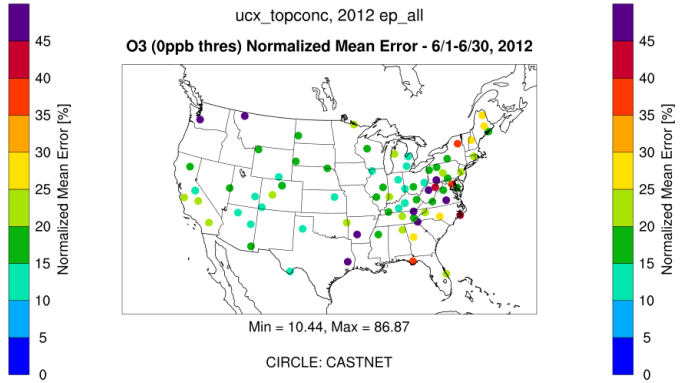
ucx_topconc, 2012 ep_all
O3 (0ppb thres) Normalized Mean Error - 6/1-6/30, 2012
Min = 10.44, Max = 86.87
CIRCLE: CASTNET

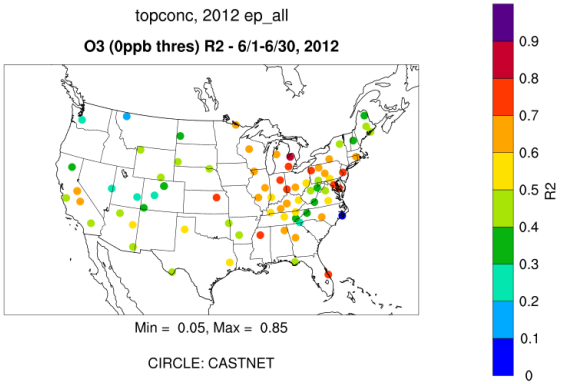
topconc, 2012 ep_all
O3 (0ppb thres) R2 - 6/1-6/30, 2012
Min = 0.05, Max = 0.85
CIRCLE: CASTNET

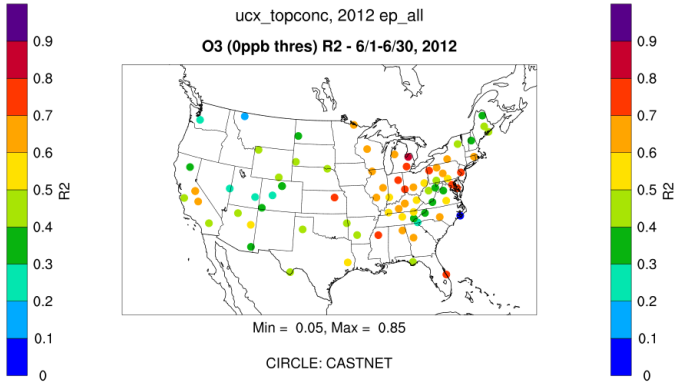
ucx_topconc, 2012 ep_all
O3 (0ppb thres) R2 - 6/1-6/30, 2012
Min = 0.05, Max = 0.85
CIRCLE: CASTNET

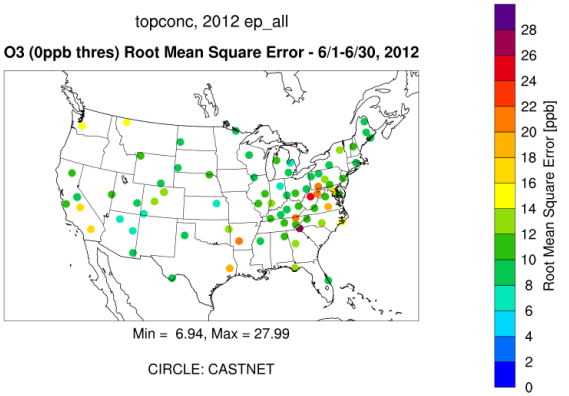
topconc, 2012 ep_all
O3 (0ppb thres) Root Mean Square Error - 6/1-6/30, 2012
Min = 6.94, Max = 27.99
CIRCLE: CASTNET

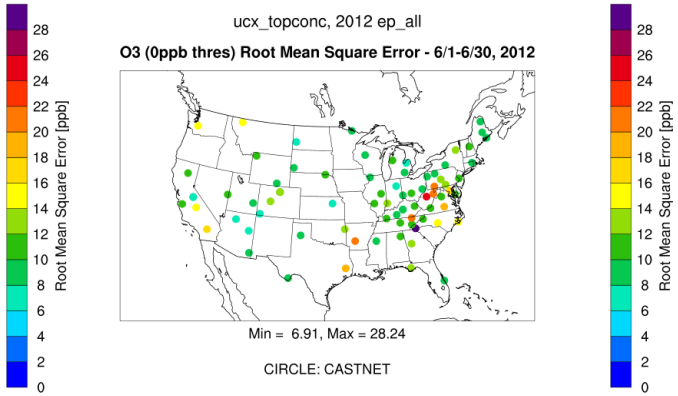
Root Mean Square Error [ppb]
0
2
4
6
8
10
12
14
16
18
20
22
24
26
28

ucx_topconc, 2012 ep_all
O3 (0ppb thres) Root Mean Square Error - 6/1-6/30, 2012
Min = 6.91, Max = 28.24
CIRCLE: CASTNET

Root Mean Square Error [ppb]
0
2
4
6
8
10
12
14
16
18
20
22
24
26
28

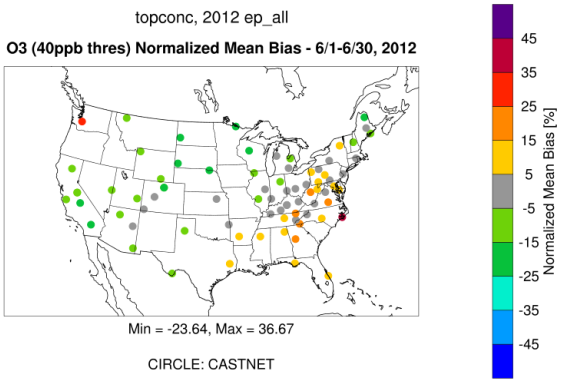
topconc, 2012 ep_all
O3 (40ppb thres) Normalized Mean Bias - 6/1-6/30, 2012
Min = -23.64, Max = 36.67
CIRCLE: CASTNET

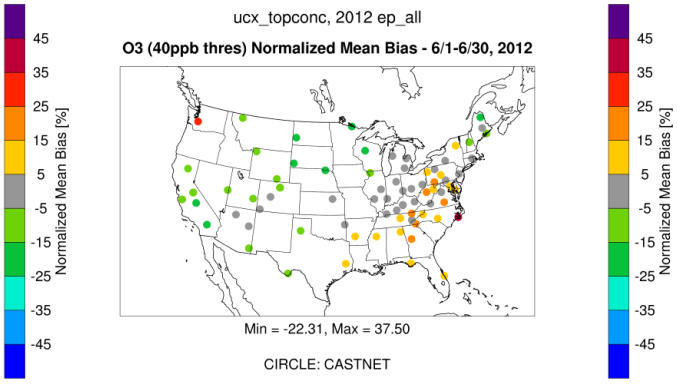
Normalized Mean Bias [%]
-45
-35
-25
-15
-5
5
15
25
35
45

ucx_topconc, 2012 ep_all
O3 (40ppb thres) Normalized Mean Bias - 6/1-6/30, 2012
Min = -22.31, Max = 37.50
CIRCLE: CASTNET

Normalized Mean Bias [%]
-45
-35
-25
-15
-5
5
15
25
35
45

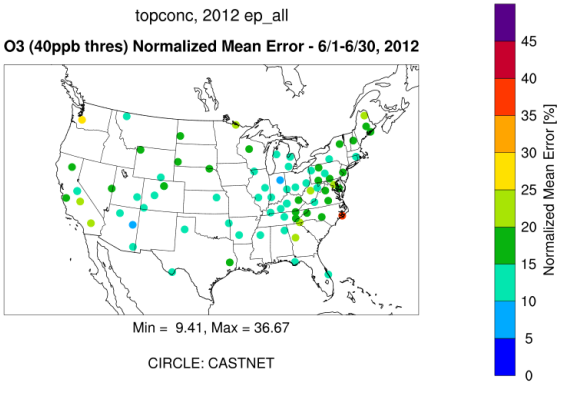
topconc, 2012 ep_all
O3 (40ppb thres) Normalized Mean Error - 6/1-6/30, 2012
Min = 9.41, Max = 36.67
CIRCLE: CASTNET

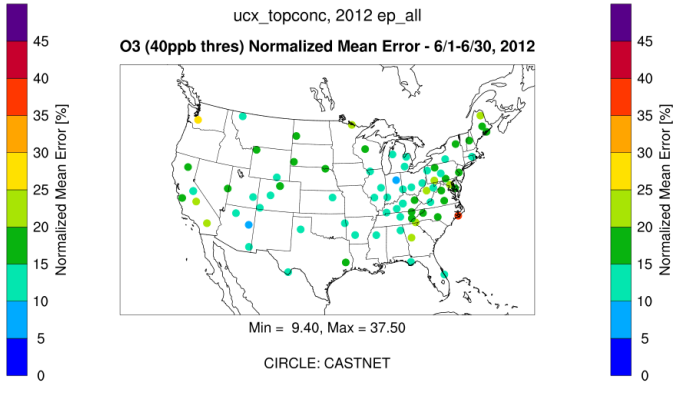
Normalized Mean Error [%]
0
5
10
15
20
25
30
35
40
45

ucx_topconc, 2012 ep_all
O3 (40ppb thres) Normalized Mean Error - 6/1-6/30, 2012
Min = 9.40, Max = 37.50
CIRCLE: CASTNET

Normalized Mean Error [%]
0
5
10
15
20
25
30
35
40
45

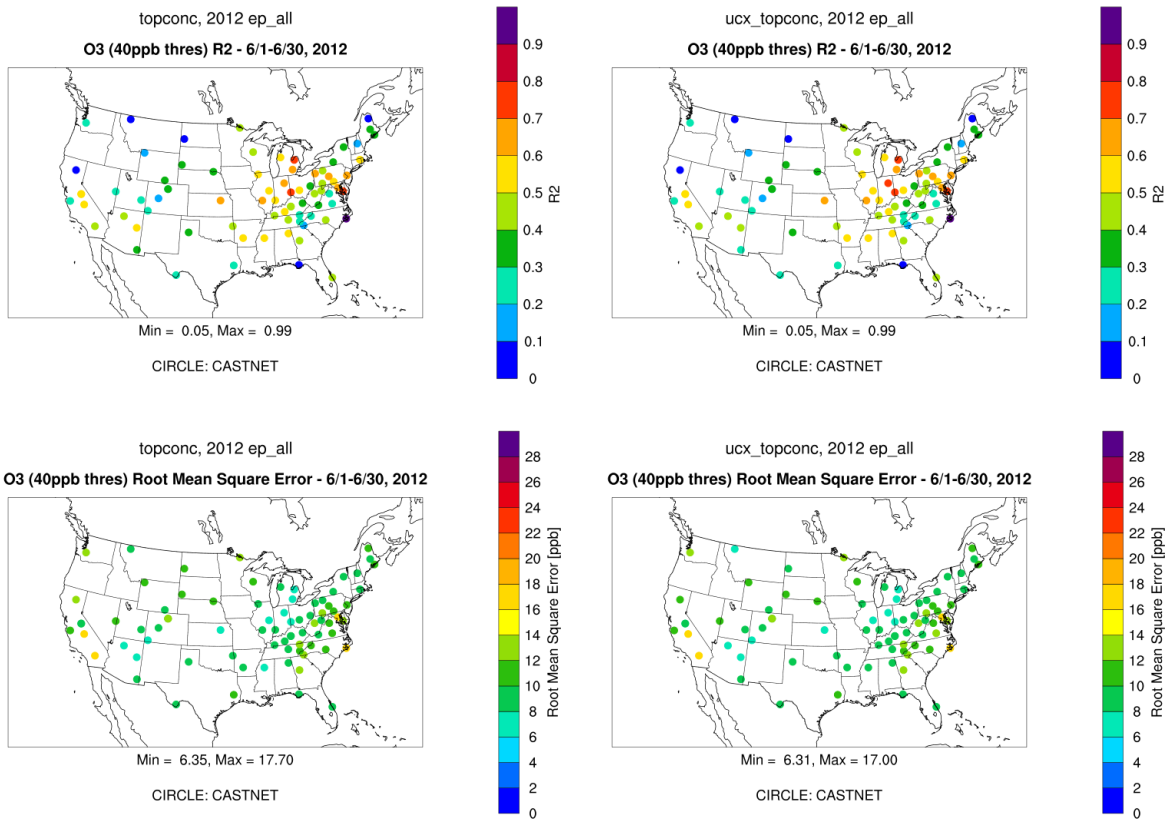

Figure 4-22. Ozone NMB (1st row), NME (2nd row), R^2 (3rd row), and RMSE (4th row) of G-C Std CAMx run (run2; 1st column), and G-C UCX CAMx run (2nd column) Evaluation performed with respect to 8-hour average ozone at CASTNET sites for the period of 6/1 – 6/30, 2012. Comparison was performed using a 40 ppb threshold in the observed ozone.

4.2 Aloft Performance Evaluation

We evaluated the effect of the use the two different GEOS-Chem top boundary conditions on CAMx ozone and NOy above the surface layer through comparison with aircraft and ozonesonde data.

4.2.1 Aloft Performance Evaluation for Ozone

We compared ozonesonde observations, paired in time and space, against the GEOS-Chem standard and UCX runs and the two CAMx simulations that used boundary conditions extracted from the GOES-Chem runs. For the aloft ozone evaluation of both GEOS-Chem and CAMx in the 2012 episode, we used weekly ozonesonde vertical profile data collected by the NOAA Climate Monitoring and Diagnostics Laboratory (CMDL) at sites in Huntsville, Alabama and Boulder Colorado from May 5 to June 30, 2012, the time period of interest for the Deep Convective Clouds and Chemistry Project (DC3) 2012 project[21] (Figure 4-23). Weekly ozonesonde profiles for Trinidad Head, CA are available from NOAA's Earth System Research Laboratory Global Monitoring Division[22] (Figure 4-23) for June 2012. We also used ozonesonde data for Idabel, OK, Beaumont, TX and Houston, TX collected by Valparaiso University and the University of Houston as part of the Tropospheric Ozone Pollution Project[23]. These six ozonesonde stations cover a range of elevations and regions of the U.S. The Boulder site has the highest elevation, at 1,743 m above sea level, while Trinidad Head is located on the west coast at 20 m elevation. Huntsville is located inland in the southeast at an elevation of 196 m and the Houston and Beaumont launch sites are in near-coastal locations.

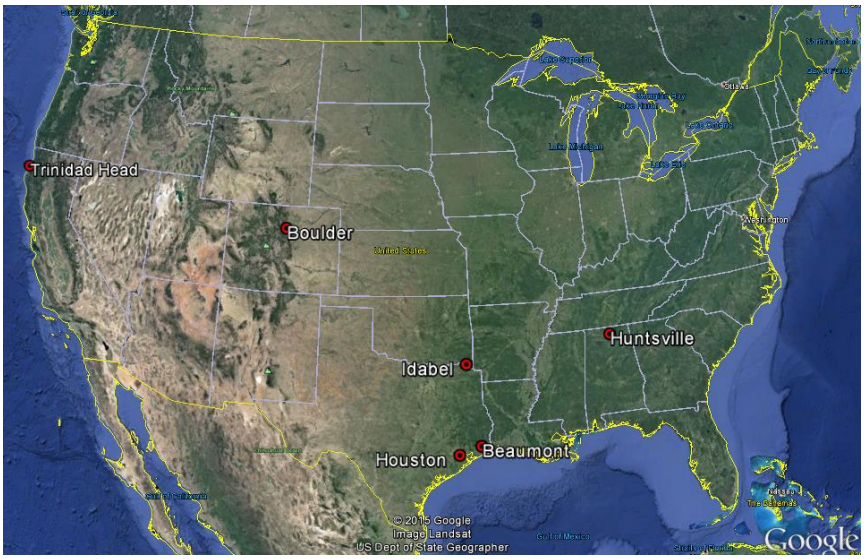

Figure 4-23. Location of ozonesonde launch sites.

[21] Data provided by NCAR/EOL under sponsorship of the National Science Foundation. http://data.eol.ucar.edu/
[22] http://www.esrl.noaa.gov/gmd/ozwv/ozsondes/
[23] http://physics.valpo.edu/ozone/

We evaluated the standard and UCX versions of GEOS-Chem against ozonesonde data from the stations shown in Figure 4-23. The ozonesondes typically reported data from near the surface up to about 30 km. We show episode average soundings for all sites in Figure 4-24 through Figure 4-26. Individual soundings were very similar to the episode averages and are not reproduced here. The ozone profiles from the two GEOS-Chem runs agree closely with one another in the troposphere. The UCX versions of GEOS-Chem tended to have slightly more ozone in the troposphere than the standard version (see Figure 4-27), but this difference is not apparent at the scale in Figure 4-24 through Figure 4-26 which was set to show differences in the lower stratosphere. Both the standard and UCX versions of GEOS-Chem have a high bias above 15 km relative to the observed profile. The UCX profile is closer to the observed profile that the standard GEOS-Chem profile at all sites in the episode averages as well as the individual soundings (not shown).

The ozonesonde comparison indicates that the UCX version of GEOS-Chem provides a simulation of lower stratospheric ozone that is closer to the observations for these sites during the June 2012 episode. We note that the observations used in this evaluation are sparse in both space and time and so must be interpreted with caution. The fact that the UCX run may not have been fully spun up by June 1, 2012 may also affect the results of the evaluation. Long-lived tracer species that can affect ozone loss may not yet have reached equilibrium, and it is possible that the UCX simulation could be brought closer to the observed ozone profiles by a full five-year spinup period.

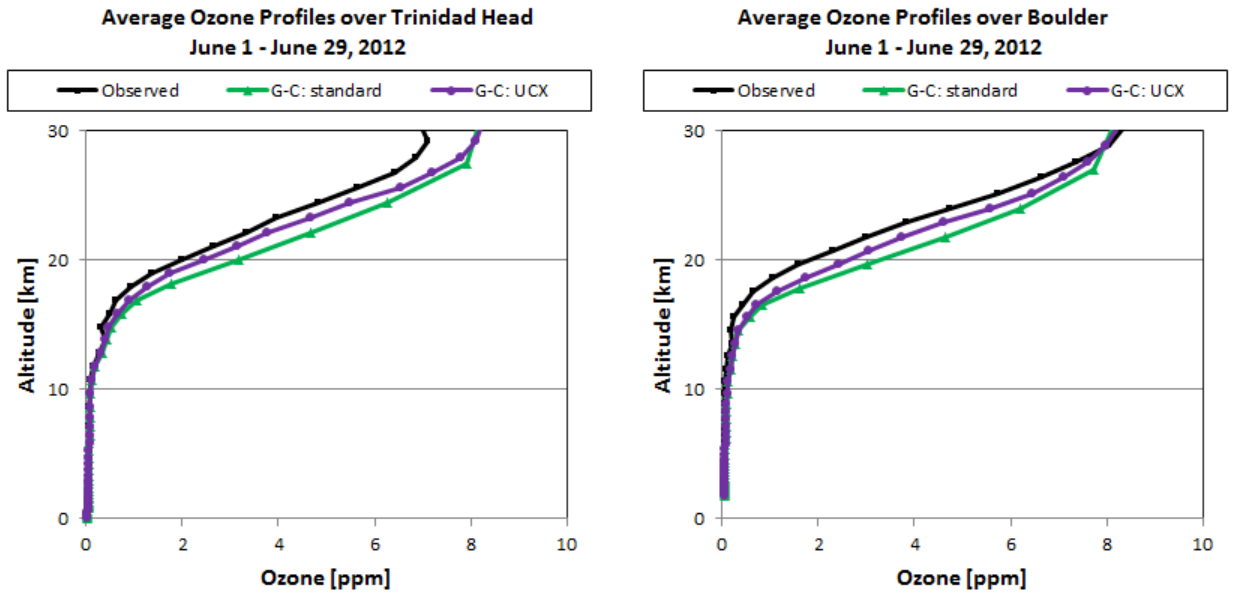

Figure 4-24. Comparison of GEOS-Chem run ozonesonde profiles for Trinidad Head, CA (left) and Boulder, CO (right).

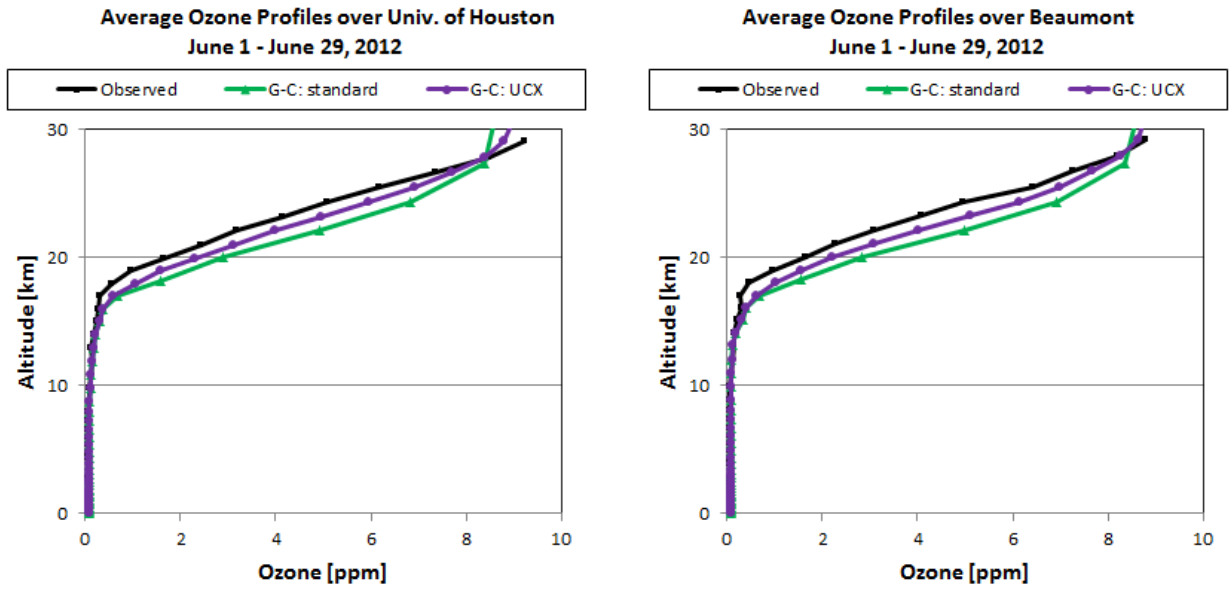

Figure 4-25. Comparison of GEOS-Chem run ozonesonde profiles for Houston, TX (left) and Beaumont, TX (right).

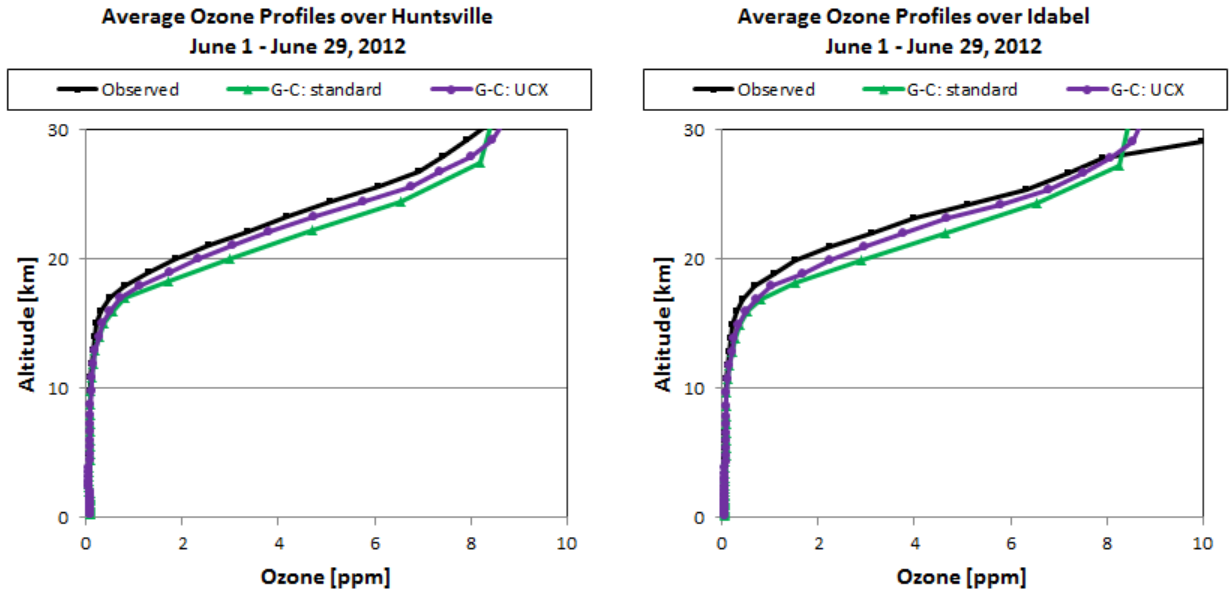

Figure 4-26. Comparison of GEOS-Chem run ozonesonde profiles for Huntsville, AL (left) and Idabel, OK (right).

In Figure 4-27, we focus on the tropospheric portion of the GEOS-Chem model run profiles at the Trinidad Head site. Trinidad Head is located on the California coast. In CAMx, the site is strongly influenced by the 36 km grid lateral boundary conditions, as air arriving at Trinidad Head has not passed over topography that would generate vertical motions. We compare the GEOS-Chem profiles at this site to examine GEOS-Chem concentrations at site close to the

CAMx western boundary. Figure 4-27 shows that the standard and UCX versions of GEOS-Chem have similar tropospheric ozone profiles at this site located downwind of the CAMx western boundary. The UCX version of GEOS-Chem has slightly higher ozone in UCX below 10 km. This is consistent with the slightly higher surface concentrations seen in CAMx when driven with the UCX version of GEOS-Chem compared to when CAMx is driven with the standard version of GEOS-Chem.

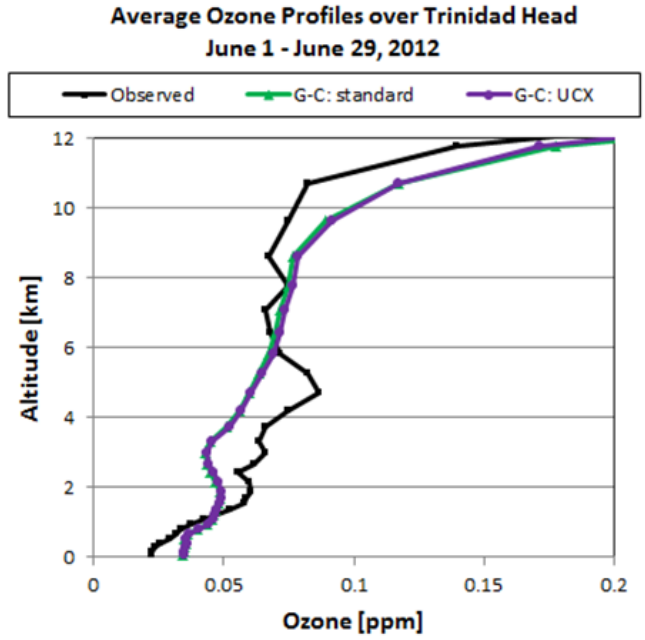

Figure 4-27. Comparison of tropospheric GEOS-Chem run ozonesonde profiles for Trinidad Head, CA. This figure displays the same data as the left panel of Figure 4-24, but is shown on a different scale to show the tropospheric portion of the profiles.

Modeled and observed vertical ozone profiles in the troposphere and stratosphere are compared in Figure 4-28 through Figure 4-33 for the CAMx runs using the standard and UCX GEOS-Chem boundary conditions. The results of the comparison are summarized below.

- For all sites, the two CAMx runs agree well below 6 km, but begin to diverge above 6 km due to the influence of their different model top boundary conditions.
- Both CAMx runs have a high bias for ozone in the upper troposphere/lower stratosphere. This is consistent with the high bias for ozone noted in the GEOS-Chem runs (Figure 4-24 through Figure 4-26)
- The high bias for upper troposphere/lower stratosphere ozone is slightly smaller in the CAMx run using GEOS-Chem UCX boundary conditions and this is consistent with the smaller bias for upper troposphere/lower stratosphere ozone in the GEOS-Chem UCX run compared to the standard version of GEOS-Chem.

- Consistent with the results of the surface model performance evaluation, the, ozonesonde profile shows that CAMx using GEOS-Chem UCX boundary condition has higher ozone below 6 km than CAMx using the standard GEOS-Chem boundary condition in the lower and middle troposphere.

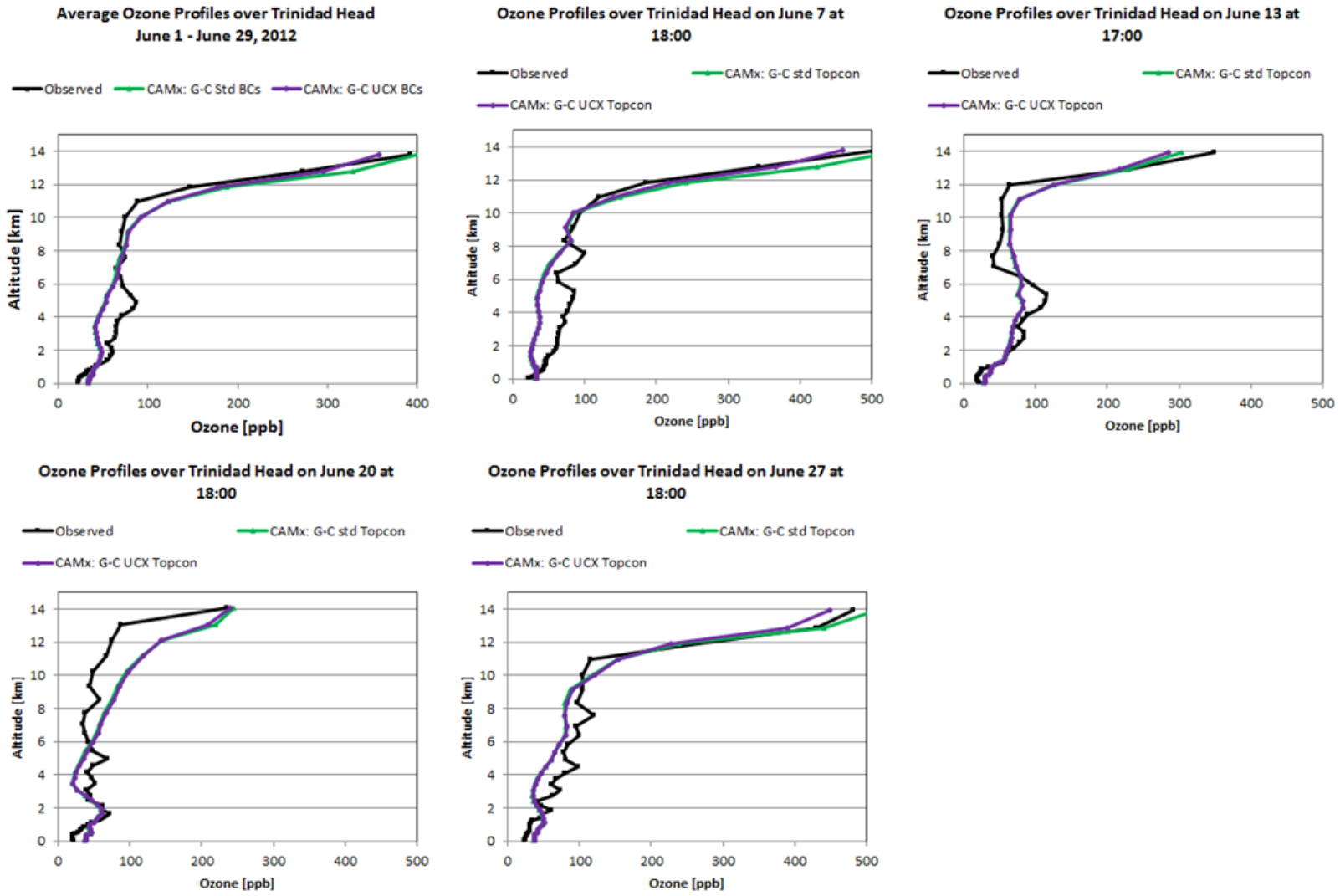

Figure 4-28. CAMx and observed ozonesonde profiles for Trinidad Head, CA.

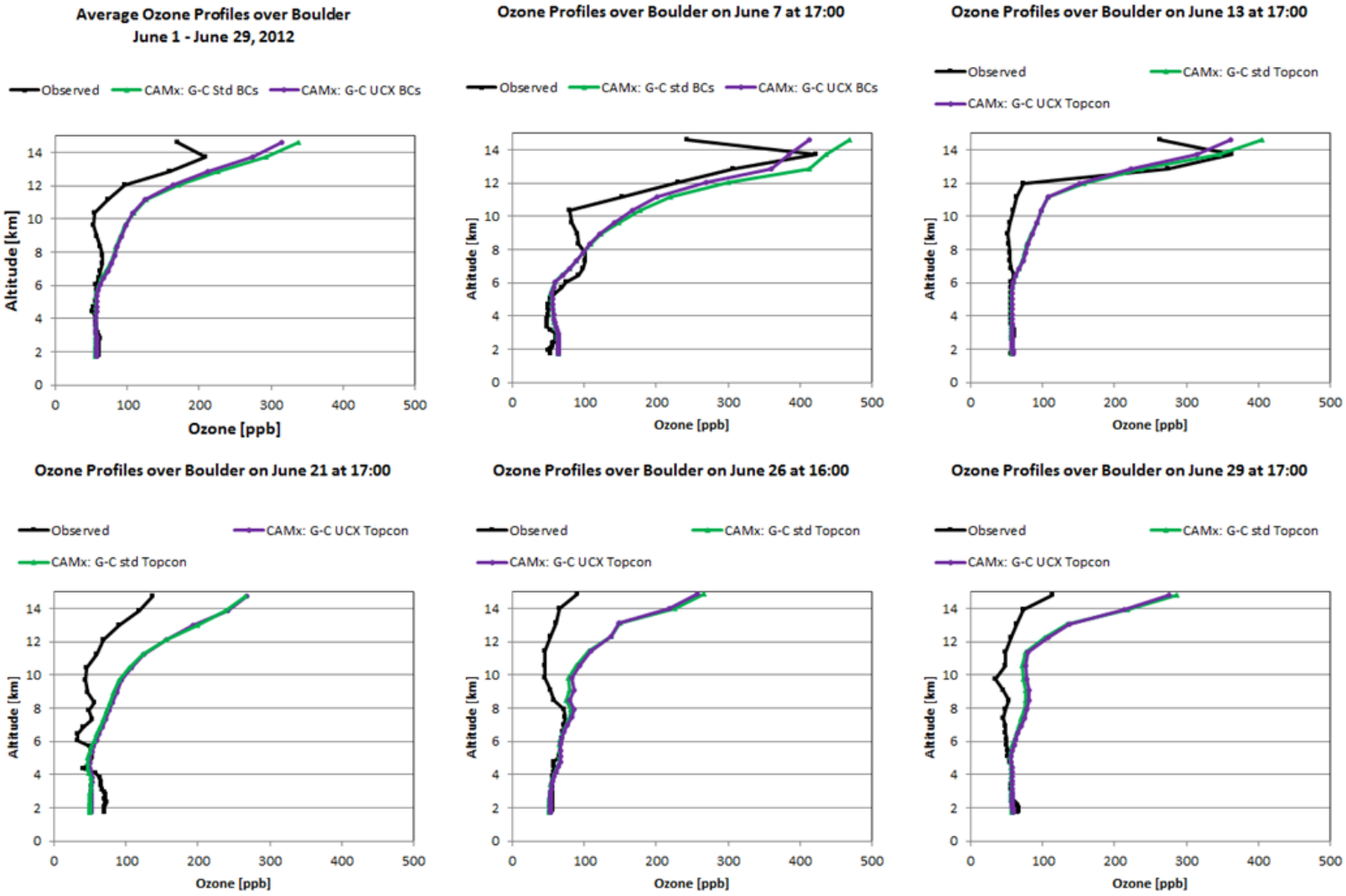

Figure 4-29. CAMx and observed ozonesonde profiles for Boulder, CO.

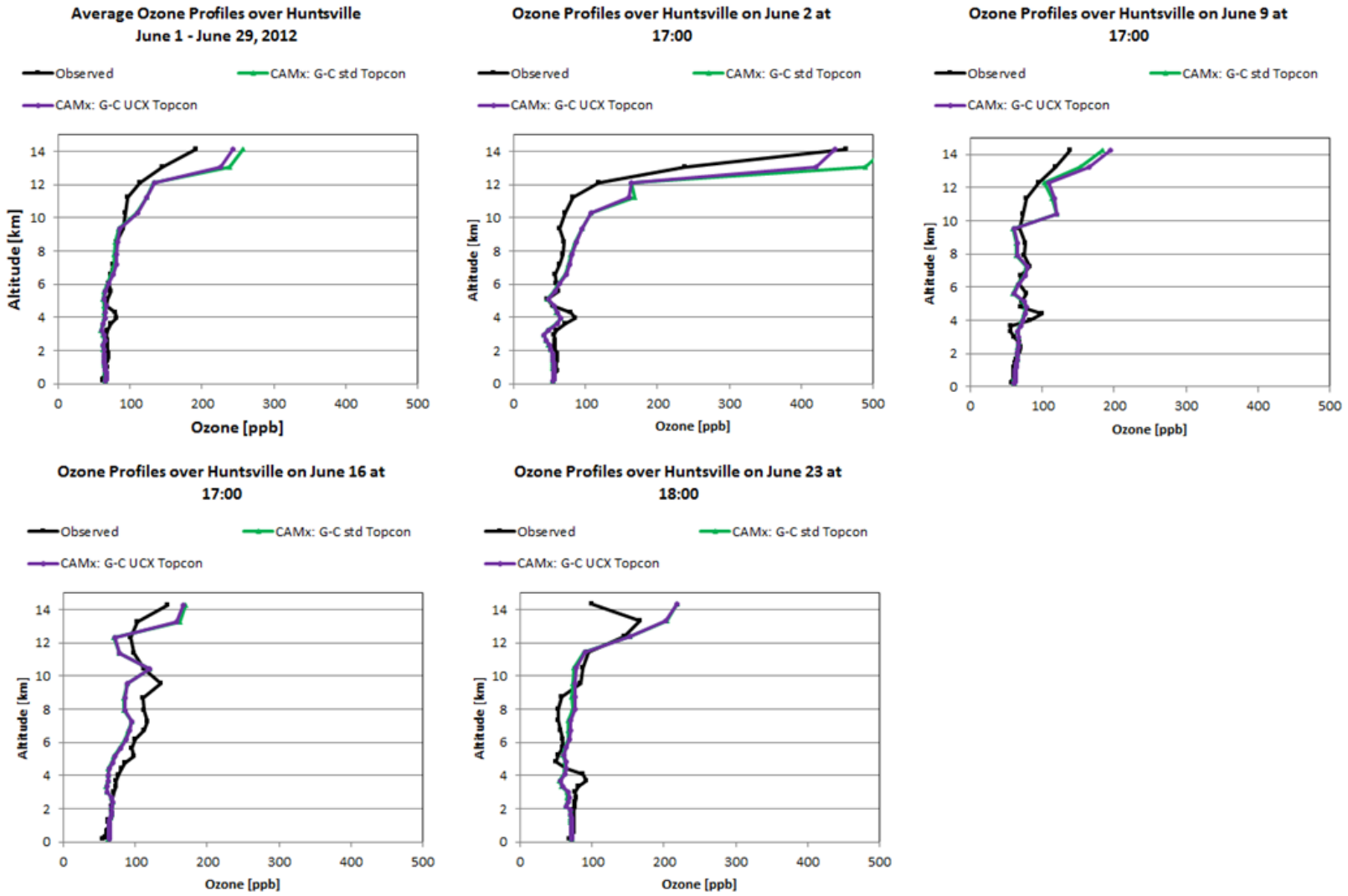

Figure 4-30. CAMx and observed ozonesonde profiles for Huntsville, AL.

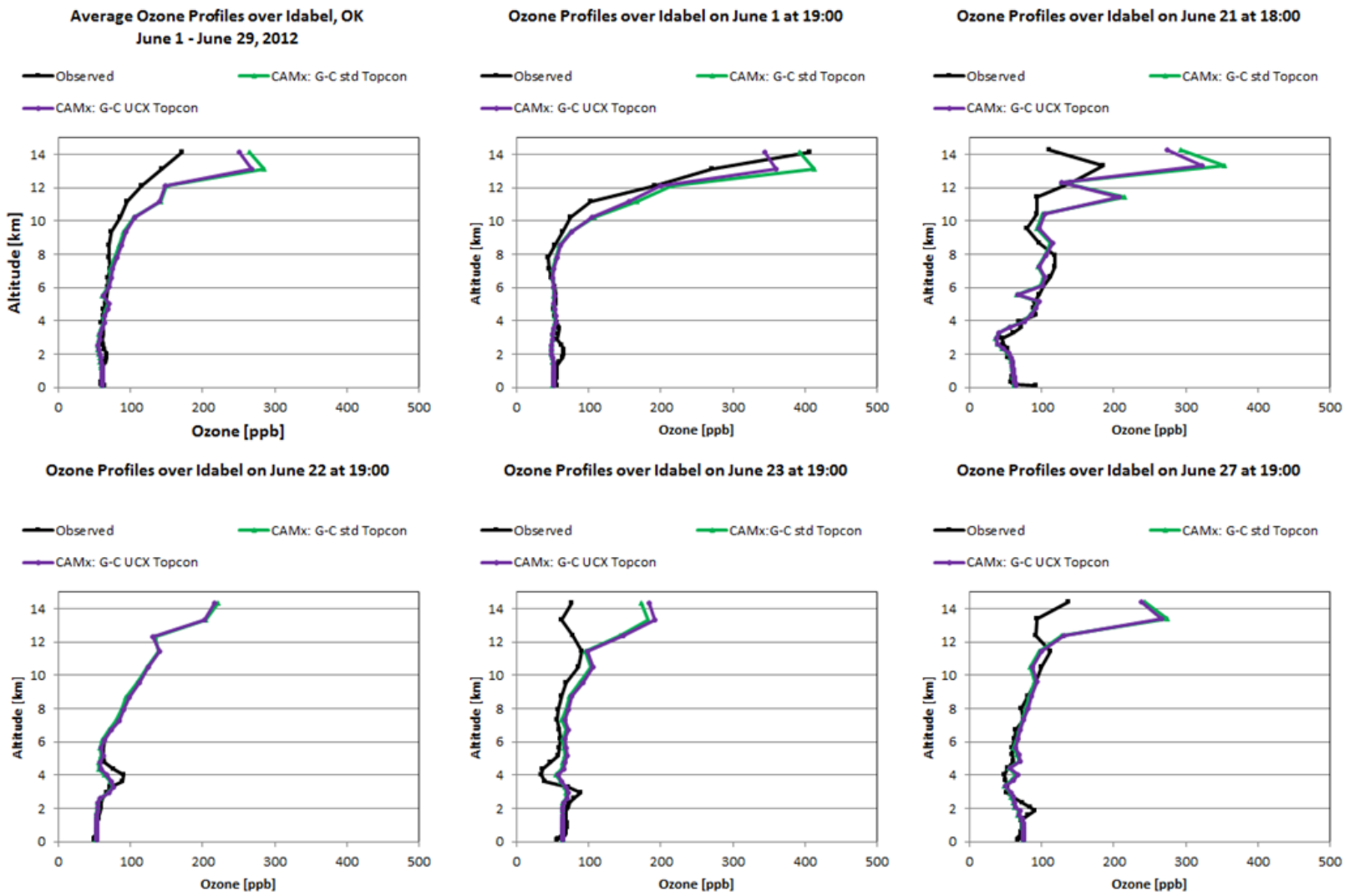

Figure 4-31. CAMx and observed ozonesonde profiles for Idabel, OK.

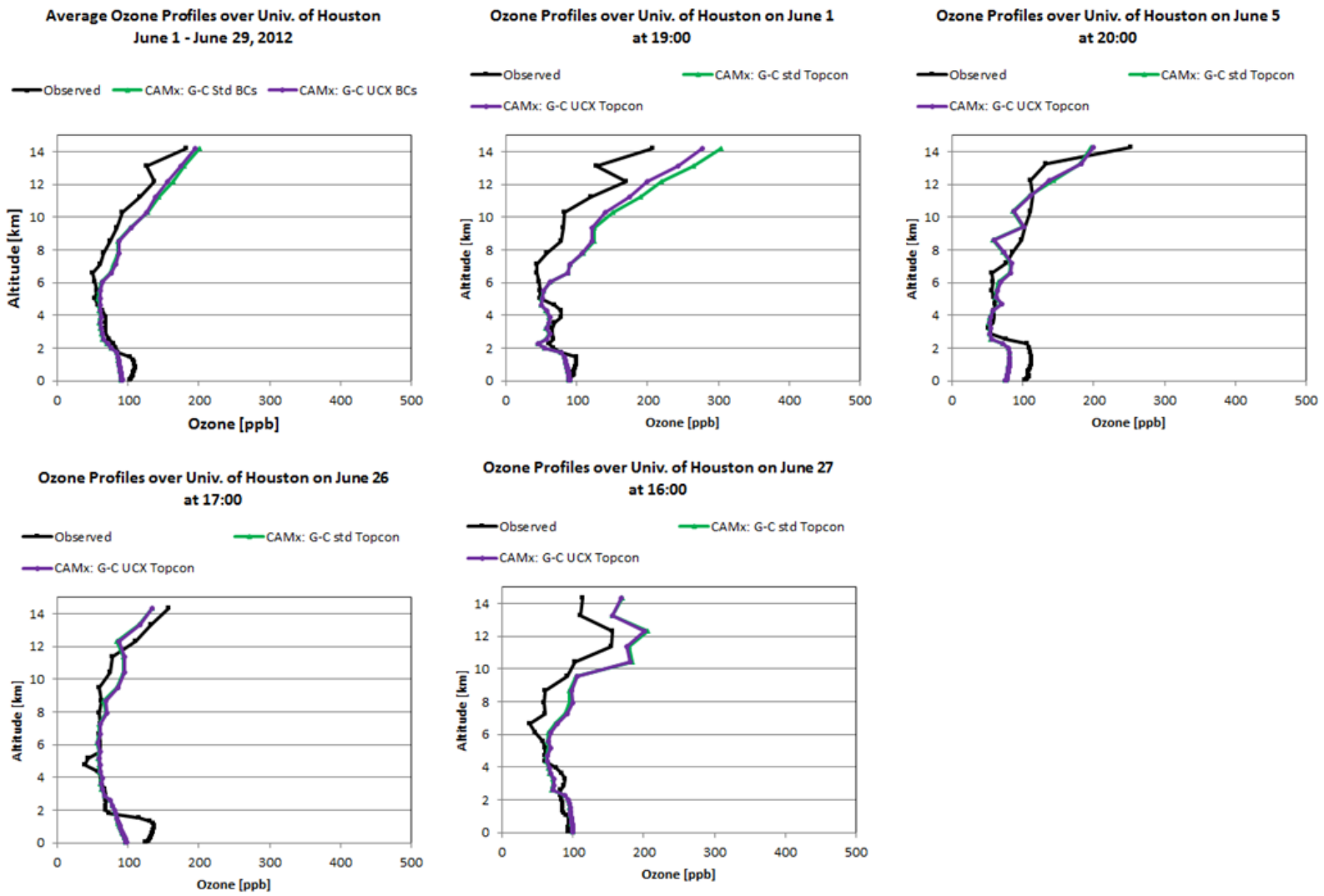

Figure 4-32. CAMx and observed ozonesonde profiles for Houston, TX.

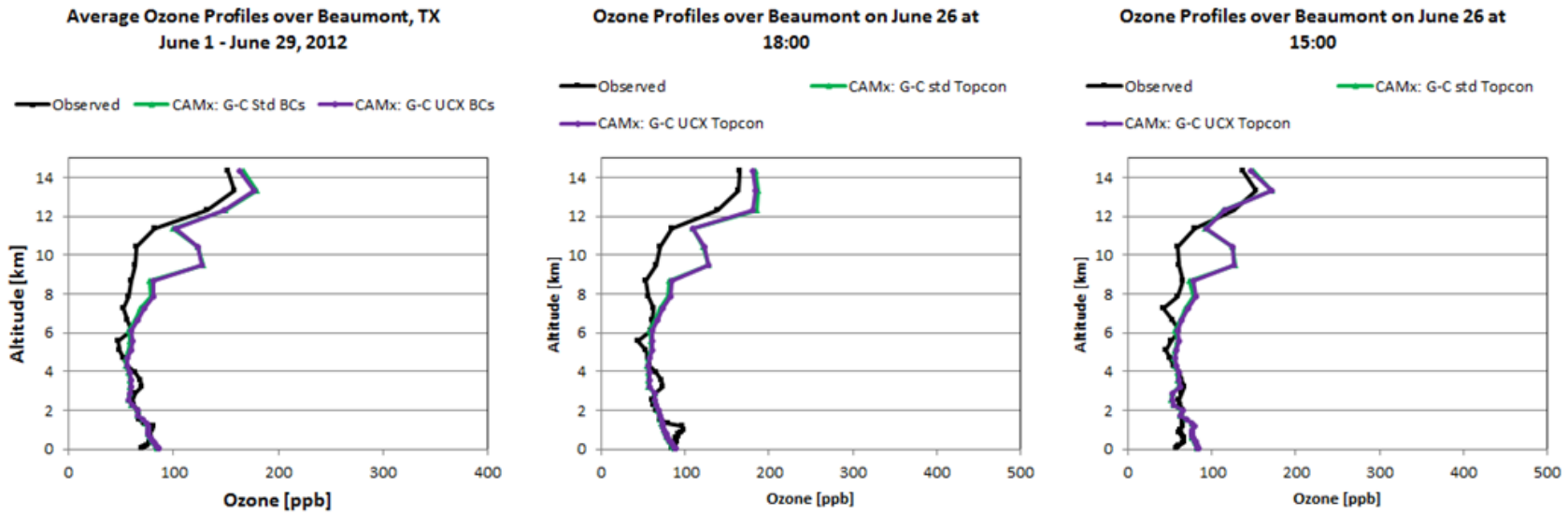

Figure 4-33. CAMx and observed ozonesonde profiles for Beaumont, TX.

4.2.2 Aloft Performance Evaluation for NOy

In 2004, the Intercontinental Chemical Transport Experiment - North America (INTEX-A) field study was held in the U.S. under the auspices of the International Consortium for Atmospheric Research on Transport and Transformation (Singh et al. 2006). Several aircraft flew missions over North America and the Atlantic and Pacific Oceans. We use measurements from the NASA DC-8 aircraft, which flew 18 missions over North America during July 1-August 15, 2004 and measured trace gases in the troposphere and lower stratosphere from 0.2-12 km (Singh et al. 2006; 2007). The DC-8 flight tracks for all flights are shown in red in Figure 4-34. The 1-minute average DC-8 measurements were provided to ENVIRON by Barron Henderson (personal communication, 2012).

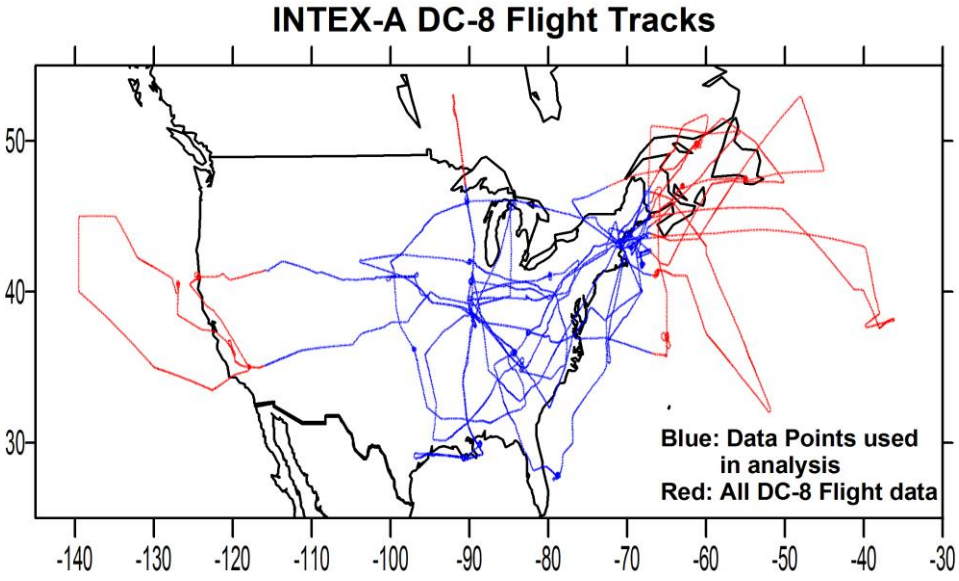

Figure 4-34. NASA DC-8 flight tracks during the INTEX-A field study (red) and flight data used in this study (superimposed on red flight tracks in blue).

Although the INTEX-A experiment does not overlap the June 2012 episode in time, we used this data to compare the mean measured state of the atmosphere with that predicted by CAMx. We do not expect the model to exactly reproduce the INTEX-A measurements, but do expect the modeled episode mean vertical species profiles to agree in shape and approximate magnitude with the measured mean vertical profiles, given that the flights and modeled episode both occur during summer over the same geographic region.

We compare campaign-average vertical profiles of trace gas species from the INTEX-A flights with episode average CAMx NOy profiles over similar geographic regions as shown in Figure 4-34. We then averaged together all INTEX-A DC-8 flight data in each CAMx layer and plotted INTEX-A layer average and CAMx 36 km region-wide layer average at the CAMx layer center altitudes. We did not plot the results for model layers with centers above 11,000 m because of low number of INTEX observations taken in this region and the variability of measured values. The same is true for the results in CAMx model layers whose layer centers lie below 1,000 m.

On the INTEX-A DC-8 flights, NO_2 was measured via laser-induced fluorescence (LIF) and thermal dissociation (Singh et al. 2006). The INTEX-A measurements are biased high due to interference from methyl peroxy nitrate, (MPN, $CH_3O_2NO_2$), and peroxy nitric acid, (PNA; HO_2NO_2) (Browne et al., 2011). Because $CH_3O_2NO_2$ and HO_2NO_2 are weakly bound, thermal dissociation was possible as ambient air passed through the inlet to the LIF instrument located in the DC-8 aircraft cabin. The NO_2 that is the product of this dissociation would then be detected as ambient NO_2. Based on data gathered during the Arctic Research of the Composition of the Troposphere from Aircraft and Satellites (ARCTAS) field study, Browne et al. (2011) developed a method for removing the estimated interference that can be applied to the original INTEX-measured NO_2, denoted XNO_2. This method was applied in the dataset that was supplied to ENVIRON by Barron Henderson (personal communication, 2012) and the corrected NO_2 is denoted NO_2 below.

Figure 4-35 shows the observed and modeled NO_2 profiles. The CAMx profiles using both sets of GEOS-Chem boundary conditions have the "C" shaped profile apparent in the observed profile and are similar to one another below 8 km. Above 8 km, the two CAMx profiles diverge, with the CAMx run with UCX boundary condition having higher NO_2. The higher NO_2 values in the UCX case reflect the influence of higher NO_2 concentrations in the stratosphere in UCX.

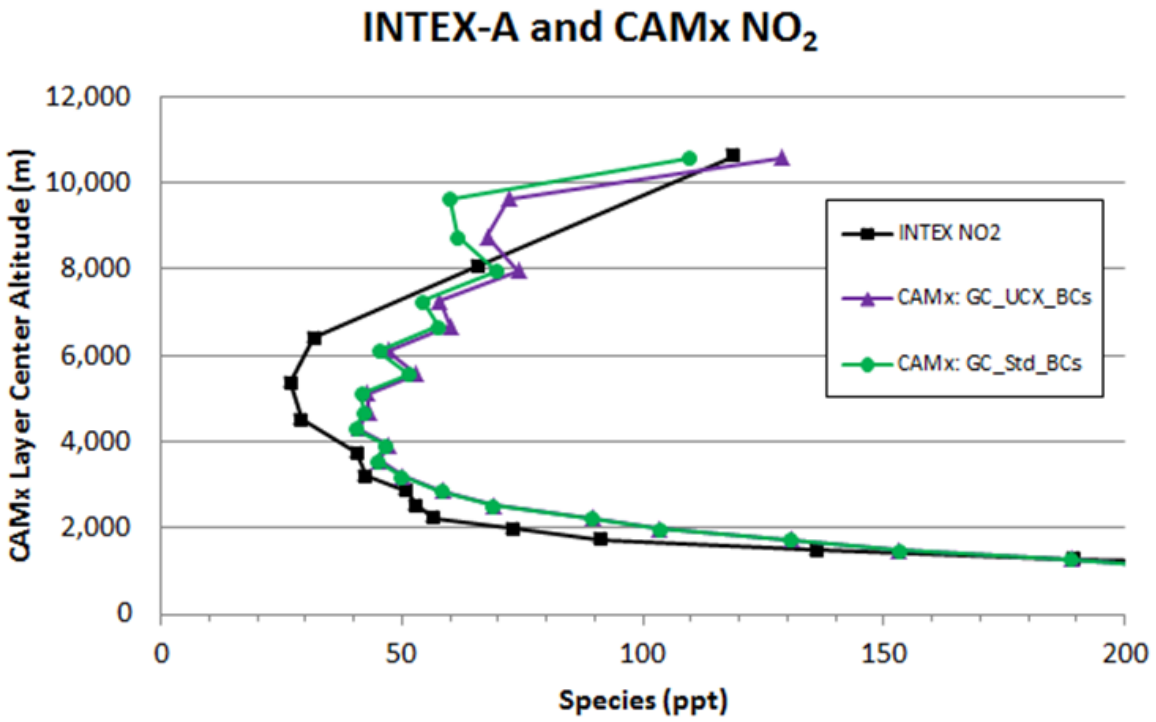

Figure 4-35. Comparison of CAMx and INTEX-A domain-average NO_2 vertical profiles.

There is a high bias for NO_2 in both CAMx runs in the mid-troposphere. This is likely due to the influence of the tropospheric emissions incorporated into the TCEQ 2012 emission inventory for

the final CAMx runs. Figure 4-36 shows the CAMx NO_2profiles for both GEOS-Chem runs before and after the introduction of aircraft and LNOx emissions. In Project 14-15, we examined the influence of increasing the CAMx vertical resolution from 28 to 38 layers (i.e. removing layer collapsing) on the modeled NO_2 profile. There were only minor differences in the 28 layer and 38 layer CAMx simulations of NO_2 in the 4,000-8,000 m range (Kemball-Cook et al., 2014). Therefore, we suspect that the differences in the initial and final CAMx runs in this altitude range in Figure 4-36 are due to the additional mid-tropospheric emissions rather than the increase in model vertical resolution. Evaluation of the new TCEQ LNOx and aircraft emission inventories against aircraft data should be a priority once these inventories are complete, as they have a significant impact on NO_2 in the mid-troposphere and can affect column-integrated comparisons with satellite NO_2 data.

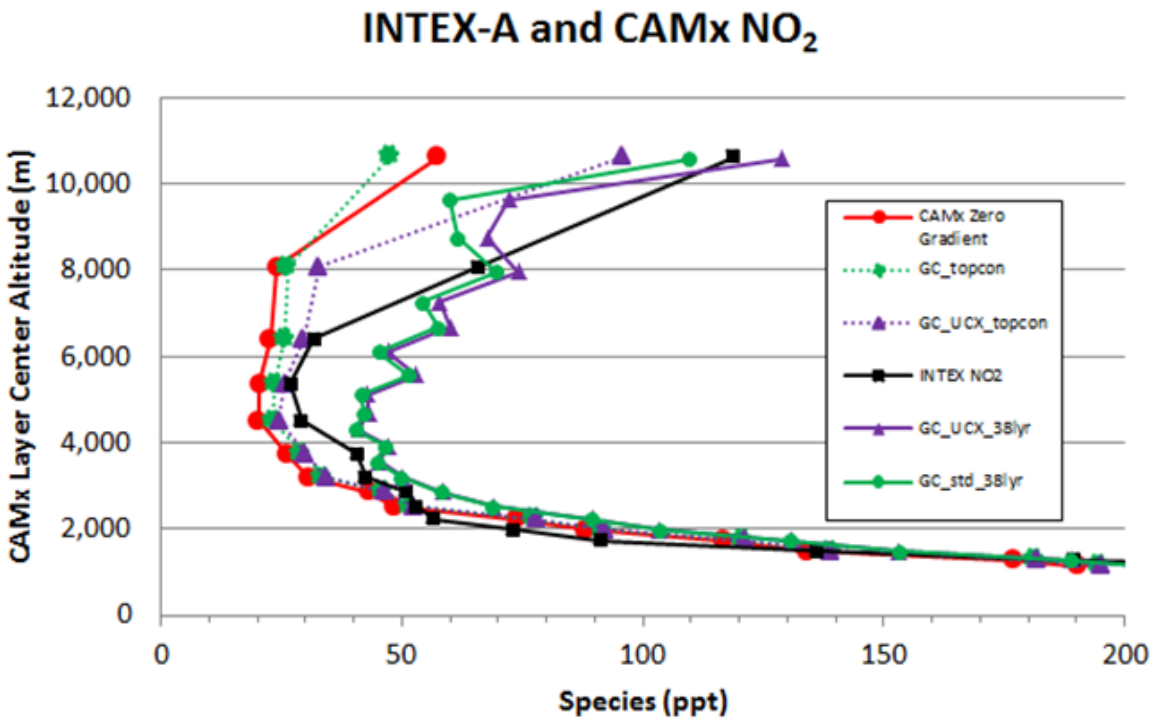

Figure 4-36. Comparison of CAMx and INTEX-A domain-average NO_2 vertical profiles for CAMx runs with augmented emission inventory and no layer collapsing (38 layer runs) and CAMx runs with layer collapsing and no LNOx and aircraft emissions (28 layer runs).

The modeled CAMx profiles for peroxyacetyl nitrate (PAN) both show a pronounced low bias above 2 km, consistent with the low bias seen in the TCEQ's 2006 ozone modeling (Kemball-Cook et al., 2014) (Figure 4-37). PAN is a long-lived reservoir species whose values in the free troposphere are driven by the CAMx boundary conditions. PAN is known to be underestimated in GEOS-Chem, and this is a subject of current research. Agreement between modeled and observed nitric acid (HNO_3; Figure 4-38) and ozone (Figure 4-39) is very good for both CAMx

runs. For ozone and all NOy species, UCX boundary conditions produced slightly higher CAMx values throughout the troposphere than the standard GEOS-Chem boundary conditions,

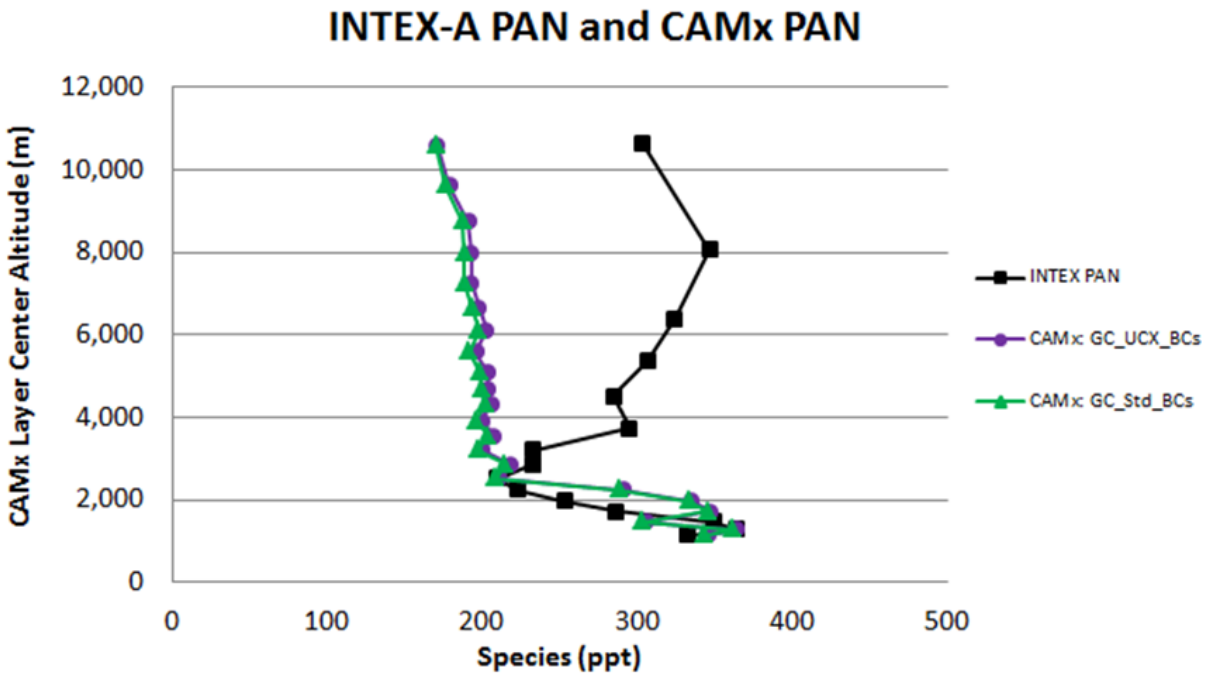

Figure 4-37. Comparison of CAMx and INTEX-A domain-average PAN vertical profiles.

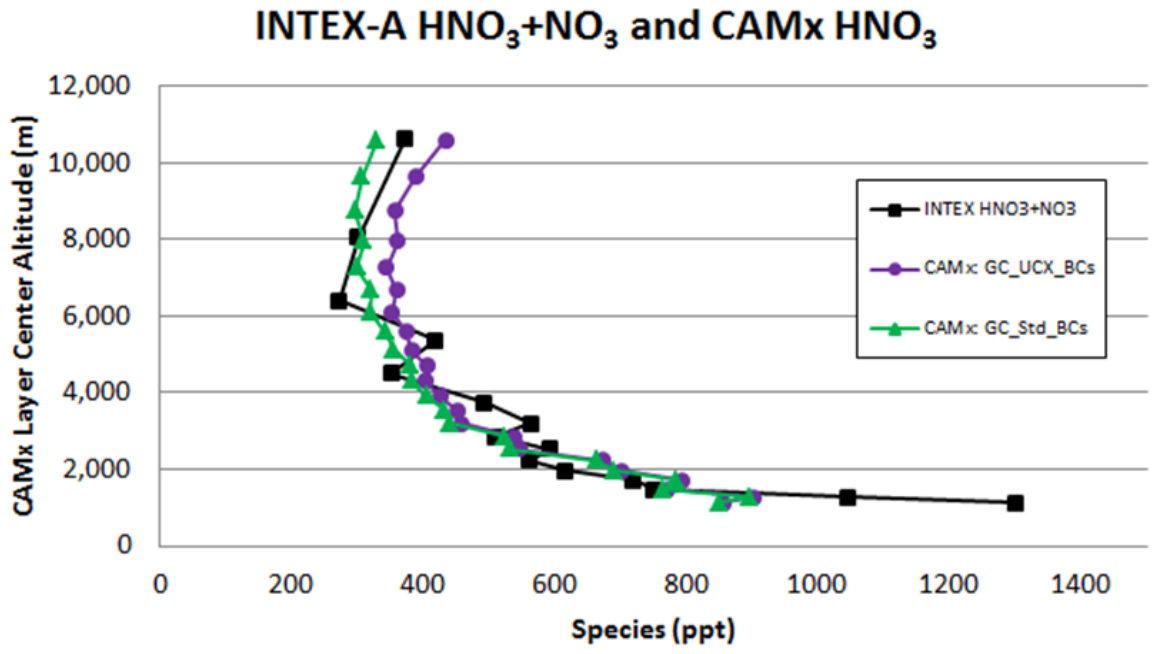

Figure 4-38. Comparison of CAMx and INTEX-A domain-average HNO_3 vertical profiles.

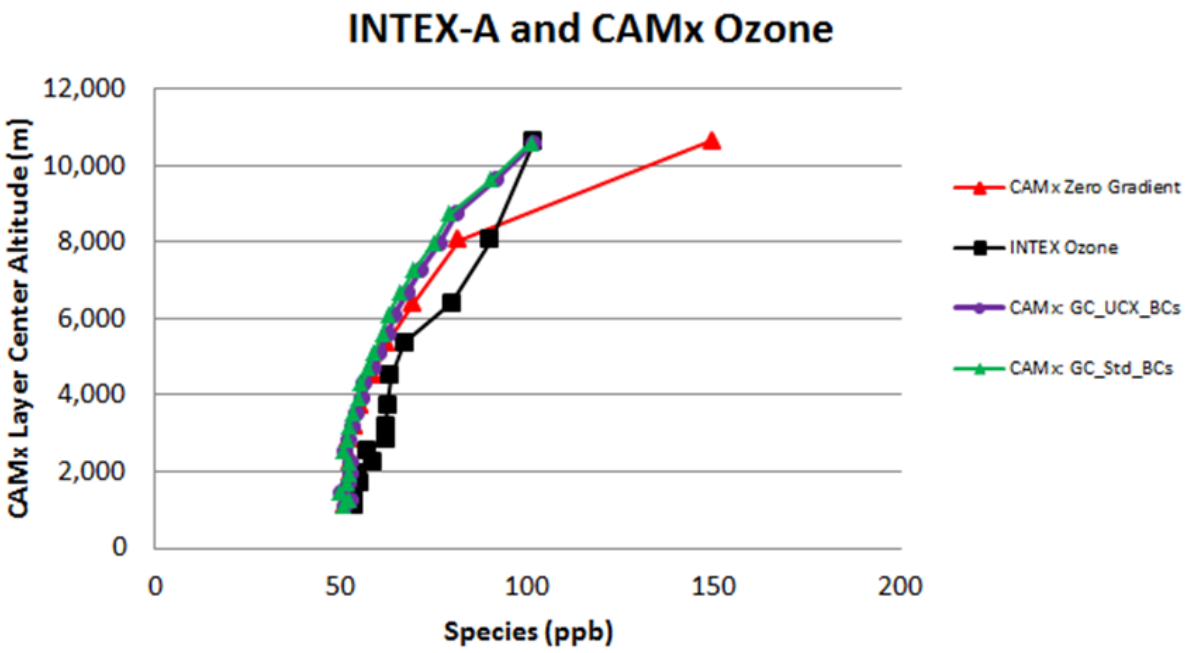

Figure 4-39. Comparison of CAMx and INTEX-A domain-average ozone vertical profiles.

4.3 Model Performance Evaluation Summary

The GEOS-Chem ozonesonde profile evaluation showed that UCX performs better than the standard version of GEOS-Chem in simulating ozone in the lower stratosphere.

The model performance evaluation of the two CAMx runs showed that the UCX and standard GEOS-Chem boundary conditions produce similar CAMx surface ozone simulations in East Texas. Comparison with ozonesonde data showed that both sets of GEOS-Chem boundary conditions give similar CAMx profiles, with UCX showing only slightly better agreement in the upper troposphere. The aircraft evaluation showed that for PAN, HNO3 and ozone, differences between the two CAMx runs were small. There were larger differences in the upper troposphere for NO_2, but it is difficult to say whether one CAMx simulation is more accurate than the other.

The CAMx model performance evaluation using surface and aloft measurements indicates that for air quality planning applications focused on ground level ozone during typical summer conditions, either the standard or UCX version of GEOS-Chem could be used to develop top and lateral boundary conditions. The UCX version of GEOS-Chem has a more complete representation of the chemistry of the stratosphere than the simplified chemistry of the standard version of GEOS-Chem and produces a more realistic simulation of stratospheric ozone, but is more resource–intensive. The model run time for a GEOS-Chem UCX simulation is twice that of the standard version of GEOS-Chem. The UCX version of GEOS-Chem requires a 5-year spinup period, while the standard version requires a 1-year spinup period. The difference in spinup is due to the slower time scale of dynamical processes in the stratosphere relative to

the troposphere, which is the main focus of the standard version of GEOS-Chem. The UCX version, which explicitly simulates both the stratosphere and the troposphere, requires a longer period of time to remove the influence of the initial conditions from the simulation of the stratosphere. The developers of UCX are considering providing UCX initial conditions files for a range of simulation years so that users of the model would not be required to perform a 5-year spinup. This would significantly reduce the computation burden of using the UCX version of GEOS-Chem.

5.0 CAMX LOWER STRATOSPHERIC CHEMISTRY EVALUATION

In this Section, we summarize efforts to determine whether it is appropriate to use a UCX-like stratospheric chemistry mechanism for the lower stratosphere. We give an overview of the CAMx layer structure and its relationship to the mean structure of the atmosphere in the vicinity of the tropopause. We examine the chemistry of SIP-relevant species in the lower stratosphere and the time-scales on which they vary. We use this analysis together with an estimate of the residence time of lower stratospheric air in the modeling domain to infer the relative importance of boundary conditions and CAMx chemistry in the lower stratosphere. We then discuss the potential impact of incorporating UCX-like chemistry into CAMx.

5.1 Simulation of Stratospheric Chemistry in CAMx

The June 2012 ozone modeling database developed by the TCEQ has its model top at an altitude of approximately 15 km above ground level. Depending on latitude, season and weather conditions, the model top can be located within either the troposphere or the stratosphere. The CB6r2 chemical mechanism (Yarwood et al., 2012) used in CAMx treats the chemistry of the troposphere. In this section, we consider the question of whether use of the Cb6r2 chemical mechanism in the lower stratosphere affects the CAMx model's ability to accurately simulate ozone and NOx in this region.

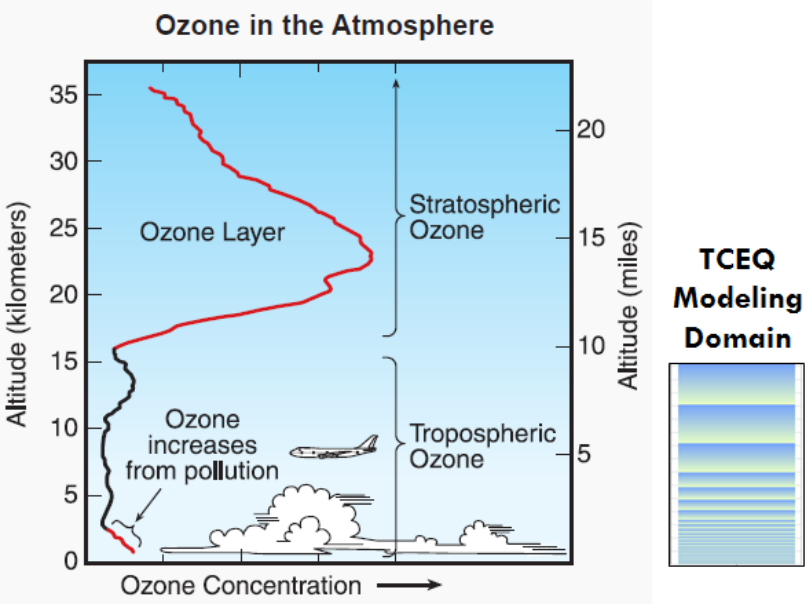

Figure 5-1. TCEQ 2012 model vertical structure and extent and climatological profile of mid-latitude ozone. Left panel is EPA figure[24]. Right panel is TCEQ figure excerpted from image shown in Figure 5-2. Figure is identical to Figure 3-5 and is reproduced here for convenience.

[24] http://esrl.noaa.gov/csd/assessments/ozone/2006/chapters/Q1.pdf

Vertical Layer Structure

Corresponding WRF Layer	Layer Top (m AGL)	CAMx Layer	Layer Center (m AGL)	Thickness (m)
38	15179.1	28	13637.9	3082.5
36	12096.6	27	10631.6	2930.0
32	9166.6	26	8063.8	2205.7
29	6960.9	25	6398.4	1125.0
27	5835.9	24	5367.0	937.9
25	4898.0	23	4502.2	791.6
23	4106.4	22	3739.9	733.0
21	3373.5	21	3199.9	347.2
20	3026.3	20	2858.3	335.9
19	2690.4	19	2528.3	324.3
18	2366.1	18	2234.7	262.8
17	2103.3	17	1975.2	256.2
16	1847.2	16	1722.2	249.9
15	1597.3	15	1475.3	243.9
14	1353.4	14	1281.6	143.6
13	1209.8	13	1139.0	141.6
12	1068.2	12	998.3	139.7
11	928.5	11	859.5	137.8
10	790.6	10	745.2	90.9
9	699.7	9	654.7	90.1
8	609.7	8	565.0	89.3
7	520.3	7	476.1	88.5
6	431.8	6	387.9	87.8
5	344.0	5	300.5	87.1
4	256.9	4	213.8	86.3
3	170.6	3	127.8	85.6
2	85.0	2	59.4	51.0
1	33.9	1	17.0	33.9

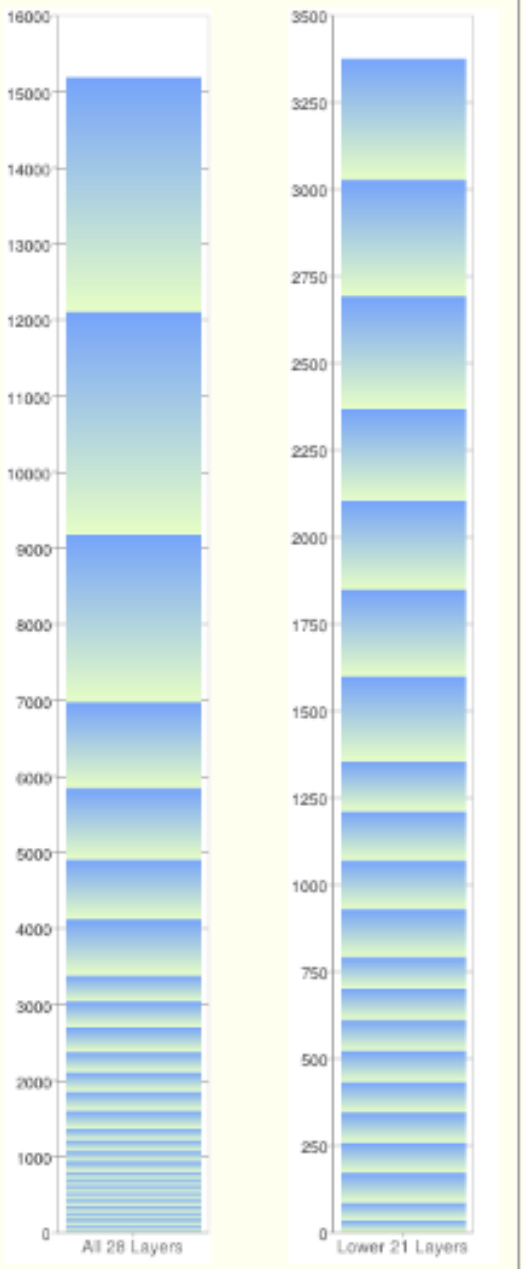

AGL - Above Ground Level.

Figure 5-2. June 2012 model WRF and CAMx layer structure. TCEQ figure[25]. Figure is identical to Figure 3-6 and is reproduced here for the reader's convenience.

[25] http://www.tceq.texas.gov/airquality/airmod/data/domain

In defining vertical and horizontal boundary conditions for photochemical modeling, it is important that the model boundary be placed far enough from the emission sources and the receptors of interest that the effect of the boundary conditions on the simulation is relatively small (e.g. EPA, 2014). EPA's Draft Modeling Guidance for Demonstrating Attainment of Air Quality Goals for Ozone, $PM_{2.5}$, and Regional Haze (EPA, 2014) recommends that the top of the modeling domain should be placed near the tropopause at the 50-100 mb level. The TCEQ model has its top at 15 km above the ground, which corresponds to a pressure of 120 mb in a U.S. Standard Atmosphere[26]. In the U.S. Standard Atmosphere, the tropopause occurs at 11 km. The tropopause is defined as the lowest level at which the lapse rate decreases to 2 °C/km or less, provided that the average lapse rate between this level and all higher levels within 2 km does not exceed 2 °C/km[27]. Figure 5-3 shows the horizontal spatial structure of the typical June-July-August (JJA) mean temperature lapse-rate tropopause as determined via Global Positioning System radio occultation measurements from the Constellation Observing System for Meteorology, Ionosphere and Climate (COSMIC) Formosa Satellite Mission 3 (Son et al., 2011). Three years of data (2006-2009) were used to form this average. Across the TCEQ 36 km continental-scale modeling domain, the typical JJA tropopause height varies vetween ~100-240 mb (or 10-16 km).

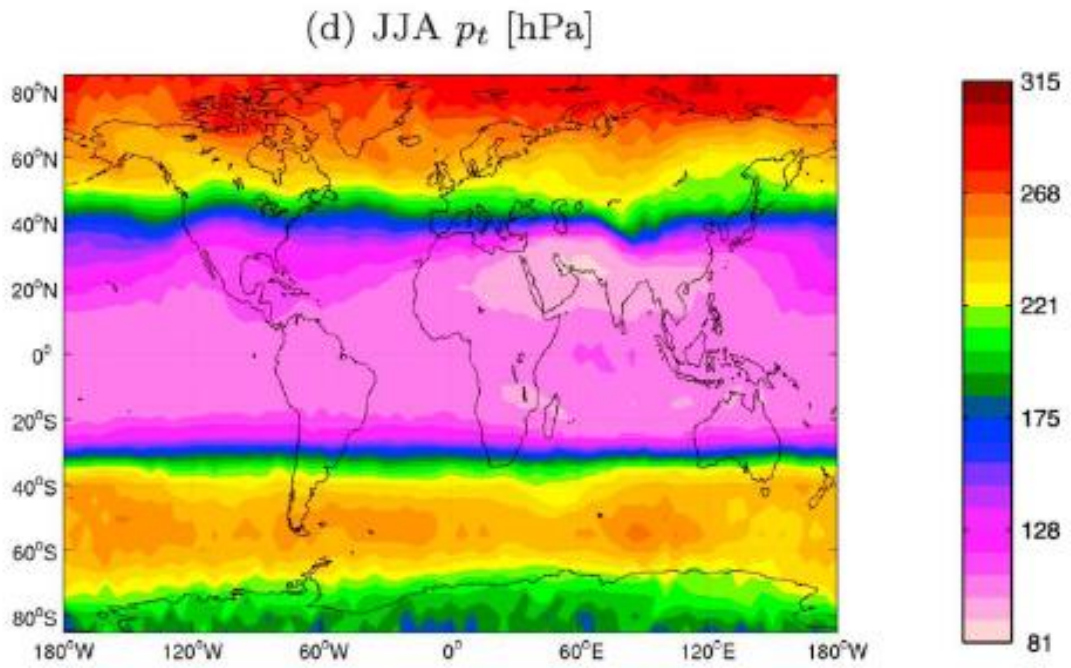

Figure 5-3. Satellite-derived 2006-2009 June-July-August (JJA) average tropopause pressure from Son et al. (2011).

[26] http://www.digitaldutch.com/atmoscalc/

[27] International Meteorological Vocabulary (2nd ed.). Geneva: Secretariat of the World Meteorological Organization. 1992. p. 636. ISBN 92-63-02182-1.

Figure 5-4 shows the NCEP-NCAR Reanalysis June 2012 zonal mean air temperature in the northern hemisphere. The red box shows the approximate meridional and vertical extent of the TCEQ 36 km modeling domain. The model top is at 15 km, but the tropopause varies from ~10-15 km (~250-125 mb) during June within the region bounded by the TCEQ 36 km modeling domain (shown as a red box in Figure 5-4). It is clear from Figure 5-4 that the altitude (pressure) of the tropopause decreases (increases) with increasing latitude so that the TCEQ modeling domain includes regions of stratospheric as well as tropospheric air.

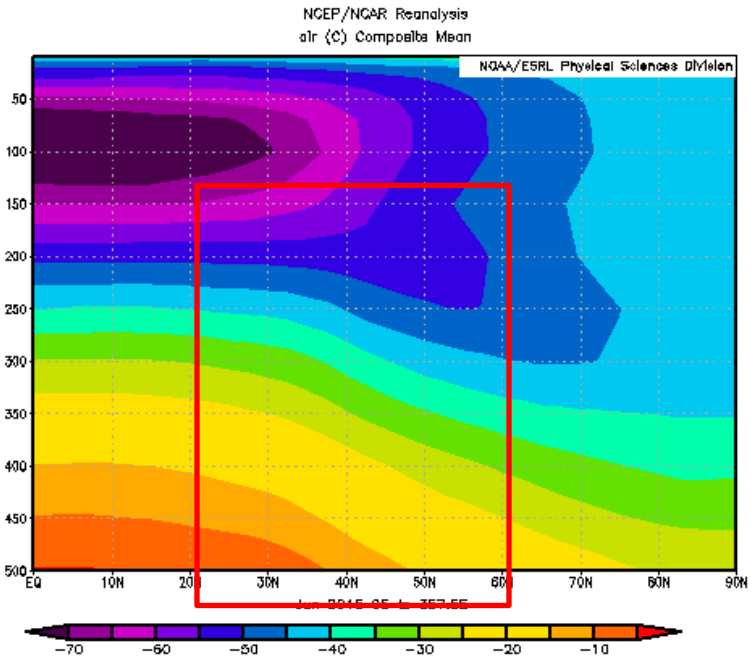

Figure 5-4. June 2012 zonal mean air temperature from the NCEP-NCAR Reanalysis. Red box indicates approximate extent of the TCEQ 36 km modeling domain.

5.1.1 Stratospheric Chemistry in CAMx

The altitude of the tropopause varies with time and location, as shown in Figure 5-3 and Figure 5-4, and the TCEQ 2012 model top at 15 km is located above the tropopause for some model columns and below the tropopause for other columns. The CB6r2 chemical mechanism used in CAMx was developed for use in tropospheric regional air quality models, while the GEOS-Chem UCX chemical mechanism extends the tropospheric chemistry in the standard version of GEOS-Chem to use an adapted version of the stratospheric chemistry of NASA's GMI model (Considine et al., 2008) between the tropopause and the stratopause. In this section, we address the question of whether it would be appropriate to use a stratospheric chemistry mechanism such as UCX for CAMx grid cells that are located above the tropopause.

In Project FY14-15 (Kemball-Cook et al., 2014), HYbrid Single-Particle Lagrangian Integrated Trajectory model (HYSPLIT; Draxler and Hess, 1997; Draxler and Rolph, 2013) trajectories were used to analyze the transport of air in the upper layers of the TCEQ's June 2006 CAMx model,

which has vertical and horizontal structure identical to that of the TCEQ June 2012 model. From HYSPLIT trajectories developed using both WRF and CAMx winds, we found that 3-5 days was a typical residence time within the continental-scale 36 km modeling domain for air in the uppermost layers of the June 2006 CAMx model, and that this time was in agreement with the residence times calculated using Eta Data Assimilation System (EDAS) analysis winds. Figure 5-5 shows an example of the trajectory analysis. The total time elapsed for air following the backward and forward trajectory paths in Figure 5-5 was about 4 days. This represents the amount of time that air spends within the 36 km modeling domain as it travels from west to east in the upper troposphere/lower stratosphere.

Figure 5-5. HYSPLIT trajectories from Project FY14-15. June 2, 2006, 2Z. Trajectory colors: blue = CAMx 28 layer run, red = WRF, Green = CAMx 38 layer run, Purple = EDAS. Left panels are back trajectories; right panels are forward trajectories. Figure from Kemball-Cook et al. (2014).

Figure 5-6 shows a cross-section of the mean zonal wind for June 2006 and June 2012 from the NCEP-NCAR Reanalysis. Zonal winds speeds for 2006 and 2012 in the upper troposphere and lower stratosphere are comparable, and zonal winds in the upper troposphere and lower stratosphere for June 2012 are consistent with the residence times in the top model layers derived for the June 2006 model through HYSPLIT trajectory analysis. Although we have not performed a HYSPLIT trajectory analysis for June 2012 to calculate model residence times, the consistency of the zonal winds for June 2006 and June 2012 suggest that residence times in 2012 are similar to those of 2006.

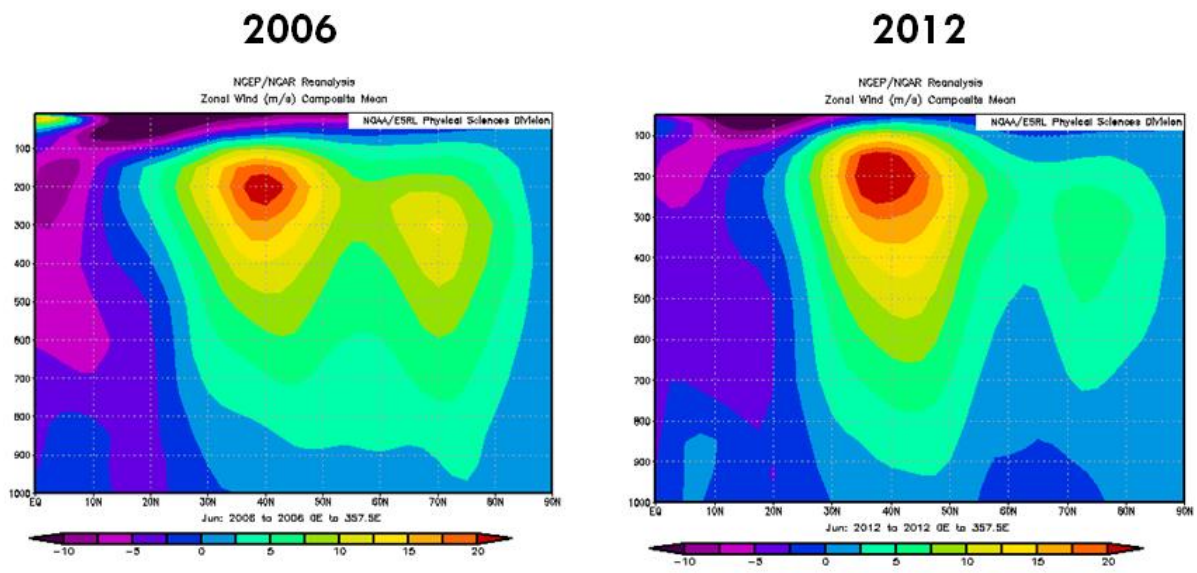

Figure 5-6. Cross-section of mean zonal wind for June 2006 (left) and June 2012 (right) from NCEP-NCAR Reanalysis developed using online tools at http://www.esrl.noaa.gov/psd/cgi-bin/data/composites/printpage.pl.

In the upper layers of CAMx, the horizontal component of the wind speed is high and the residence time of air in the upper layers of CAMx is short. Therefore, the lateral and top boundary conditions will be the most important influence on chemical species concentrations within the modeling domain unless there are chemical reactions occurring within CAMx that affect concentrations significantly on a time scale shorter than 3-5 days.

The question of whether it is appropriate to use a UCX-like stratospheric chemistry mechanism for the lower stratosphere in CAMx depends on whether UCX and CB6r2 chemical mechanisms produce significantly different concentrations of species in air parcels on the 5-day time scale of parcels' residence time in the model. One method for investigating this question would be to run the UCX and CB6r2 mechanisms in a box model for a 5-day period with initial concentrations representative of the lower stratosphere and compare species concentrations. Box modeling is outside the scope of this project, so we addressed this question by examining the chemistry of key chemical species and their lifetimes in the lower stratosphere.

We focus on ozone and NOx because these are the species whose concentrations in the upper model layers are most likely to be relevant to the TCEQ's SIP modeling. The simulation of ozone in the lower stratosphere is relevant for modeling intrusions of ozone-rich stratospheric air that can affect near-surface ozone levels in Texas or upwind states, while simulation of NO_2 and its reservoir species is relevant for comparison with satellite NO_2 column data.

We consider the time scale for changes in ozone and NOx in the lower stratosphere. Of particular relevance are the chemical lifetimes of ozone and NOx and the existence of any sources and sinks of ozone and NOx in UCX in the 10-15 km altitude range that are not present

in CB6r2 and are important on a 5-day time scale. In the stratosphere, ozone is produced via the following reactions:

$$O_2+hv \rightarrow O+O \quad [1]$$

$$O+O_2+M \rightarrow O_3+M \quad [2]$$

$$O_3+hv \rightarrow O_2+O \quad [3]$$

$$O_3+O \rightarrow O_2+O_2 \quad [4]$$

Reactions 2 and 3 are very fast, while reactions 1 and 4 occur relatively slowly and determine the concentration of ozone. Because of the rapid cycling between O and O_3 in reactions 2 and 3, they are considered to be in photochemical equilibrium with one another and are grouped together in the odd oxygen chemical family, Ox, where $Ox=O+O_3$. In the lower stratosphere, O concentrations are very low and [Ox] ≈ [O3]. Ox is destroyed by reaction of ozone and atomic oxygen on the timescale of months in the lower stratosphere (Figure 5-7). The lifetime of Ox is therefore far longer than the 3-5 day residence time of air in CAMx in the 10-15 km range of the lower stratosphere.

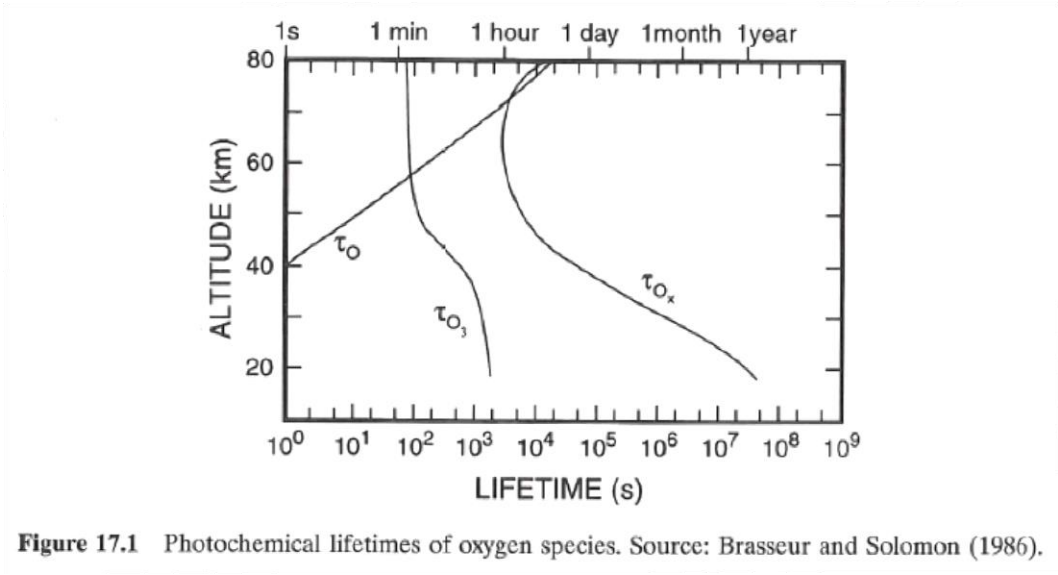

Figure 17.1 Photochemical lifetimes of oxygen species. Source: Brasseur and Solomon (1986).

Figure 5-7. Photochemical lifetimes of odd oxygen species. Figure from Salby (1996) reprinted from Brasseur and Solomon (1986).

In the stratosphere, NOx is created by the oxidation of N_2O, a very long-lived species emitted by biogenic and anthropogenic sources at the earth's surface.

$$O^1(D) + N_2O \rightarrow 2NO \qquad [5]$$

The source of $O^1(D)$ is photodissociation of ozone in 200-300 nm wavelength region. NO reacts with ozone to form NO_2, which can then photolyze.

$$NO+O_3 \rightarrow NO_2+O_2 \qquad [6]$$

$$NO_2+ h\nu \rightarrow NO +O \qquad [7]$$

$$O+O_2+M \rightarrow O_3+M \qquad [8]$$

At altitudes lower than 40 km, when the sun shines, there is rapid exchange between NO and NO_2 and a photostationary state is established within about 100 s (e.g. Warneck, 1988). The partitioning between NO and NO_2 depends on the time of day and season. Time scales for NOy species in the stratosphere are shown in Figure 5-8. The lifetime of N_2O in the lower stratosphere is on the order of years. Therefore, reaction 5 is of minimal importance in producing NO on the 5 day residence time of air within CAMx in the 10-15 km altitude range. NO and NO_2 have time scales on the order of minutes, because they can inter-convert rapidly, but the lifetime of NOx is on the order of weeks.

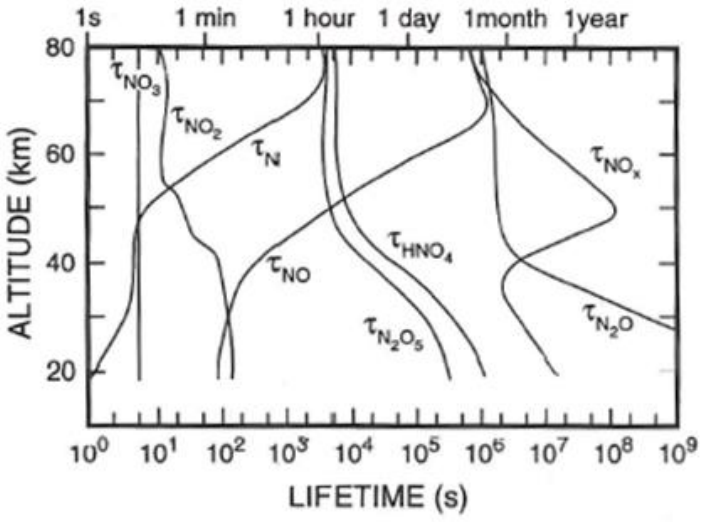

Figure 17.3 Photochemical lifetimes of nitrogen species. Source: Brasseur and Solomon (1986).

Figure 5-8. Photochemical lifetimes of NOy species. Figure from Salby (1996) reprinted from Brasseur and Solomon (1986).

Therefore, we believe it is unlikely that the use of UCX-like stratospheric chemistry would produce a significantly different simulation of ozone or NOx in the lower stratosphere than the CB6r2 chemical mechanism. There are no photochemical sources or sinks of Ox or NOx that act to change the concentrations of these species on the time scale of a few days in the lower

stratosphere. The model solution in the lower stratosphere should therefore be largely controlled by the boundary conditions.

To test this hypothesis, we ran CAMx with CB6r2 chemistry turned off in the lower stratosphere. We estimated the tropopause height by diagnosing the presence of stratospheric air in CAMx grid cells aloft using the water vapor mixing ratio. Stratospheric air is very dry. An important source of air to the stratosphere is the lifting of tropical air in deep convective towers. As the tropical air rises and cools, the water vapor in the air condenses and falls out, so that by the time air crosses the tropical tropopause, the humidity in the air is very low. The air continues to stay dry as it moves around the stratosphere because there is no significant source of water in the stratosphere. This property of stratospheric air allows us to use the water vapor mixing ratio as an indicator of stratospheric air in a CAMx grid cell (e.g. Singh et al., 2007). For simplicity, we chose a 20 ppm water vapor mixing ratio threshold based on zonal average water vapor mixing ratio measurements (Figure 5-9), but note that the tropopause height can vary from grid cell to grid cell.

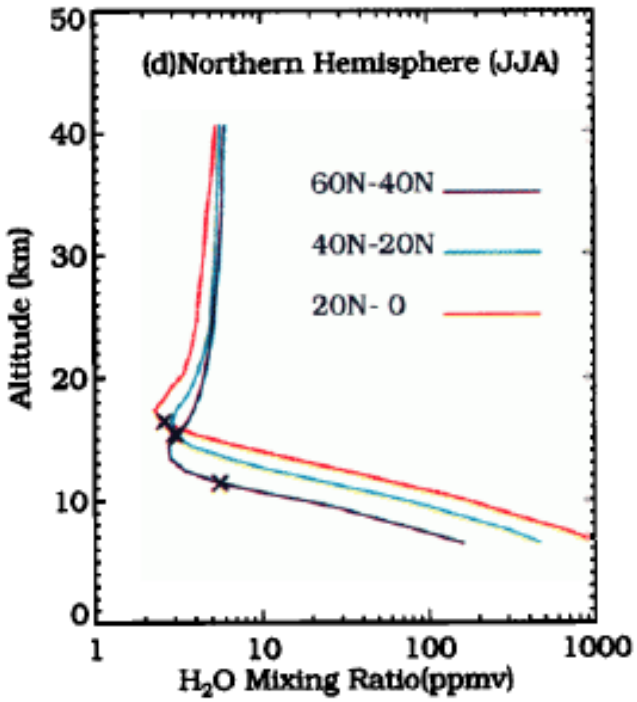

Figure 5-9. SAGE-II-derived seasonal zonal mean profiles of water vapor mixing ratios (crosses denote the mixing ratio at the average tropopause altitude). Figure from Chiou et al. (1997).

We compared the results of this CAMx sensitivity run (CAMx: GC_UCX_BCs_nostratchem) to the results of an otherwise identical CAMx simulation driven with UCX boundary conditions (CAMx: GC_UCX_BCs). Both runs used GEOS-Chem UCX boundary conditions. The comparison showed that turning off chemistry in the stratosphere had very little effect on episode average vertical profiles of ozone and NOy (Figure 5-10). The largest differences are seen in the NO_2 profiles, but even these are barely visible at the scale of Figure 5-10.

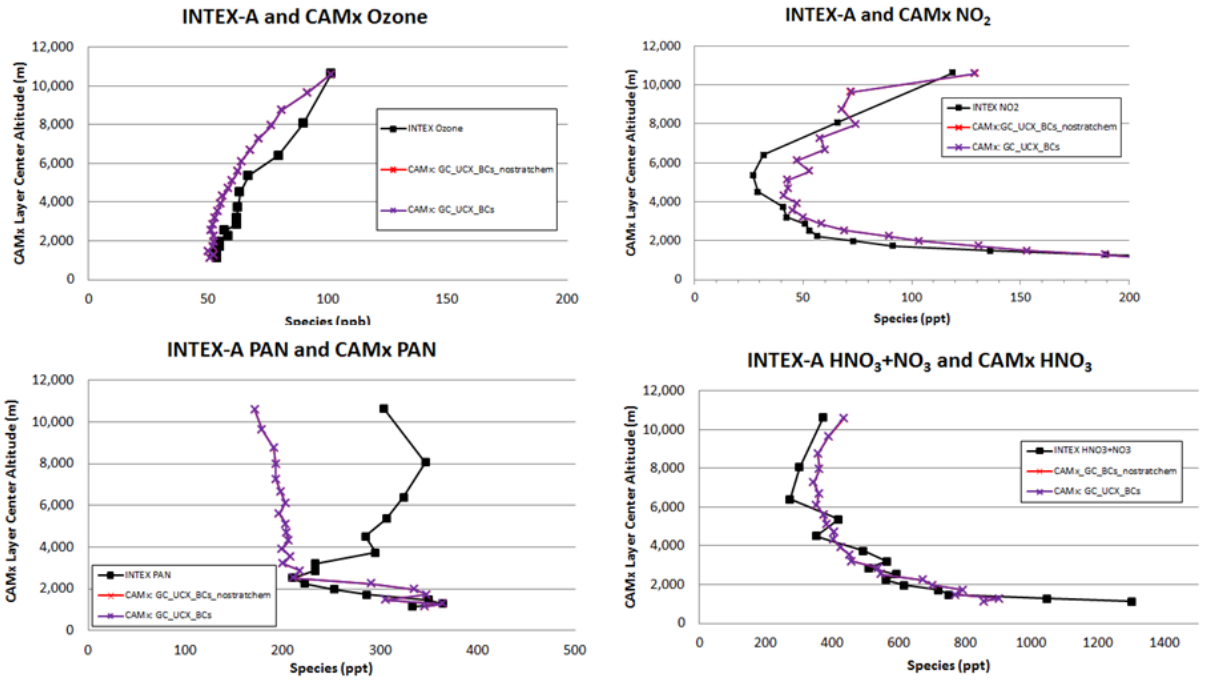

Figure 5-10. Stratospheric chemistry sensitivity test (CAMx: GC_UCX_BCs_nostratchem) comparison against INTEX-A aircraft data and CAMx run with stratospheric chemistry (CAMx: GC_UCX_BCs).

We compared ozone profiles for the two runs against ozonesonde data for individual soundings and found that the profiles for the two runs were indistinguishable, with the largest differences in ozone coming in the top two layers of the model and having magnitude on the order of 0.1 ppb (profiles not shown). We conclude that the boundary conditions are far more important than chemistry for simulation of ozone and NOx in the upper troposphere and lower stratosphere in CAMx when CB6r2 is used.

Based on the results of this sensitivity test, we suggest that the following method for improving the simulation of lower stratosphere in CAMx be investigated. For applications where simulation the upper troposphere/lower stratosphere is critical, the CAMx model top could be moved upward to an altitude of 20 km above ground level. At 20 km, the atmosphere is dynamically stable, and the CAMx model top would be located in the stratosphere throughout the 36 km TCEQ modeling domain.

Stratospheric ozone intrusions would then be simulated using the higher resolution meteorology of WRF rather than the lower resolution GEOS meteorology. The GEOS-Chem UCX, with its explicit stratospheric chemistry, would be used to determine ozone and NOy in the CAMx lower stratosphere through the model boundary conditions. A 20 km top boundary may permit CAMx when running with GC-UCX boundary conditions to perform better in in the lower stratosphere than CAMx running with GC-Std boundary conditions and a 15 km model top. CAMx chemistry in the stratosphere could be turned off to mitigate the computational burden due to addition of extra model layers. An alternate approach would be to model ozone and NOx using only the steady state approximation (reactions 6-8) above the tropopause. This method retains the gain in computational efficiency from turning off the full CB6r2 chemical mechanism while allowing for more accurate partitioning between NO and NO_2.

6.0 SUMMARY AND RECOMMENDATIONS

In this study, we developed lateral and top boundary conditions for the TCEQ's 2012 ozone modeling. We ran both the standard and UCX versions of GEOS-Chem version 10-01 for the 2012 ozone season and extracted lateral and model top boundary conditions for use in modeling with CAMx. We evaluated the performance of the standard and UCX versions of the GEOS-Chem model in simulating ozonesonde observations at U.S. sites during June, 2012. The two GEOS-Chem simulations were very similar in the lower and middle troposphere, but the UCX simulation of ozone in the lower stratosphere was consistently closer to the observed ozone profiles than the simulation using the standard version of GEOS-Chem.

Next, we ran CAMx for the TCEQ's June 2012 episode using the two sets of GEOS-Chem boundary conditions. We evaluated CAMx model performance in these two runs against surface ozone observations, aloft aircraft measurements of ozone and NOy, and ozonesonde profiles. The model performance evaluation against observed surface and aloft ozone and NOy indicated that the GEOS-Chem model was functioning correctly in both the standard and UCX configurations and provides reasonable model top boundary conditions to the CAMx model. CAMx boundary conditions developed using the UCX and standard versions of GEOS-Chem produce nearly identical CAMx ground level ozone simulations in East Texas. Small and intermittent differences in hourly surface ozone on the order of 3 ppb or less occurred at higher elevation sites such as Big Bend in Texas and sites in the Rocky Mountains. Comparison of the two CAMx simulations of ozone and NOy in the upper troposphere and lower stratosphere against aircraft data showed that differences were small between the two CAMx runs using boundary conditions developed with the UCX and standard versions of GEOS-Chem.

The CAMx model performance evaluation using surface and aloft measurements indicates that for air quality planning applications focused on ground level ozone during typical summer conditions, either the standard or UCX version of GEOS-Chem could be used to develop top and lateral boundary conditions. The UCX version of GEOS-Chem has a more complete representation of the chemistry of the stratosphere than the simplified chemistry of the standard version of GEOS-Chem and produces a more realistic simulation of stratospheric ozone, but is more resource–intensive. The model run time for a GEOS-Chem UCX simulation is twice that of the standard version of GEOS-Chem. The UCX version of GEOS-Chem requires a 5-year spinup period, while the standard version requires a 1-year spinup period. The difference in spinup is due to the slower time scale of dynamical processes in the stratosphere relative to the troposphere, which is the main focus of the standard version of GEOS-Chem. The UCX version, which explicitly simulates both the stratosphere and the troposphere, requires a longer period of time to remove the influence of the initial conditions from the simulation of the stratosphere. The developers of UCX are considering providing UCX initial conditions files for a range of simulation years so that users of the GEOS-Chem model would not be required to perform a 5-year spinup. This would significantly reduce the computation burden of using the UCX version of GEOS-Chem.

The June 2012 CAMx modeling database developed by the TCEQ has its model top at an altitude of approximately 15 km above ground level. Depending on latitude, season and weather conditions, the model top can be located within either the troposphere or the stratosphere. The CB6r2 chemical mechanism used in CAMx was developed for use in the troposphere. We evaluated whether the chemistry in CAMx should be extended to represent lower stratosphere conditions using a scheme similar to that of the GEOS-Chem UCX.

The horizontal component of the wind speed in the upper troposphere and lower stratosphere over North America is fast enough that the residence time of air in the continental-scale 36 km modeling domain within the upper layers of CAMx is typically 3-5 days. Therefore, the CAMx lateral and top boundary conditions are the most important influence on chemical species concentrations in the highest model layers unless there are chemical reactions occurring within the CAMx modeling domain that significantly affect species concentrations on a time scale shorter than 3-5 days.

The question of whether it is appropriate to use a UCX-like stratospheric chemistry mechanism for the lower stratosphere in CAMx depends on whether UCX and CAMx CB6r2 chemical mechanisms produce significantly different concentrations of species in air parcels during the parcels' 5-day residence time in the modeling domain. One method for investigating this question would be to run the UCX and CB6r2 mechanisms in a box model for a 5-day period with initial concentrations representative of the lower stratosphere and compare species concentrations. Box modeling was outside the scope of this project, so we addressed this question by examining the chemistry of key chemical species and their lifetimes in the lower stratosphere.

We focused on ozone and NOx because these are the species whose concentrations in the upper model layers are most likely to be relevant to the TCEQ's SIP modeling. The simulation of ozone in the lower stratosphere is relevant for modeling intrusions of ozone-rich stratospheric air that can affect near-surface ozone levels in Texas or upwind states, while simulation of NO_2 and its reservoir species is relevant for comparison with satellite NO_2 column data. There are no photochemical sources or sinks of odd oxygen ($Ox=O+O_3$) or NOx that act to change the concentrations of these species on the time scale of a few days in the lower stratosphere. The model solution in the lower stratosphere should therefore be largely controlled by the boundary conditions. Therefore, we believe it is unlikely that the use of UCX-like stratospheric chemistry would produce a significantly different simulation of ozone or NOx in the highest model layers than the CB6r2 chemical mechanism.

To test the sensitivity of the model to CB6r2 chemistry in the lower stratosphere, we ran CAMx with chemistry turned off in the lower stratosphere. Turning off the chemistry in the stratosphere had very little effect on the simulation. Modeled vertical profiles of NOy and ozone with chemistry turned on and off in the stratosphere were nearly indistinguishable, with differences in the lower stratospheric ozone and NOy profiles of 0.1 ppb or less. We conclude that the boundary conditions are far more important than chemistry for simulation of ozone and NOx in the upper troposphere and lower stratosphere in CAMx.

6.1 Recommendations

Below, we summarize recommendations arising from this study:

- For air quality planning applications focused on ground level ozone during typical summer conditions, either the standard or UCX version of GEOS-Chem could be used
  - UCX has an explicit representation of the stratosphere and provides a better simulation of stratospheric ozone, but is currently more resource-intensive to use
- The UCX version of GEOS-Chem should be used to develop CAMx boundary conditions for applications where simulation of the upper troposphere and lower stratosphere is critical, such as:
  - Simulation of stratospheric ozone intrusions
  - Comparison with column-integrated satellite data
- For applications where simulation of the upper troposphere and lower stratosphere is critical, we recommend evaluating whether moving the CAMx top boundary to 20 km permits CAMx with GEOS-Chem UCX-derived boundary conditions to perform better in the upper troposphere/lower stratosphere than CAMx boundary conditions developed with the standard version of GEOS-Chem
- Incorporation of UCX-like stratospheric chemistry in CAMx is not necessary because the CAMx lateral and top boundary conditions are far more important than chemistry in determining concentrations of ozone and NOx in the upper troposphere and lower stratosphere

7.0 REFERENCES

Allen, D. J., K. E. Pickering, R. W. Pinder, B. H. Henderson, K. W. Appel, and A. Prados (2012). Impact of lightning-NO on eastern United States photochemistry during the summer of 2006 as determined using the CMAQ model. *Atmos. Chem. Phys.*, 10, 107–119.

Bey, I., D. J. Jacob, R. M. Yantosca, J. A. Logan, B. Field, A. M. Fiore, Q. Li, H. Liu, L. J. Mickley, and M. Schultz. 2001. Global modeling of tropospheric chemistry with assimilated meteorology: Model description and evaluation, *J. Geophys. Res*., 106, 23,073-23,096.

Boccippio, D.J., Cummins, K.L., Christian, H.J., Goodman, S.J., (2001). Combined satellite- and surface-based estimation of the intracloud-cloud-to-ground lightning ratio over the continental United States. *Mon. Wea. Rev*. 129, 108e122.

Brasseur, G. and S. Solomon. 1986. Aeronomy of the Middle Atmosphere: Chemistry and Physics of the Stratosphere and Mesosphere. D. Reidel Publishing Co. Dordrecht.

Brohede, S., McLinden, C. A., Berthet, G., Haley, C. S., Murtagh, D., and Sioris, C. E. 2007. A stratospheric NO_2 climatology from Odin/OSIRIS limb-scatter measurements, *Can. J. Phys*., 85, 1253–1274, doi:10.1139/P07-141,

Browne, E. C., Perring, A. E., Wooldridge, P. J., Apel, E., Hall, S. R., Huey, L. G., Mao, J., Spencer, K. M., Clair, J. M. St., Weinheimer, A. J., Wisthaler, A., and Cohen, R. C.: Global and regional effects of the photochemistry of $CH_3O_2NO_2$: evidence from ARCTAS, (2011). *Atmos. Chem. Phys.*, 11, 4209–4219,doi:10.5194/acp-11-4209-2011.

Chiou, E.W., M.P. McCormick, and W.P. Chu. 1997. Global water vapor distributions in the stratosphere and upper troposphere derived from years of SAGE II observations (1986-1991). *J. Geophys. Res*., 102,D15, 19,105-19,118.

Considine, D.B., J.A. Logan, and M.A. Olsen, 2008. Evaluation of near-tropopause ozone distributions in the GMI combine stratosphere/troposphere model with ozonesonde data, *Atmos. Chem. Phys*., 8, 2365-2385.

Cooper, O. R., Langford, A. O., Parrish, D. D., and Fahey, D. W.: Challenges of a lowered U.S. ozone standard, (2015). *Science*, 348 (6239) 1096-1097, doi:10.1126/science.aaa5748.

Draxler, R.R., and G.D. Hess, 1997: Description of the HYSPLIT_4 modeling system. NOAA Tech. Memo. ERL ARL-224, NOAA Air Resources Laboratory, Silver Spring, MD, 24 pp.

Draxler, R.R. and G.D. Rolph, 2013. HYSPLIT (HYbrid Single-Particle Lagrangian Integrated Trajectory) Model access via NOAA ARL READY Website (http://www.arl.noaa.gov/HYSPLIT.php). NOAA Air Resources Laboratory, College Park, MD.

Eastham, S., D. K. Weisenstein, S.R.H. Barrett, 2014. Development and evaluation of the unified tropospheric-stratospheric chemistry extension (UCX) for the global chemistry-transport model GEOS-Chem. *Atmos. Env*. 89 (2014) 52-63. http://dx.doi.org/10.1016/j.atmosenv.2014.02.001.

Emmons, L. K., S. Walters, P. G. Hess, J.-F. Lamarque, G. G. Pfister, D. Fillmore, C. Granier, A. Guenther, D. Kinnison, T. Laepple, J. Orlando, X. Tie, G. Tyndall, C. Wiedinmyer, S. L. Baughcum, and S. Kloster, (2010), Description and evaluation of the Model for Ozone and Related Tracers, version 4 (MOZART-4), *Geosci. Model Dev*., 3, 43–67.

ENVIRON, 2010, Modeling Transport Analysis: Work Order No. 582-7-84005-FY10-21, Prepared for TCEQ, 12100 Park 35 Circle Austin, TX, July.

ENVIRON, 2011, Analysis of Ozone Contributions from Different Source Regions: Work Order No. 582-11-10396-FY11-01, Prepared for: Jocelyn Mellberg, Fernando Mercado and Mark Estes, TCEQ, 12100 Park 35 Circle Austin, TX, July.

EPA, 2014. Draft Modeling Guidance for Demonstrating Attainment of Air Quality Goals for Ozone, PM2s, and Regional Haze. U.S. Environmental Protection Agency, Office of Air Quality and Planning Standards, Research Triangle Park, North Carolina. April. http://www.epa.gov/ttn/scram/guidance/guide/Draft_O3-PM-RH_Modeling_Guidance-2014.pdf.

Fortuin, J.P.F. and H. Kelder, 1998. An ozone climatology base on ozonesonde and satellite measurements. *J. Geophys. Res.* 103, 31,709-31,734.

Hansen, A., H. E. Fuelberg and K. E. Pickering, (2010), Vertical distributions of lightning sources and flashes over Kennedy Space Center, Florida. *J. Geophys. Res.*, 115, D14203.

Herwehe, J., T. Otte, R. Mathur, S. Rao, 2011. Diagnostic analysis of ozone concentrations simulated by two regional-scale air quality models. *Atmos. Env.* 45, 5957-5969.

Holler, H., Schumann, U., (2000). EULINOX (European Lightning Nitrogen Oxides Project) final report. http://www.pa.op.dlr.de/eulinox/publications/finalrep/index.html.

Johnson, J., G. Wilson, DJ Rasmussen, and G. Yarwood. 2015. Daily Near Real-Time Ozone Modeling for Texas. WO 582-11-10365-FY14-16 Final Report. Prepared for Mark Estes, TCEQ. January.

Jung, J., S. Kemball-Cook and G. Yarwood. Interim Report on Tasks 2 and 3: Simulation of the Stratospheric Contribution to Surface Ozone. Prepared for Jim Smith, TCEQ. July, 2015.

Kemball-Cook, S., J. Johnson and G. Yarwood, 2012. Evaluating TCEQ NOx Emission Inventories Using Satellite NO_2 Data: Final Report: WO 10365-FY12-08. Prepared for Bright Dornblaser, TCEQ. August.

Kemball-Cook, S. J. Johnson, and G. Yarwood, 2013. Continuation on Use of Satellite Nitrogen Dioxide (NO_2) Data. WO 582-11-10365-FY13-10 Final Report. Prepared for Bright Dornblaser, TCEQ. August.

Kemball-Cook, S. C. Emery, E. Tai, J. Jung J. Johnson, and G. Yarwood, 2014. Improved Stratosphere-to-Troposphere Transport and Evaluation of Upper Tropospheric Winds in CAMx. WO582-11-10365-FY14-15 Final Report. Prepared for Bright Dornblaser, TCEQ. August.

Koo, B., Chien, C.-J., Tonnesen, G., Morris, R., Johnson, J., Sakulyanontvittaya, T., Piyachaturawat, P., and Yarwood, G., (2010). Natural emissions for regional modeling of background ozone and particulate matter and impacts on emissions control strategies, *Atmos. Environ.*, 44, 2372–2382., doi:10.1016/j.atmosenv.2010.02.041.

Lee, D.S., Kohler, I., Grobler, E., Rohrer, F., Sausen, R., Gallardo-Klenner, L., Olivier, J.G. J., Dentener, F.J., Bouwman, A.F., (1997). Estimations of global NOx emissions and their uncertainties. *Atmos. Environ*. 31 (12), 1735.

McLinden, C., S. Olsen, B. Hannegan, O. Wild, M.J. Prather, and J. Sundet, 2000. Stratospheric ozone in 3-D models: A simple chemistry and the cross-tropopause flux. *J. Geophys. Res*., 105, 14653-14665.

Murray, L. 2012. Stratospheric Chemistry in GEOS-Chem. http://wiki.seas.harvard.edu/geos-chem/index.php/Stratospheric_chemistry.

Orville, R.E., Huffines, G.R., Burrows,W.R., Holle, R.L., Cummins, K.L., 2002. The North American Lightning Detection Network (NALDN)-first results: 1998e2000. *Mon. Wea. Rev.* 130, 2098-2109.

Ott, L. E., K. E. Pickering, G. L. Stenchikov, D. J. Allen, A. J. DeCaria, B. Ridley, R.-F. Lin, S. Lang, and W.-K. Tao (2010), Production of lightning NOx and its vertical distribution calculated from three-dimensional cloud-scale chemical transport model simulations, *J. Geophys. Res.*, 115, doi:10.1029/2009JD011880.

Parrella, J.P., Jacob, D.J., Liang, Q., Zhang, Y., Mickley, L.J., Miller, B., Evans, M.J., Yang, X., Pyle, J. a., Theys, N., and Van Roozendael, M. 2012. Tropospheric bromine chemistry: implications for present and pre-industrial ozone and mercury. *Atmos. Chem. and Phys*. 12, 6723e6740.

Park, R. J., D. J. Jacob, B. D. Field, R. M. Yantosca, and M. Chin, (2004). Natural and transboundary pollution influences on sulfate-nitrate-ammonium aerosols in the United States: implications for policy, *J. Geophys. Res.*, 109, D15204, 10.1029/2003JD004473.

Ramboll Environ, 2015. "The User's Guide to the Comprehensive Air Quality Model with Extensions Version 6.10". Available from Ramboll Environ, 773 San Marin Drive, Novato, CA. 94998 and at http://www.camx.com.

Salby, M. 1996. Fundamentals of Atmospheric Physics. Academic Press, Elsevier. San Diego.

Sander, S.P., et al., 2011. Chemical Kinetics and Photochemical Data for Use in Atmospheric Studies, Evaluation 17. JPL Publication 10-6. http://jpldataeval.jpl.nasa.gov/pdf/JPL%2010-6%20Final%2015June2011.pdf.

Sauvage, B., R. V. Martin, A. van Donkelaar, X. Liu, K. Chance, L. Jaeglé, P. I. Palmer, S. Wu, and T. M. Fu (2007), Remote sensed and in situ constraints on processes affecting tropical tropospheric ozone, *Atmos. Chem. Phys*., 7, 815–838.

Schumann, U., Huntrieser, H., 2007. The global lightning-induced nitrogen oxides source. *Atmos. Chem. Phys*. Discuss. 7, 2623-2818.

Simon, H., Baker, K. R., Phillips, S, (2012), Compilation and interpretation of photochemical model performance statistics published between 2006 and 2012, *Atmos. Env.*, 61, 124-139.

Singh, H. B., W. H. Brune, J. H. Crawford, D. J. Jacob, and P. B. Russell, (2006). Overview of the summer 2004 Intercontinental Chemical Transport Experiment-North America (INTEX-A). *J. Geophys. Res.*, 111(D24S01), doi:10.1029/2006JD007905.

Singh, H. B., L. Salas, D. Herlth, R. Kolyer, E. Czech, M. Avery, J. H. Crawford, R. B. Pierce, G. W. Sachse, D. R. Blake, R. C. Cohen, T. H. Bertram, A. Perring, P. J. Wooldridge, J. Dibb, G. Huey, R. C. Hudman, S. Turquety, L. K. Emmons, F. Flocke, Y. Tang, G. R. Carmichael, and L. W. Horowitz, (2007). Reactive nitrogen distribution and partitioning in the North American troposphere and lowermost stratosphere. *J. Geophys. Res*., 112(D12S04), doi:10.1029/2006JD007664.

Skamarock, W. C., J. B. Klemp, J. Dudhia, D. O. Gill, D. M. Barker, W. Wang, and J. G. Powers, 2005. "A description of the Advanced Research WRF Version 2". NCAR Tech Notes-468+STR. http://www.mmm.ucar.edu/wrf/users/docs/arw_v2.pdf.

Son, S.W., N.F. Tandon, and L.M. Polvani. 2011. The fine-scale structure of the global tropopause derived from COSMIC GPS radio occultation measurements. *J. Geophys. Res*., 116(D201113), doi:10.1029/2011JD016030.

Thompson, A. M., et al. (2007a), Intercontinental chemical transport experiment Ozonesonde Network Study (IONS) 2004: 1. Summertime upper troposphere/lower stratosphere ozone over northeastern North America, *J. Geophys. Res*., 112, D12S12, doi:10.1029/2006JD007441.

Thompson, A. M., et al. (2007b), Intercontinental chemical transport experiment Ozonesonde Network Study (IONS) 2004: 2. Tropospheric ozone budgets and variability over northeastern North America, *J. Geophys. Res.*, 112, D12S13, doi:10.1029/2006JD007670.

Wang, Y., D.J. Jacob, and J.A. Logan, (1998). Global simulation of tropospheric O3-NOx-hydrocarbon chemistry, 1. Model formulation, *J. Geophys. Res.*, 103, D9,10,713-10,726.

Warneck, P. 1988. Chemistry of the Natural Atmosphere. Academic Press. San Diego.

Weisenstein, D.K., Yue, G.K., Ko, M.K.W., Sze, N.-D., Rodriguez, J.M., Scott, C.J., 1997. A two-dimensional model of sulfur species and aerosols. *J. Geophys. Res.* 102. D11, 13,019–13,035.

Weisenstein, D., S. Eastham, J. Sheng, S. Barrett, T. Peter and D. Keith. 2013. Modeling Stratospheric Aerosols at Background Levels: New Results from SOCOL and GEOS-CHEM. Presentation to SSiRC Meeting, 28-30 October 2013. www.sparcssirc.org/downloads/Weisenstein.pptx

Yantosca, et al., 2014, GEOS–Chem v9–02 Online User's Guide, http://acmg.seas.harvard.edu/geos/doc/man/.

Yarwood, G., H. Gookyoung, W.P.L. Carter, G.Z. Whitten. 2012. "Environmental Chamber Experiments to Evaluate NOx Sinks and Recycling in Atmospheric Chemical

Mechanisms." Final Report prepared for the Texas Air Quality Research Program, University of Texas, Austin, Texas (AQRP Project 10-042, February 2012).

Zhang, X., Helsdon, J.J.H., Farley, R.D., (2003a). Numerical modeling of lightning produced NOx using an explicit lightning scheme: 1. Two-dimensional simulation as a 'proof of concept'. *J. Geophys. Res.* 108 (D18) ACH 5-1-ACH 5-20.

Zhang, X., Helsdon, J.J.H., Farley, R.D., (2003b). Numerical modeling of lightning produced NOx using an explicit lightning scheme: 2. Three-dimensional simulation and expanded chemistry. *J. Geophys. Res*. 108 (D18) ACH 6-1-ACH 6-17.

APPENDIX A

Model Performance Evaluation for Initial CAMx Runs

(Excerpt from Jung et al., 2015)

Appendix A. Model Performance Evaluation of 28-Layer CAMx Runs with Original TCEQ 2012 Emission Inventory

In the initial CAMx modeling for Project 15-46, we ran CAMx for the TCEQ's June 2012 episode using the two sets of GEOS-Chem boundary conditions. The model was run with 28 layers in the vertical with layer collapsing, as shown in Figure 3-5. We made a third run in the same configuration with the CAMx zero gradient mixing ratio top boundary condition; this CAMx run did not use a model top boundary condition supplied by GEOS-Chem. We evaluated CAMx model performance in these three runs against surface ozone observations, aloft aircraft measurements of ozone and NOy, and ozonesonde profiles. In Appendix A, we present the results of the model performance evaluation at the surface and aloft that was reported in Jung et al. (2015).

A.1 Surface Performance Evaluation for Ozone

The performance of the three CAMx runs in simulating surface layer ozone was evaluated at rural sites within the 36 km CAMx modeling grid and at sites in Texas in the 4 km modeling grid. We evaluated CAMx against ground level observations from CASTNET sites within the 36 km grid (right panel of Figure 4-1). The CASTNET monitors are located in rural areas and were used in this study because regions outside of Texas and surrounding states were modeled using a 36 km grid, which cannot be expected to accurately simulate variations in ozone within an urban area.

We also evaluated ozone at monitors within Texas using the modeling output from the 4 km grid. Within the 4 km grid centered on East Texas (Figure 3-3), ozone data from the TCEQ's CAMS sites were used for the model performance evaluation. The goal of the evaluation was to determine the effect of the different CAMx top boundary conditions on modeled ground level ozone at sites within Texas. When selecting sites for display in this section, we chose sites that had the largest differences in surface ozone between the three CAMx runs. These CAMS sites tended to be in rural and coastal locations, where the boundary conditions make a larger relative contribution to the total ozone than at urban sites, which are more heavily influenced by local emissions.

Consistent with EPA Modeling Guidance (EPA, 2014), we used multiple statistical metrics in the model performance evaluation. We evaluated the root mean square error (RMSE), normalized mean bias (NMB), normalized mean error (NME), and the coefficient of determination (r^2).

A.1.1 Evaluation on 4 km Grid

Below, we summarize the main points of the model performance evaluation for surface ozone on the 4 km grid.

- The CAMx model has an overall high bias for ozone. The normalized mean bas (NMB) plots in Figures A-1 through A-6 frequently show positive values of the NMB for days with 8-hour average ozone exceeding the 40 ppb threshold.

- The high bias was generally largest in the Zero Gradient Run, and smallest in the G-C std CAMx run, with the G-C UCX CAMx run NMB often falling between those of the other two runs.

- The three CAMx runs agree well for surface ozone throughout most of the June 2012 episode. This indicates that the effect of the model top boundary on ground level ozone in Texas is generally small.

- The largest differences in surface layer ozone among all three runs occurred during June 10-15, a period of relatively low observed ozone at most East Texas CAMS sites.

- During the last week of June, East Texas experienced a period of widespread high ozone, and differences among the three CAMx runs were relatively small. At most sites, the time series for the three runs are nearly indistinguishable during June 24-29.

- Differences between the two CAMx runs using the GEOS-Chem top boundary condition were generally smaller than differences between the CAMx run with Zero Gradient Mixing Ratio boundary condition and the two CAMx runs with using GEOS-Chem boundary conditions.

- At the coastal sites Aransas Pass (Figure A-2) and Galveston (Figure A-3), differences between the three CAMx runs were largest of all East Texas monitors and the differences reached their largest values during the low ozone period June 10-15. Even for these coastal sites, the period with high ozone at end of June showed very little difference in ozone among the three runs.

In general, the differences in surface ozone between the three CAMx runs are small, which indicates that the influence of the top boundary condition is generally small at the surface, especially during periods of high ozone. However, differences in the specification of the top boundary condition affected surface 1-hour average ozone by as much as 5 ppb during the June 2012 episode.

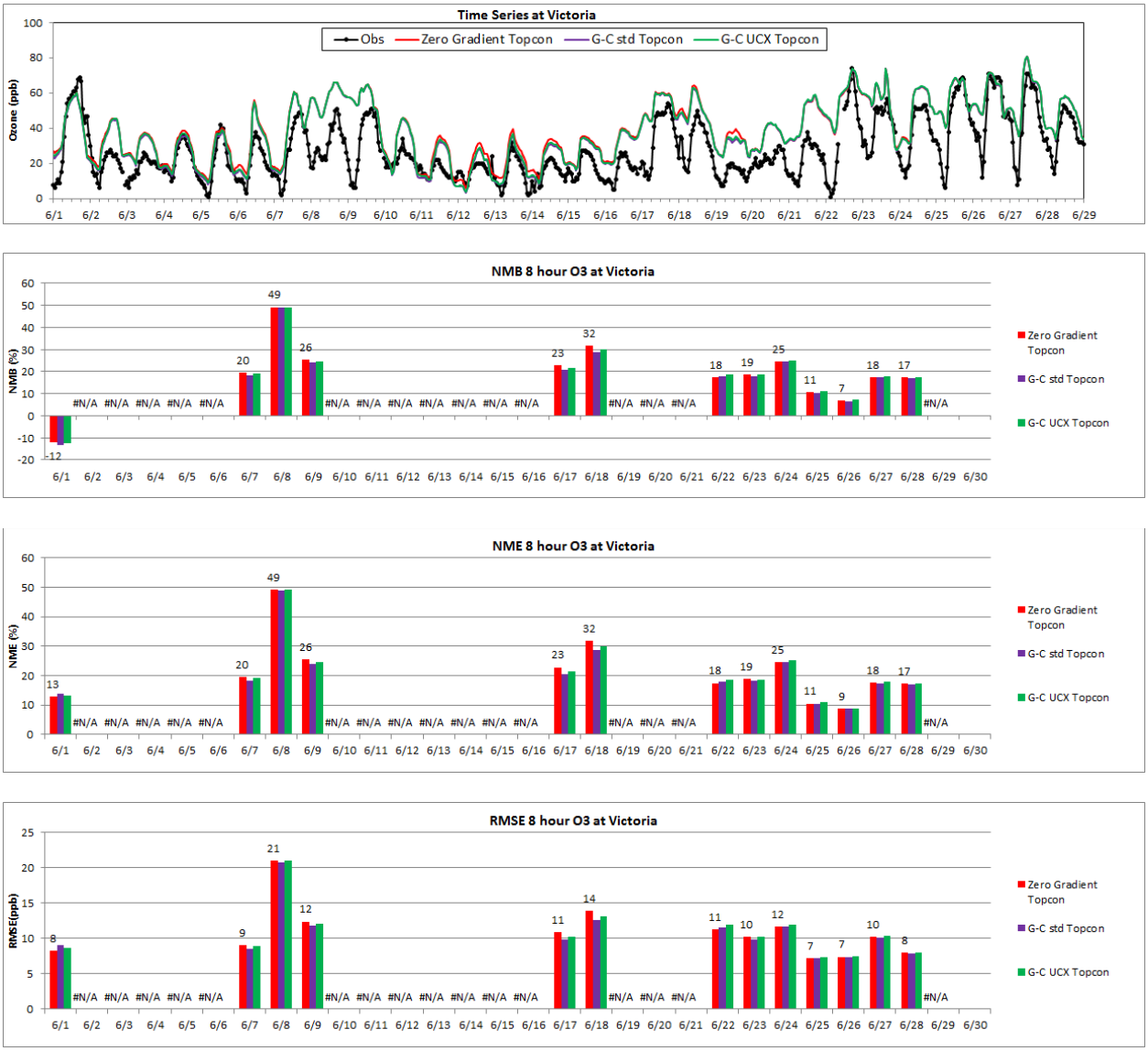

Figure A-1. Upper panel: observed 1-hour ozone (black) at the Victoria (CAMS 87) monitor versus modeled 1-hour average surface layer ozone during the June 1-30, 2012 period for the Zero Gradient CAMx Run (red), G-C Std CAMx run (purple) and G-C UCX CAMx Run (green). 2nd panel from top: normalized mean bias (NMB) for 8-hour average ozone. 3rd panel from top: normalized mean error (NME) for 8-hour average ozone. 4th panel from top: root mean square error (RMSE) for 8-hour average ozone.

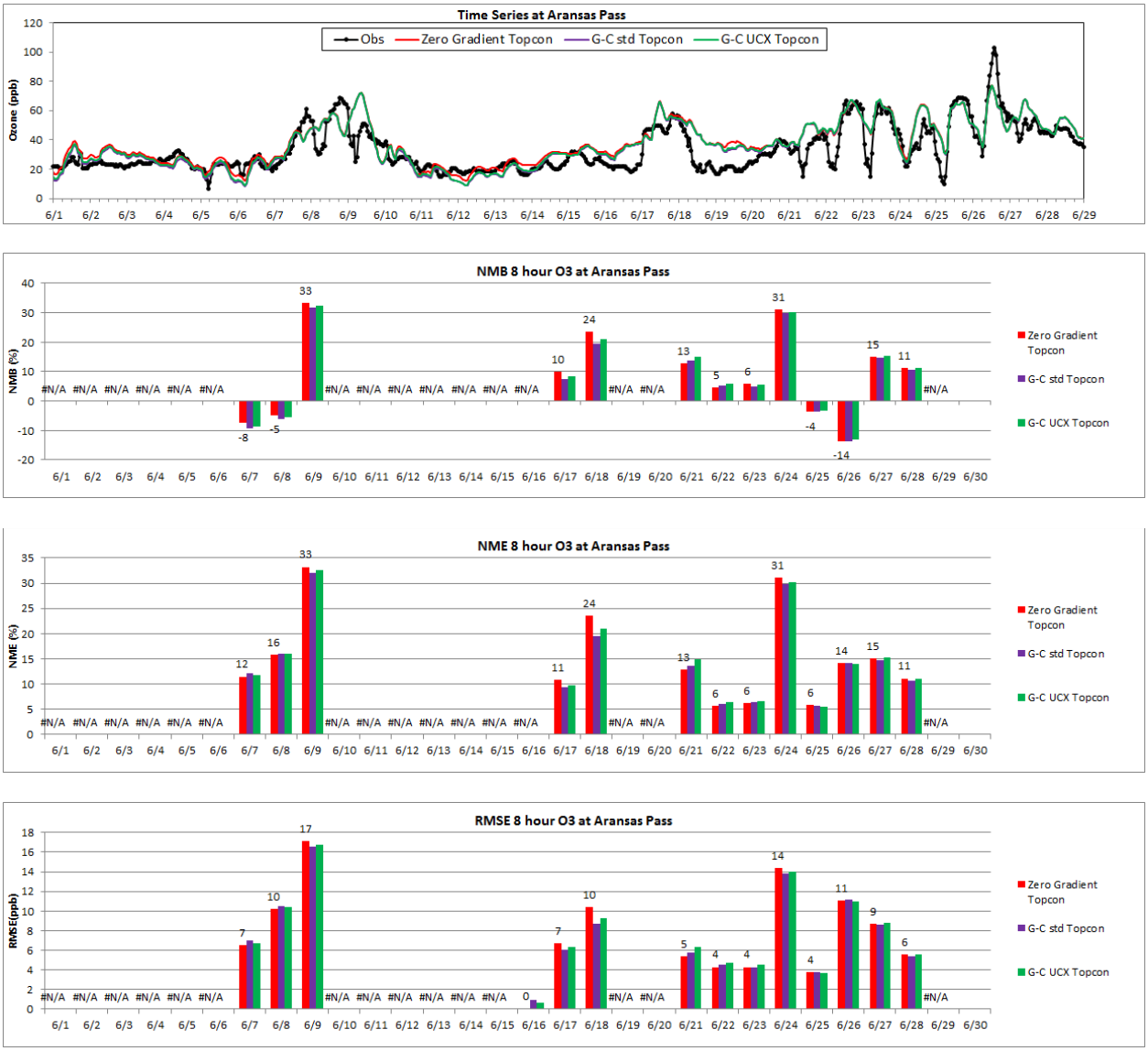

Figure A-2. Upper panel: observed 1-hour ozone (black) at the Aransas Pass (CAMS 659) monitor versus modeled 1-hour average surface layer ozone during the June 1-30, 2012 period for the Zero Gradient CAMx Run (red), G-C Std CAMx run (purple) and G-C UCX CAMx Run (green). 2nd panel from top: normalized mean bias (NMB) for 8-hour average ozone. 3rd panel from top: normalized mean error (NME) for 8-hour average ozone. 4th panel from top: root mean square error (RMSE) for 8-hour average ozone.

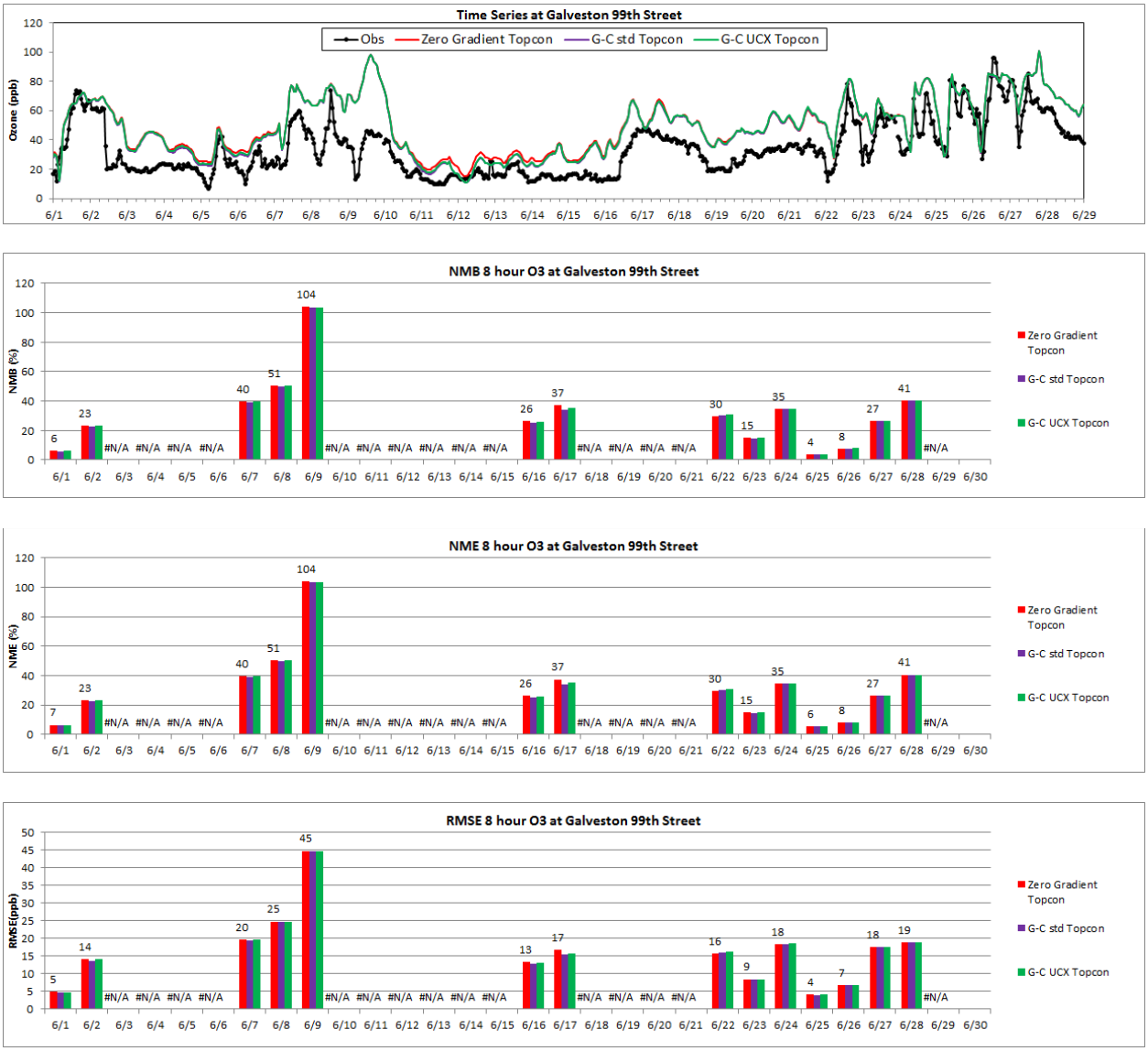

Figure A-3. Upper panel: observed 1-hour ozone (black) at the Galveston 99th St. (CAMS 1034) monitor versus modeled 1-hour average surface layer ozone during the June 1-30, 2012 period for the Zero Gradient CAMx Run (red), G-C Std CAMx run (purple) and G-C UCX CAMx Run (green). 2nd panel from top: normalized mean bias (NMB) for 8-hour average ozone. 3rd panel from top: normalized mean error (NME) for 8-hour average ozone. 4th panel from top: root mean square error (RMSE) for 8-hour average ozone.

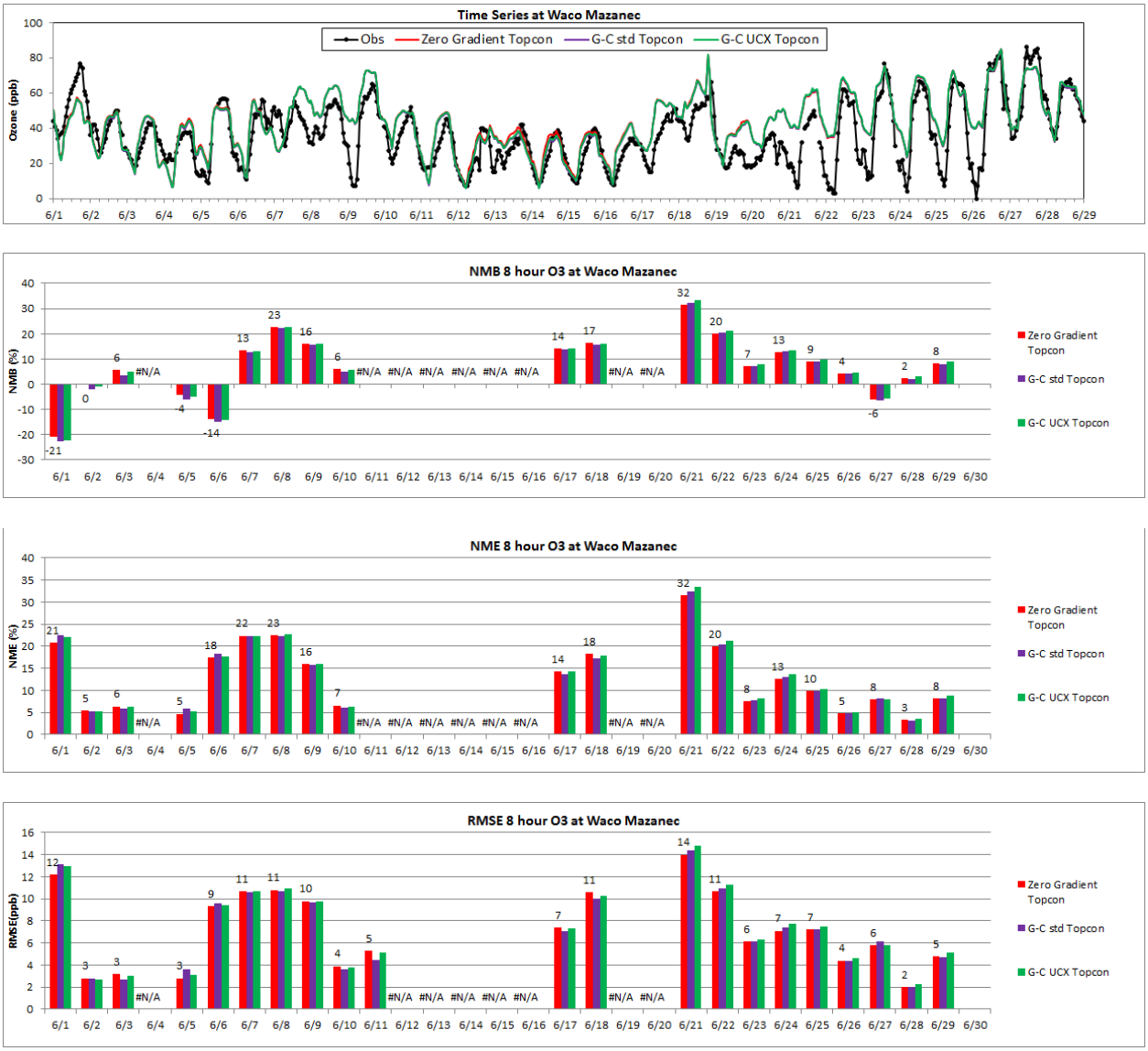

Figure A-4. Upper panel: observed 1-hour ozone (black) at the Waco Mazanec (CAMS 1037) monitor versus modeled 1-hour average surface layer ozone during the June 1-30, 2012 period for the Zero Gradient CAMx Run (red), G-C Std CAMx run (purple) and G-C UCX CAMx Run (green). 2nd panel from top: normalized mean bias (NMB) for 8-hour average ozone. 3rd panel from top: normalized mean error (NME) for 8-hour average ozone. 4th panel from top: root mean square error (RMSE) for 8-hour average ozone.

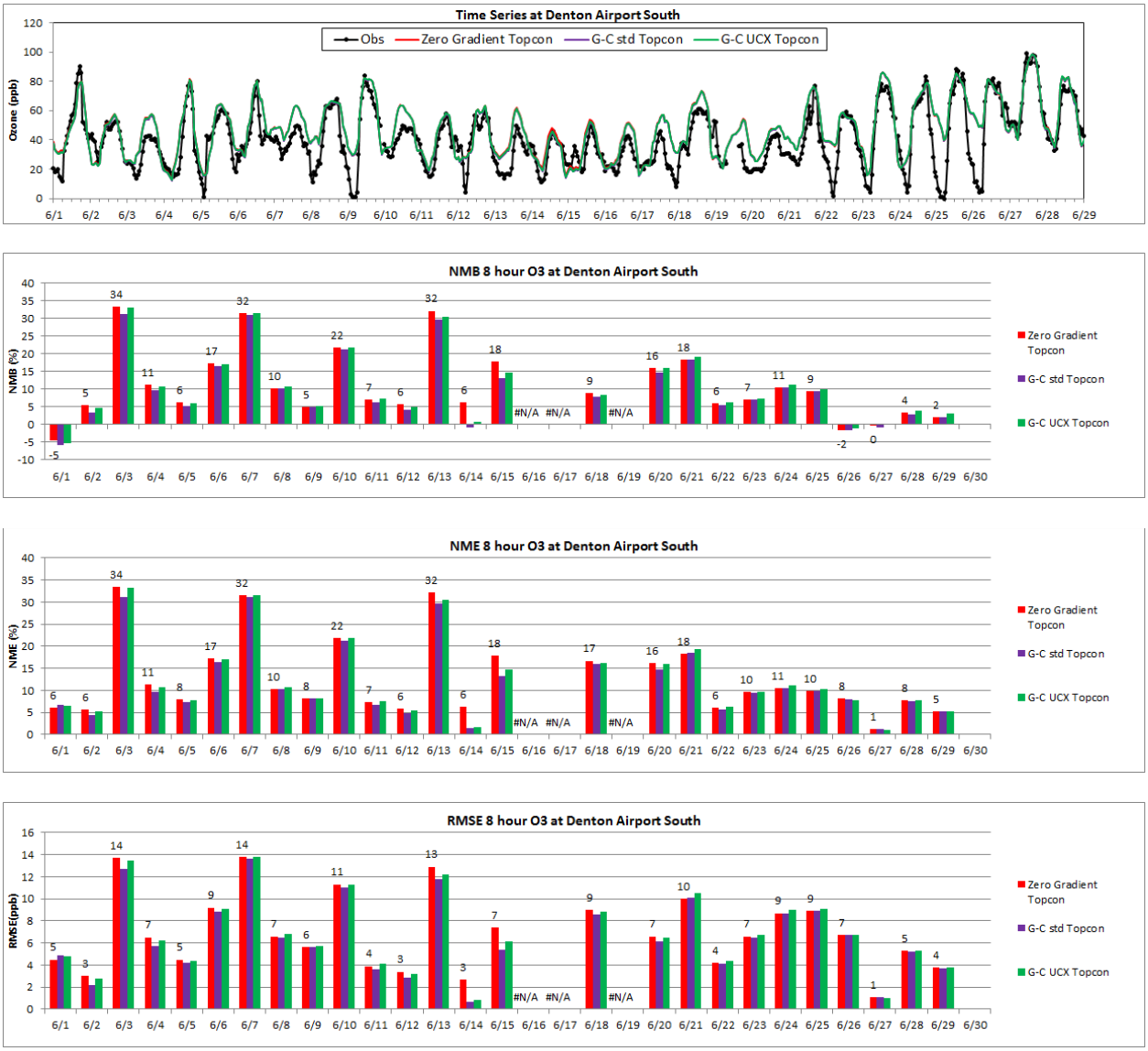

Figure A-5. Upper panel: observed 1-hour ozone (black) at the Denton Airport South (CAMS 56) monitor versus modeled 1-hour average surface layer ozone during the June 1-30, 2012 period for the Zero Gradient CAMx Run (red), G-C Std CAMx run (purple) and G-C UCX CAMx Run (green). 2nd panel from top: normalized mean bias (NMB) for 8-hour average ozone. 3rd panel from top: normalized mean error (NME) for 8-hour average ozone. 4th panel from top: root mean square error (RMSE) for 8-hour average ozone.

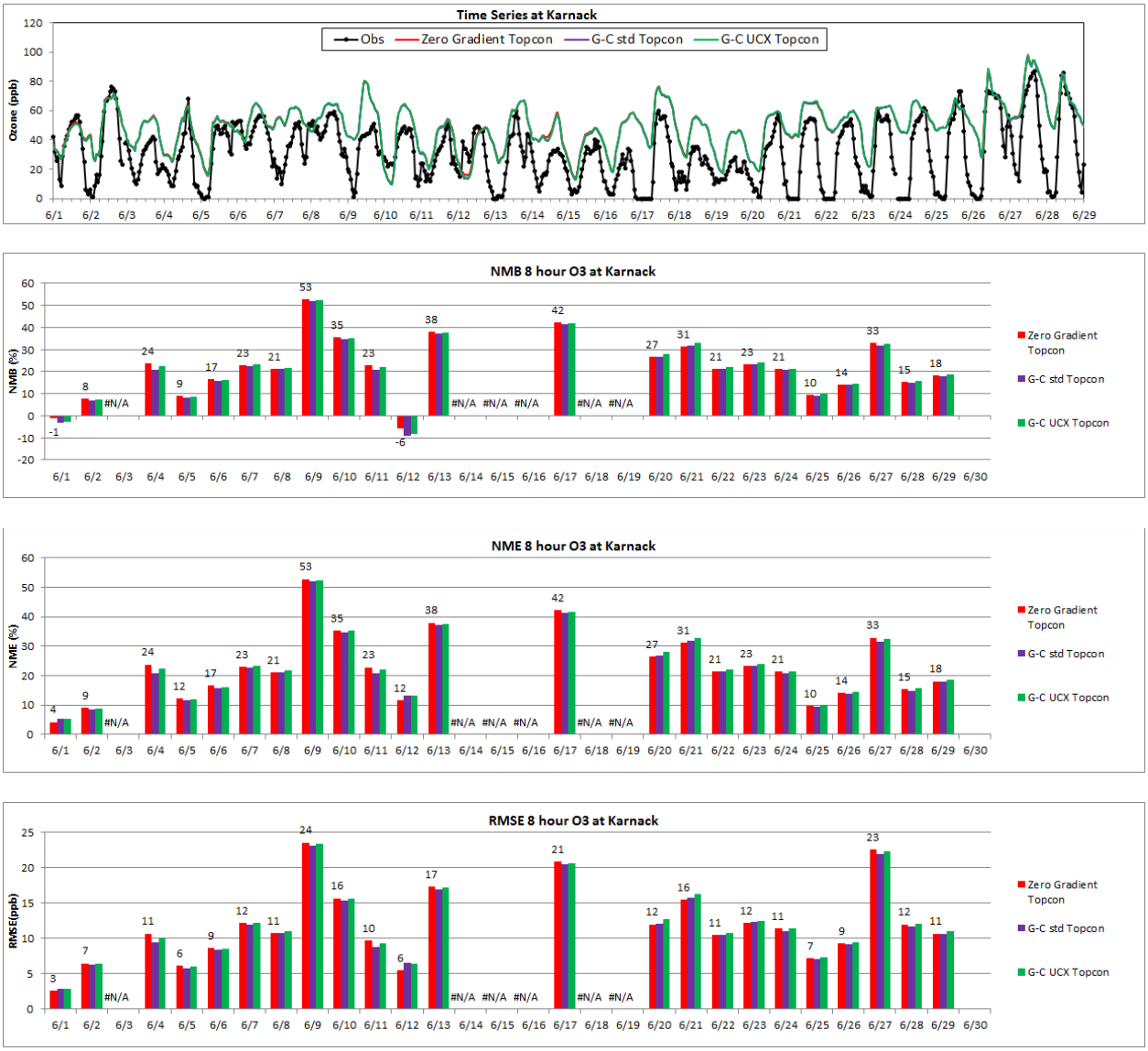

Figure A-6. Upper panel: observed 1-hour ozone (black) at the Karnack (CAMS 85) monitor versus modeled 1-hour average surface layer ozone during the June 1-30, 2012 period for the Zero Gradient CAMx Run (red), G-C Std CAMx run (purple) and G-C UCX CAMx Run (green). 2nd panel from top: normalized mean bias (NMB) for 8-hour average ozone. 3rd panel from top: normalized mean error (NME) for 8-hour average ozone. 4th panel from top: root mean square error (RMSE) for 8-hour average ozone.

A.1.2 Evaluation on 36 km Grid

In Figure A-7 through Figure A-20, we summarize the surface model performance evaluation on the continental-scale 36 km grid. Figure A-7 through Figure A-20 show observed and modeled 1-hour ozone time series for a subset of sites shown in the right panel of Figure 4-1. Figure A-21 shows the episode average MNB for 8-hour ozone for the June 1-30, 2012 period. All three runs have a pronounced high bias over the eastern U.S. and minimal or low bias over the western U.S. The tendency of ozone models to overestimate ozone in the southeastern U.S. and Ohio River Valley has been noted previously in TCEQ's CAMx modeling (e.g. ENVIRON, 2010, 2011) as well as by other groups using other regional air quality models (e.g. Herwehe et al., 2011). Because the episode average differences between the two CAMx runs are small for most sites, we focus on time series of observed ground layer ozone and modeled surface layer ozone for both runs.

The results of the time series comparison are summarized below:

- Sites that are in the eastern U.S. (Abington, CT) and/or are at relatively low elevation (Ann Arbor, MN) tended to have smaller and less frequent differences among the three model runs. Sites that are at higher elevation or are otherwise influenced by the presence of nearby high terrain showed more frequent and larger differences between the runs.

- The sites with the largest sustained differences between CAMx runs are the Florida sites Indian River Lagoon (Figure A-7) and Everglades National Park (Figure A-8). At both of these sites, the Zero Gradient CAMx run had consistently higher ozone than the two CAMx runs with GEOS-Chem top boundary conditions. Differences between the two CAMx runs with GEOS-Chem top boundary conditions were small.

- At the Texas CASTNET sites, Big Bend (Figure A-10), Alabama-Coushatta (Figure A-9) and Palo Duro (Figure A-11), differences between the three runs were small.

- At western sites (Lassen Volcanic Park [Figure A-12] and Mount Rainier [Figure A-16]), there were large and sustained differences between the Zero Gradient and the two GEOS-Chem topcon CAMx runs. Where differences were apparent between the CAMx runs with GEOS-Chem top boundary conditions, the G-C UCX CAMx run generally had higher ozone than the G-C Std CAMx run.

- Sites at higher elevations (Figure A-13, Figure A-14 and Figure A-15) tended to have larger differences between the runs, while eastern sites (Figure A-20) and sites in the Midwest (Figure A-17) and Southeast (Figure A-18) tended to have smaller differences between the Zero Gradient and GEOS-Chem CAMx runs.

- Where the Zero Gradient CAMx run had a positive bias, the use of the GEOS-Chem top boundary condition improved model performance by lowering surface layer ozone so that modeled ozone agreed more closely with observations. Agreement was generally

better for the CAMx G-C Std run than the CAMx G-C UCX because the UCX case generally had higher ozone. The NMB for 8-hour average ozone shows a similar pattern (Figure A-21).

- Where the Zero Gradient CAMx run had a negative bias, the use of the GEOS-Chem top boundary condition degraded model performance by lowering surface layer ozone so that modeled ozone agreed less closely with observations. Agreement was generally better for the CAMx G-C UCX run than the CAMx G-C Std run because the CAMx G-C UCX run generally had higher ozone.

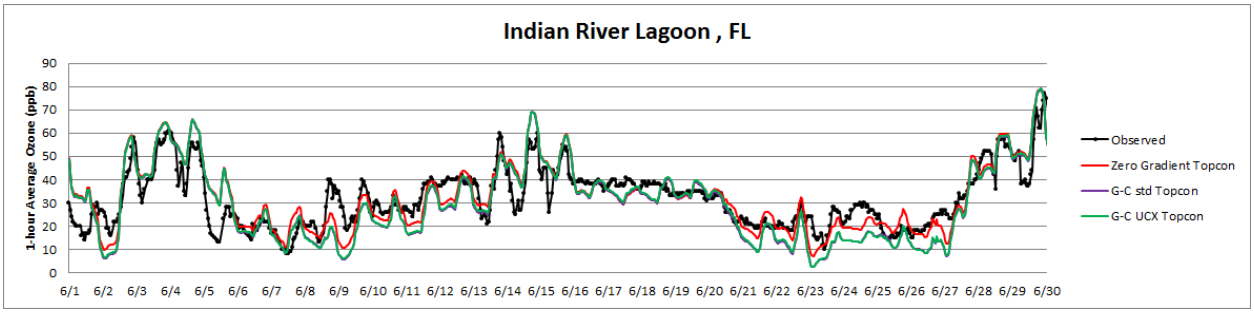

Figure A-7. Indian River Lagoon, FL. Elevation 2 m.

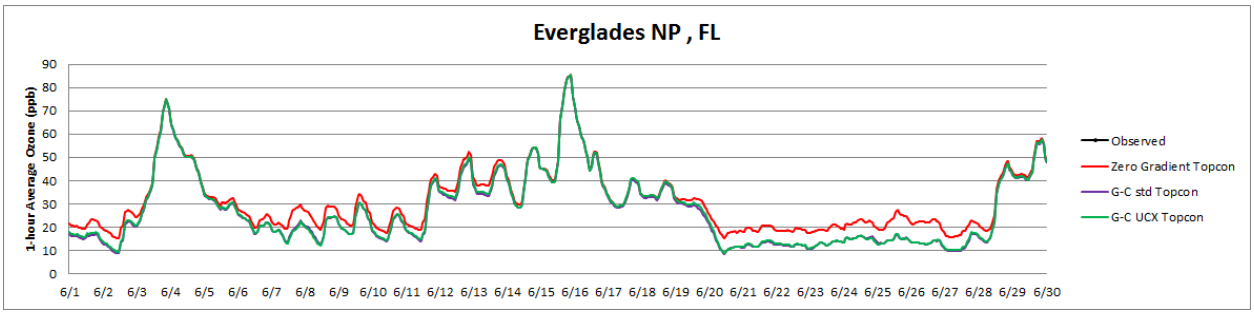

Figure A-8. Everglades NP, FL. Elevation 2 m. (Note: no observations available).

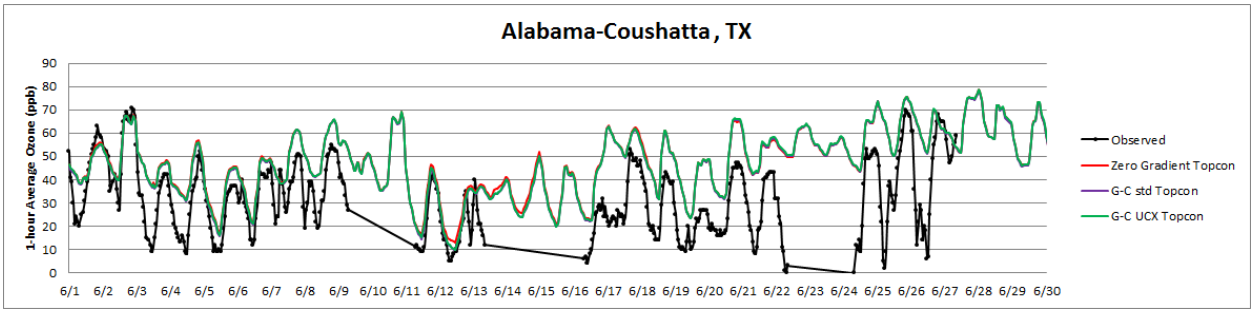

Figure A-9. Alabama-Coushatta, TX. Elevation 105 m.

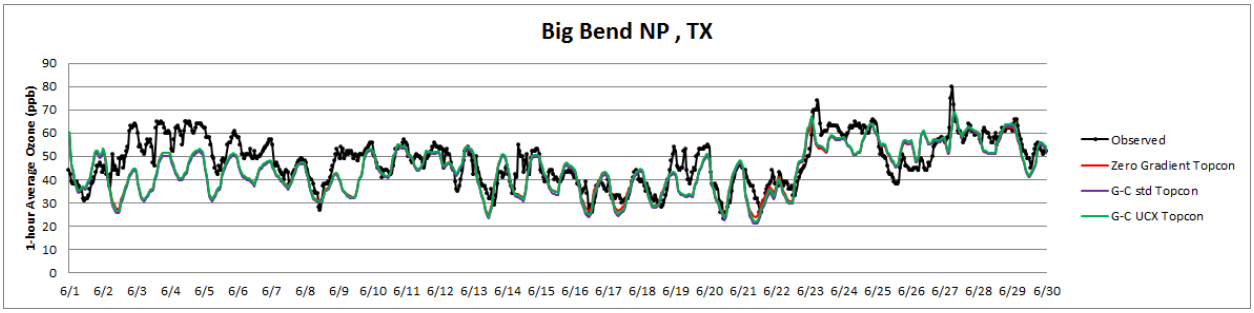

Figure A-10. Big Bend NP, TX. Elevation 1,052 m.

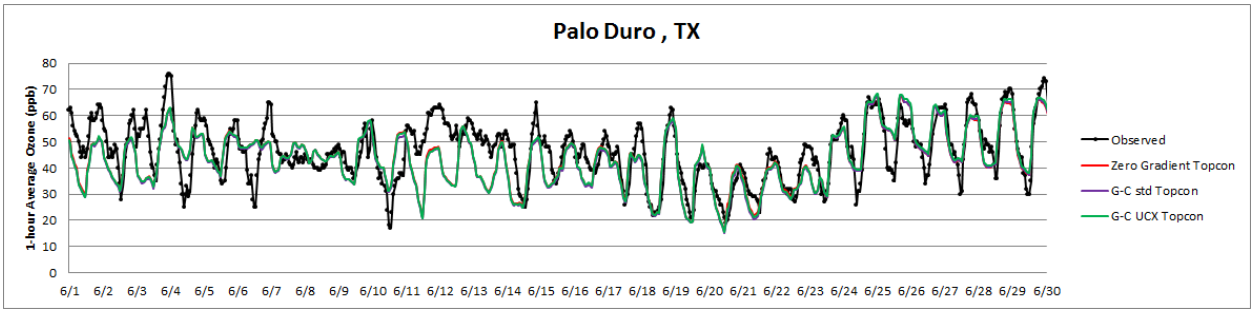

Figure A-11. Palo Duro, TX. Elevation 1,053 m.

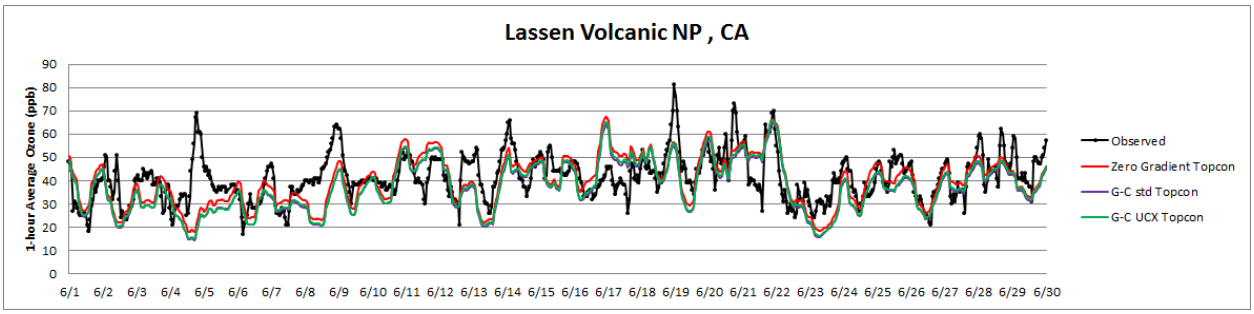

Figure A-12. Lassen Volcanic NP, CA. Elevation 1,756 m.

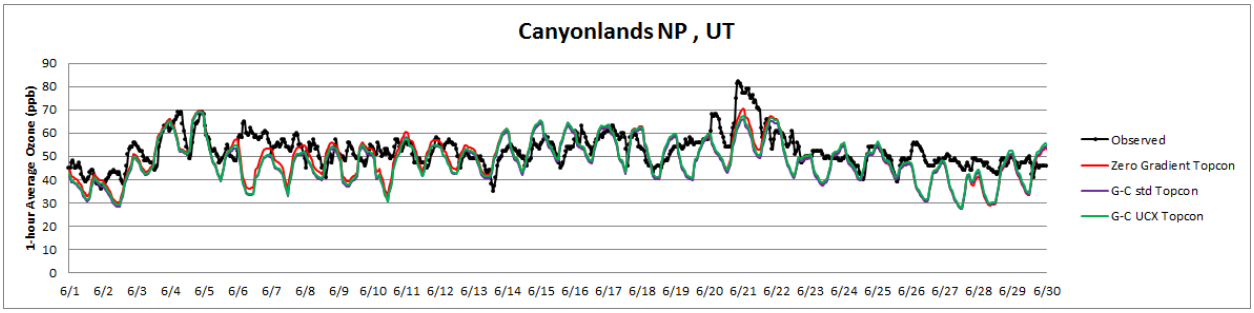

Figure A-13. Canyonlands NP, UT. Elevation 1,809 m.

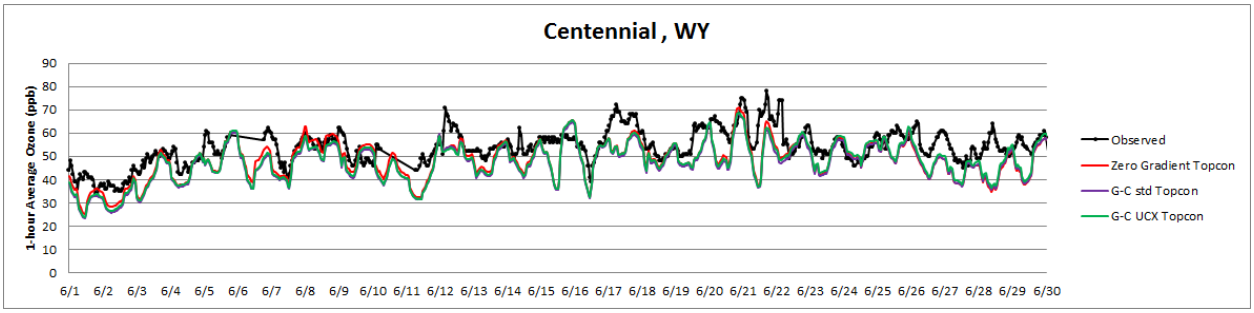

Figure A-14. Centennial, WY. Elevation 3,175 m.

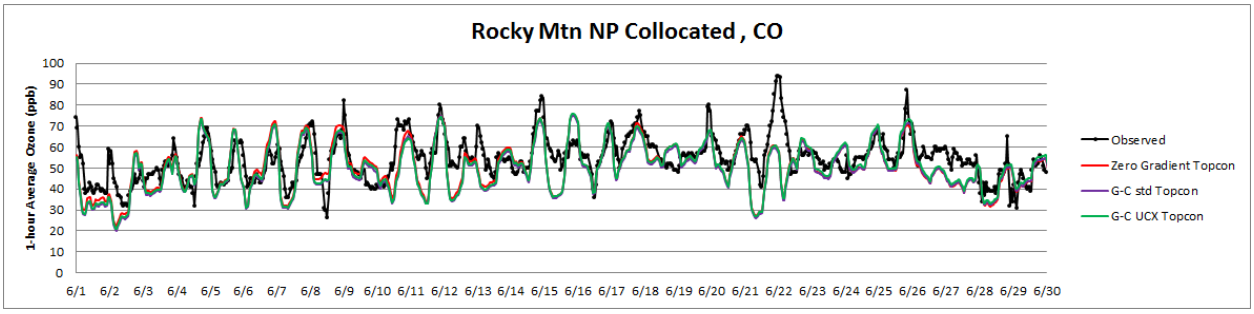

Figure A-15. Rocky Mountain National Park, Collocated. Elevation 2,742 m.

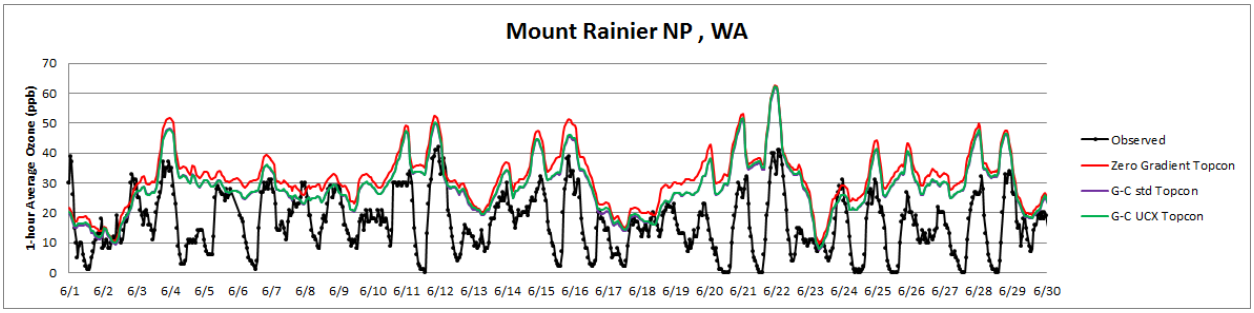

Figure A-16. Mount Rainier, WA. Elevation 415 m.

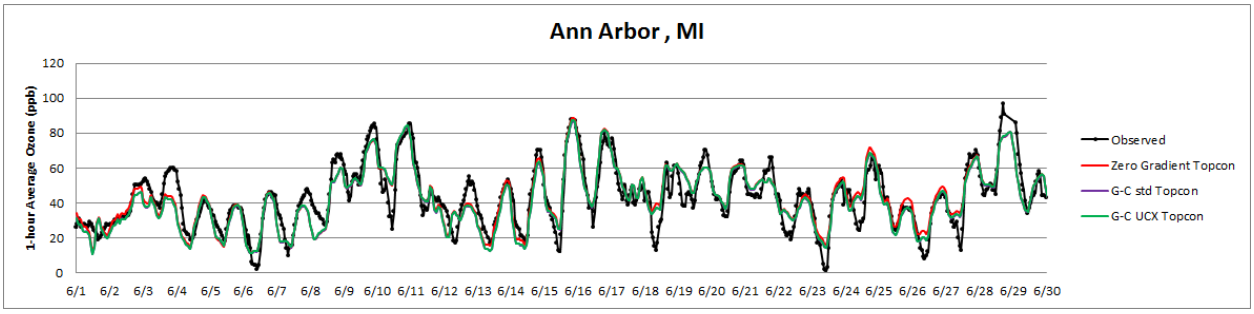

Figure A-17. Ann Arbor, MI. Elevation 266 m.

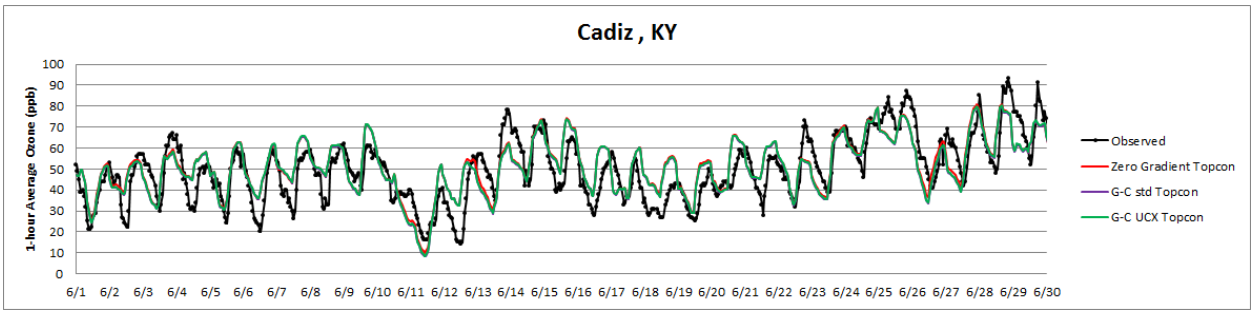

Figure A-18. Cadiz, KY. Elevation 190 m.

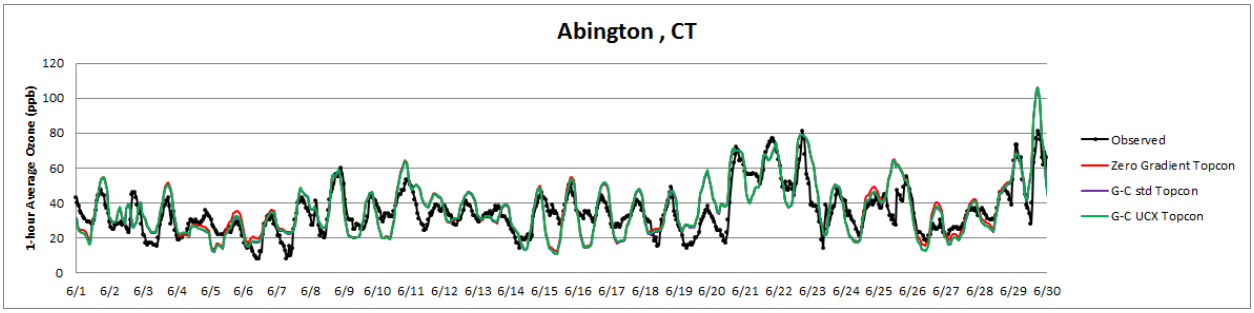

Figure A-19. Abington, CT. Elevation 202 m.

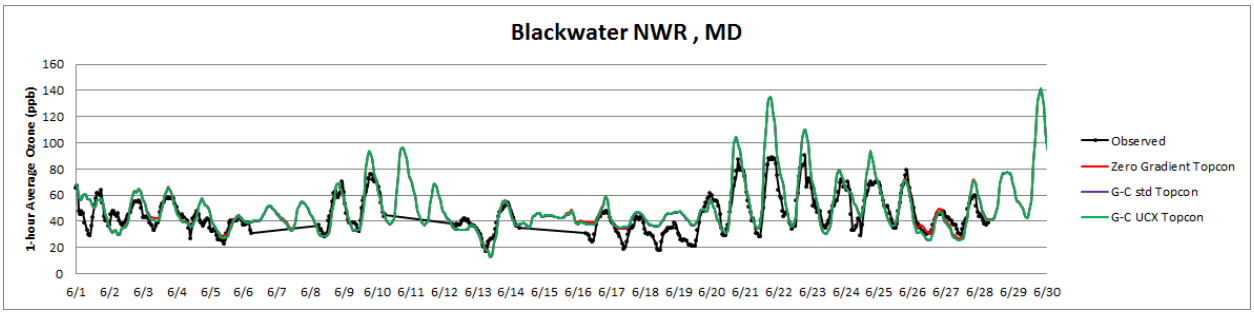

Figure A-20. Blackwater NWR, MD. Elevation 1 m.

Table A-1. Summary of CASTNET Site Episode Average Statistical Evaluation. Sites with positive (negative) NMB are shaded red (green).

	NMB (%)			NME (%)			R^2		
Site ID	Zero Gradient	GEOS-Chem Standard	GEOS-Chem UCX	Zero Gradient	GEOS-Chem Standard	GEOS-Chem UCX	Zero Gradient	GEOS-Chem Standard	GEOS-Chem UCX
ABT147	2.02	1.16	1.61	14.19	13.76	13.87	0.56	0.58	0.58
ACA416	-9.04	-8.43	-8.00	16.59	16.13	16.03	0.32	0.32	0.32
ALC188	15.32	14.52	15.15	17.59	17.30	17.69	0.34	0.33	0.32
ALH157	-4.32	-5.61	-5.00	11.45	11.86	11.73	0.63	0.63	0.63
ANA115	-3.08	-4.80	-4.26	10.65	11.05	10.92	0.68	0.68	0.68
ARE128	-2.90	-3.77	-3.32	15.77	16.12	16.03	0.58	0.59	0.59
ASH135	-15.68	-17.17	-16.45	21.99	23.40	22.87	0.04	0.04	0.04
BBE401	-8.76	-9.50	-8.01	13.25	13.93	13.34	0.26	0.25	0.25
BEL116	8.72	8.20	8.75	21.86	21.85	22.00	0.69	0.69	0.69
BFT142	35.07	35.16	35.96	35.07	35.16	35.96	0.99	0.99	0.99
BVL130	-1.17	-2.78	-2.12	10.84	10.96	10.91	0.51	0.51	0.51
BWR139	8.41	7.52	7.91	15.08	14.97	15.06	0.76	0.76	0.76
CAD150	7.27	6.30	6.83	12.41	12.33	12.59	0.54	0.53	0.53
CAN407	-6.44	-8.83	-7.19	12.70	13.75	13.22	0.31	0.27	0.26
CDR119	20.36	18.45	19.09	20.86	19.47	19.93	0.45	0.43	0.44
CDZ171	-1.31	-2.62	-2.07	13.52	13.73	13.67	0.43	0.42	0.43
CHA467	-6.48	-7.65	-5.86	14.65	14.57	14.29	0.28	0.30	0.29
CHE185	-3.44	-4.11	-3.47	12.10	12.40	12.27	0.48	0.47	0.47
CKT136	3.68	2.49	3.00	15.25	15.11	15.16	0.34	0.35	0.35
CND125	13.41	12.31	12.87	17.38	17.15	17.42	0.47	0.46	0.46
CNT169	-9.70	-11.71	-10.13	11.72	12.99	12.15	0.34	0.35	0.34
COW137	19.52	18.25	18.86	20.84	20.16	20.60	0.17	0.14	0.15
CTH110	-4.04	-4.95	-4.46	14.57	14.82	14.72	0.36	0.38	0.38
CVL151	12.91	11.75	12.38	14.20	13.40	13.85	0.63	0.61	0.62

Site ID	NMB (%)			NME (%)			R^2		
	Zero Gradient	GEOS-Chem Standard	GEOS-Chem UCX	Zero Gradient	GEOS-Chem Standard	GEOS-Chem UCX	Zero Gradient	GEOS-Chem Standard	GEOS-Chem UCX
DCP114	2.70	1.22	1.78	12.30	12.58	12.50	0.55	0.55	0.55
ESP127	7.03	5.78	6.32	13.94	13.79	13.95	0.46	0.45	0.45
GAS153	15.49	14.35	14.92	20.30	19.93	20.19	0.45	0.43	0.43
GLR468	-8.64	-14.71	-13.59	11.62	15.76	14.94	0.10	0.06	0.06
GRB411	-10.40	-13.52	-11.91	14.75	16.51	15.78	0.21	0.22	0.22
GRC474	-3.84	-6.15	-4.39	10.00	10.70	10.52	0.48	0.45	0.43
GRS420	-4.48	-5.47	-5.05	16.85	17.08	17.00	0.22	0.21	0.22
GTH161	-1.19	-2.33	-0.01	12.40	13.27	13.20	0.29	0.19	0.19
HOW132	-4.88	-4.61	-4.04	18.85	18.54	18.42	0.35	0.35	0.34
HOX148	-0.76	-2.36	-1.80	11.41	11.35	11.32	0.50	0.52	0.52
HWF187	6.23	5.21	5.74	15.70	16.17	16.30	0.32	0.32	0.32
IRL141	6.48	4.79	5.42	12.41	12.42	12.52	0.44	0.43	0.43
JOT403	-18.19	-20.67	-19.34	19.33	21.51	20.53	0.45	0.43	0.42
KEF112	3.81	2.68	3.16	15.11	15.15	15.28	0.44	0.46	0.46
KNZ184	-6.83	-8.22	-7.58	11.72	12.53	12.17	0.58	0.58	0.59
LAV410	-9.34	-14.70	-13.31	16.80	19.07	18.47	0.09	0.09	0.10
LRL117	15.43	13.81	14.38	20.26	19.32	19.64	0.42	0.42	0.43
MAC426	1.86	0.73	1.26	10.96	11.20	11.15	0.56	0.55	0.55
MCK131	0.63	-0.47	0.06	11.46	11.58	11.59	0.51	0.51	0.51
MCK231	1.34	0.24	0.78	11.55	11.61	11.64	0.51	0.51	0.51
MEV405	1.12	-1.07	0.76	11.45	11.38	11.66	0.30	0.28	0.27
MKG113	7.74	6.37	6.82	14.83	14.41	14.56	0.62	0.62	0.62
MOR409	31.68	26.82	28.12	31.68	26.82	28.12	0.28	0.27	0.27
OXF122	-3.71	-5.43	-4.90	10.23	11.06	10.81	0.69	0.68	0.69
PAL190	-10.17	-10.79	-9.79	13.63	14.08	13.61	0.40	0.40	0.40
PAR107	10.06	8.24	8.86	13.67	12.89	13.16	0.44	0.43	0.43

Site ID	NMB (%)			NME (%)			R^2		
	Zero Gradient	GEOS-Chem Standard	GEOS-Chem UCX	Zero Gradient	GEOS-Chem Standard	GEOS-Chem UCX	Zero Gradient	GEOS-Chem Standard	GEOS-Chem UCX
PED108	16.57	15.37	16.01	19.25	18.52	18.95	0.25	0.25	0.26
PET427	-1.36	-2.90	-1.16	9.27	9.26	9.30	0.52	0.53	0.52
PIN414	-7.86	-11.64	-10.79	15.55	17.20	16.86	0.26	0.28	0.28
PNF126	5.05	3.59	4.15	16.35	16.28	16.37	0.24	0.24	0.24
PRK134	-14.66	-16.59	-16.16	16.45	17.58	17.25	0.43	0.48	0.48
PSU106	9.13	8.02	8.53	13.83	13.66	13.80	0.65	0.66	0.66
QAK172	-3.03	-4.84	-4.27	12.61	12.89	12.77	0.32	0.32	0.33
ROM206	-6.68	-8.51	-7.03	13.74	14.29	14.02	0.31	0.31	0.30
ROM406	-12.84	-14.62	-13.21	15.84	16.94	16.18	0.37	0.37	0.36
SAL133	-4.67	-6.40	-5.83	9.45	10.34	10.05	0.69	0.69	0.69
SAN189	-16.12	-17.93	-17.37	17.81	19.48	19.09	0.32	0.34	0.34
SEK430	-20.74	-23.48	-22.30	21.45	23.80	22.71	0.57	0.59	0.59
SHN418	-4.40	-5.69	-5.16	16.70	17.12	16.99	0.19	0.19	0.19
SND152	10.63	9.79	10.22	13.16	12.81	13.03	0.57	0.56	0.56
SPD111	15.80	14.36	14.87	18.89	18.43	18.67	0.32	0.31	0.31
STK138	-9.98	-11.92	-11.34	12.54	13.89	13.47	0.57	0.59	0.59
SUM156	7.01	5.40	6.01	13.37	12.45	12.80	0.07	0.07	0.07
THR422	-16.15	-19.61	-18.83	17.83	20.21	19.49	0.08	0.11	0.11
UVL124	-4.92	-6.28	-5.81	10.58	11.31	11.12	0.72	0.73	0.73
VIN140	-1.78	-3.03	-2.43	11.10	11.14	11.07	0.50	0.51	0.51
VOY413	-20.24	-22.90	-22.58	21.47	23.32	23.08	0.34	0.41	0.41
VPI120	0.22	-1.33	-0.76	12.93	12.98	12.97	0.31	0.31	0.31
WNC429	-16.33	-18.48	-17.40	17.21	19.04	18.19	0.38	0.39	0.39
WSP144	1.99	0.95	1.45	15.81	15.96	16.02	0.62	0.62	0.62
WST109	-8.72	-10.90	-10.45	15.58	17.52	17.28	0.10	0.13	0.13
YEL408	-11.02	-14.50	-12.92	15.48	17.49	16.73	0.20	0.20	0.20

Site ID	NMB (%)			NME (%)			R^2		
	Zero Gradient	GEOS-Chem Standard	GEOS-Chem UCX	Zero Gradient	GEOS-Chem Standard	GEOS-Chem UCX	Zero Gradient	GEOS-Chem Standard	GEOS-Chem UCX
YOS204	-6.43	-10.03	-8.64	10.92	12.67	11.73	0.51	0.55	0.55
YOS404	-7.28	-10.89	-9.51	11.22	13.16	12.19	0.52	0.55	0.56
Overall	-3.07	-4.82	-3.92	14.31	14.92	14.68	0.37	0.36	0.37

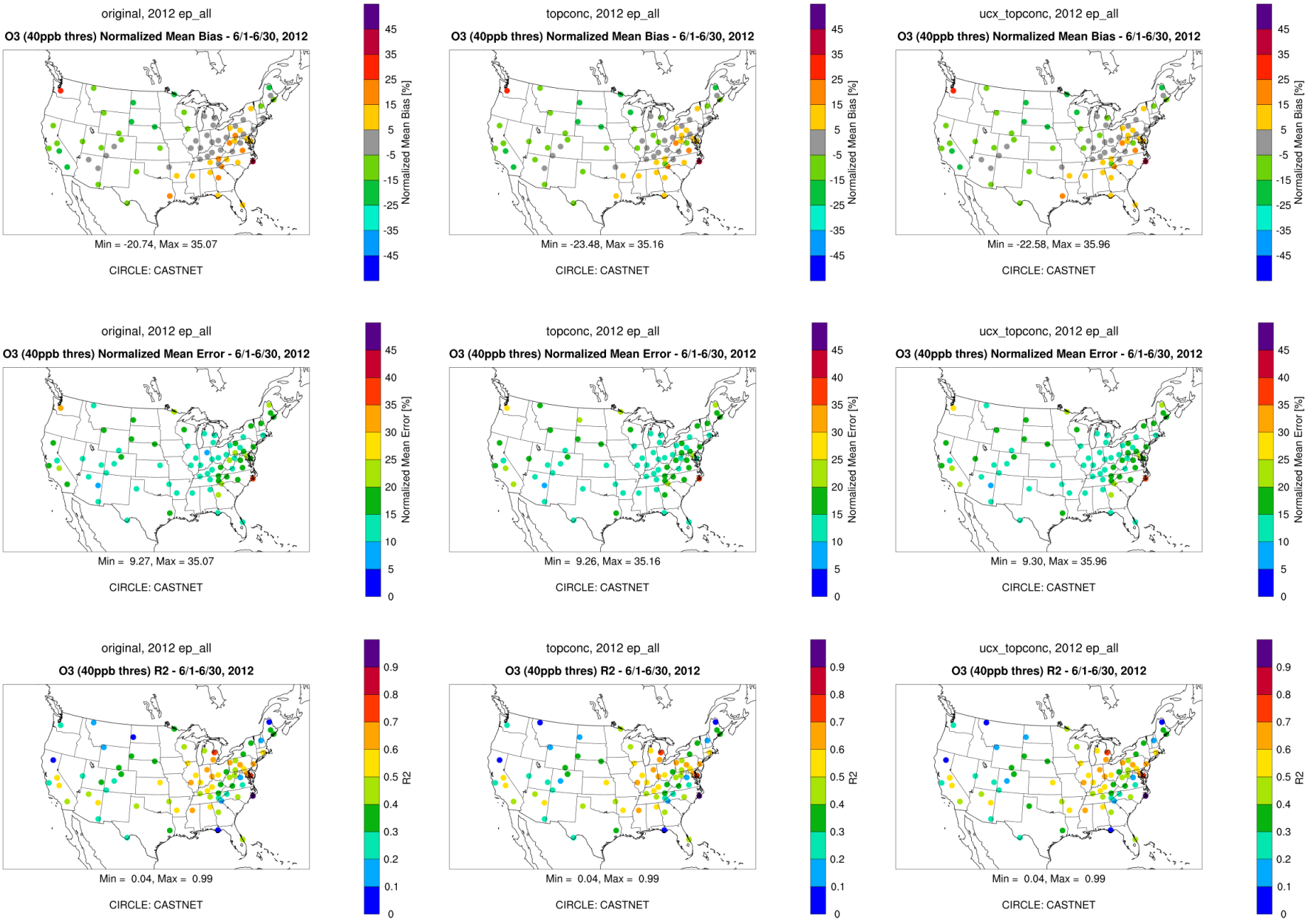
original, 2012 ep_all
O3 (40ppb thres) Normalized Mean Bias - 6/1-6/30, 2012
Min = -20.74, Max = 35.07
CIRCLE: CASTNET
Normalized Mean Bias [%]
topconc, 2012 ep_all
O3 (40ppb thres) Normalized Mean Bias - 6/1-6/30, 2012
Min = -23.48, Max = 35.16
CIRCLE: CASTNET
Normalized Mean Bias [%]
ucx_topconc, 2012 ep_all
O3 (40ppb thres) Normalized Mean Bias - 6/1-6/30, 2012
Min = -22.58, Max = 35.96
CIRCLE: CASTNET
Normalized Mean Bias [%]
original, 2012 ep_all
O3 (40ppb thres) Normalized Mean Error - 6/1-6/30, 2012
Min = 9.27, Max = 35.07
CIRCLE: CASTNET
Normalized Mean Error [%]
topconc, 2012 ep_all
O3 (40ppb thres) Normalized Mean Error - 6/1-6/30, 2012
Min = 9.26, Max = 35.16
CIRCLE: CASTNET
Normalized Mean Error [%]
ucx_topconc, 2012 ep_all
O3 (40ppb thres) Normalized Mean Error - 6/1-6/30, 2012
Min = 9.30, Max = 35.96
CIRCLE: CASTNET
Normalized Mean Error [%]
original, 2012 ep_all
O3 (40ppb thres) R2 - 6/1-6/30, 2012
Min = 0.04, Max = 0.99
CIRCLE: CASTNET
R2
topconc, 2012 ep_all
O3 (40ppb thres) R2 - 6/1-6/30, 2012
Min = 0.04, Max = 0.99
CIRCLE: CASTNET
R2
ucx_topconc, 2012 ep_all
O3 (40ppb thres) R2 - 6/1-6/30, 2012
Min = 0.04, Max = 0.99
CIRCLE: CASTNET
R2

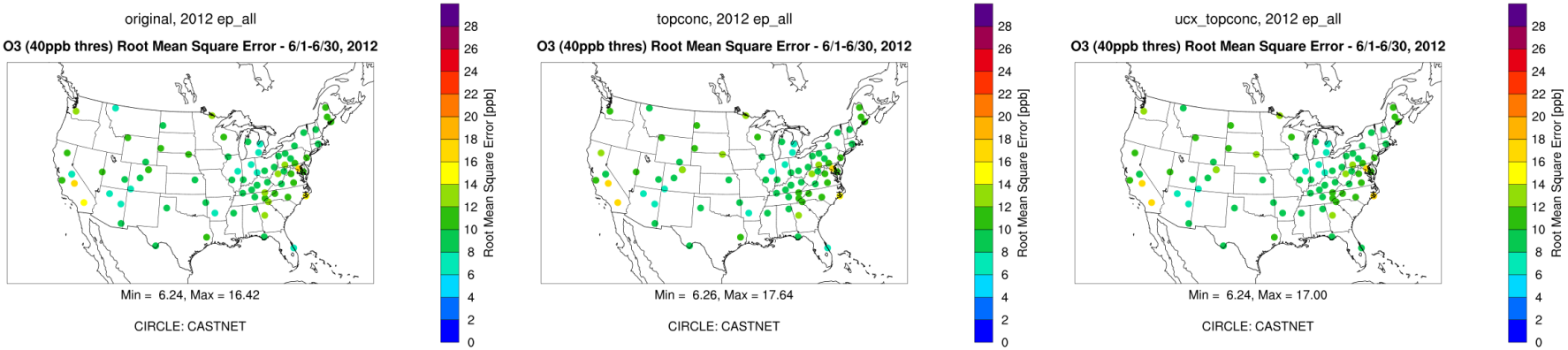

Figure A-21. Ozone NMB (1st row), NME (2nd row), R^2 (3rd row), and RMSE (4th row) of Zero Gradient CAMx run (run1; 1st column), G-C Std CAMx run (run2; 2nd column), and G-C UCX CAMx run (run3; 3rd column) Evaluation performed with respect to 8-hour average ozone at CASTNET sites for the period of 6/1 – 6/30, 2012. In the first to the third columns the comparison was performed using a 40 ppb threshold in the observed ozone.

A.2 Aloft Performance Evaluation

We evaluated the effect of the use of the zero gradient and GEOS-Chem top boundary conditions on CAMx ozone and NOy above the surface layer through comparison with aircraft data and ozonesonde data.

A.2.1 Aloft Performance Evaluation for Ozone

We compared ozonesonde observations, paired in time and space, against the three CAMx simulations using the same data and methods described in Section 4.2.1.

Modeled and observed vertical ozone profiles in the troposphere and stratosphere were compared for the CAMx runs using standard and UCX versions of GEOS-Chem as top boundary conditions and the Zero Gradient CAMx run. The results of the comparison are shown in Figure A-22 and are summarized below.

- For all sites, the three CAMx runs agree well below 6 km, but begin to diverge above 6 km due to the influence of their different model top boundary conditions.
- For all sites except Trinidad Head, the two CAMx runs using GEOS-Chem top boundary conditions have higher ozone than the Zero Gradient run above 9 km.
- For all sites, the CAMx model runs have a strong high bias in the upper troposphere relative to the observations. This is likely due at least in part to the limited model resolution in the upper troposphere and lower stratosphere in these 28-layer runs with layer collapsing (e.g. Kemball-Cook et al., 2014)
- For several sites, the shape of the CAMx ozone profile in the upper troposphere is more similar to the observed profile in the two runs that use GEOS-Chem top boundary conditions than in the Zero Gradient run. In the Zero Gradient run, the CAMx profile remains relatively constant with height above 10 km at Boulder, Huntsville, Houston and Idabel while ozone continue to increase (similar to the observed profile) in the CAMx run using GEOS-Chem top boundary conditions. This indicates that use of the Zero Gradient approach can result in ozone profiles that differ significantly from observations and should not be used in applications in which the simulation of ozone and NOy in the upper troposphere and lower stratosphere is important.
- Consistent with the results of the surface model performance evaluation, the ozonesonde profiles show that CAMx using GEOS-Chem UCX boundary condition has higher ozone below 6 km than CAMx using the standard GEOS-Chem boundary condition in the lower and middle troposphere (not shown).

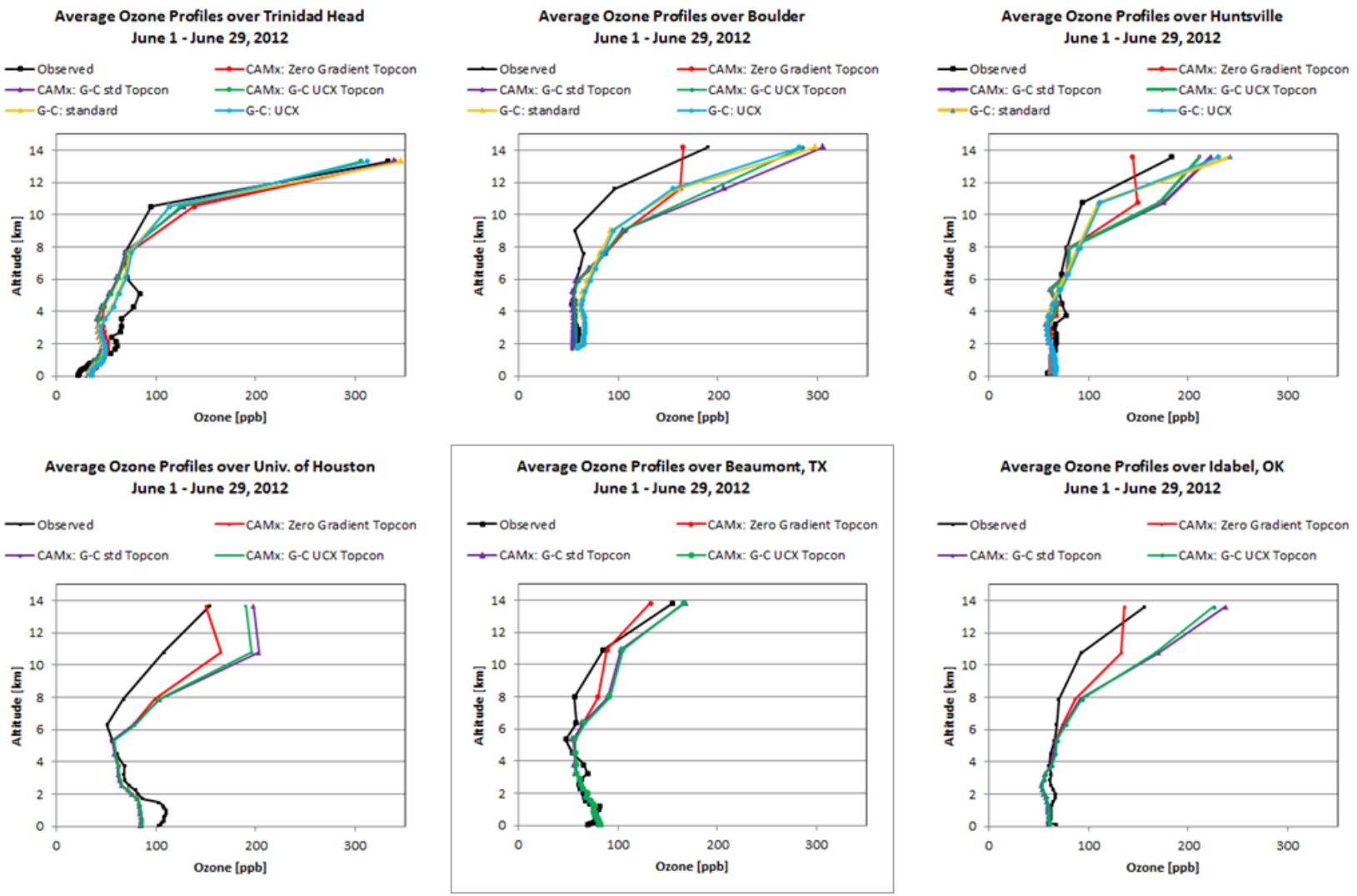

Figure A-22. Episode average ozonesonde, GEOS-Chem, (GC) and CAMx ozone profile comparison.

A.2.2 Aloft Performance Evaluation for NOy

The three initial CAMx runs were evaluated against INTEX-A aircraft data using the data and methods described in Section 4.2.2. We summarize the results of the evaluation below.

Figure A-23 shows the observed and modeled NO_2 profiles. In the upper troposphere, the modeled profiles show large differences relative to one another and the observations. All modeled profiles are significantly lower than the observed NO_2 above 6 km. This low bias is likely due in part to the fact that aircraft cruise NOx emissions and lightning NOx emissions that were not present in the emission inventory at the time of the initial CAMx runs. This confounded comparison with the observations and highlighted the need for additional CAMx modeling.

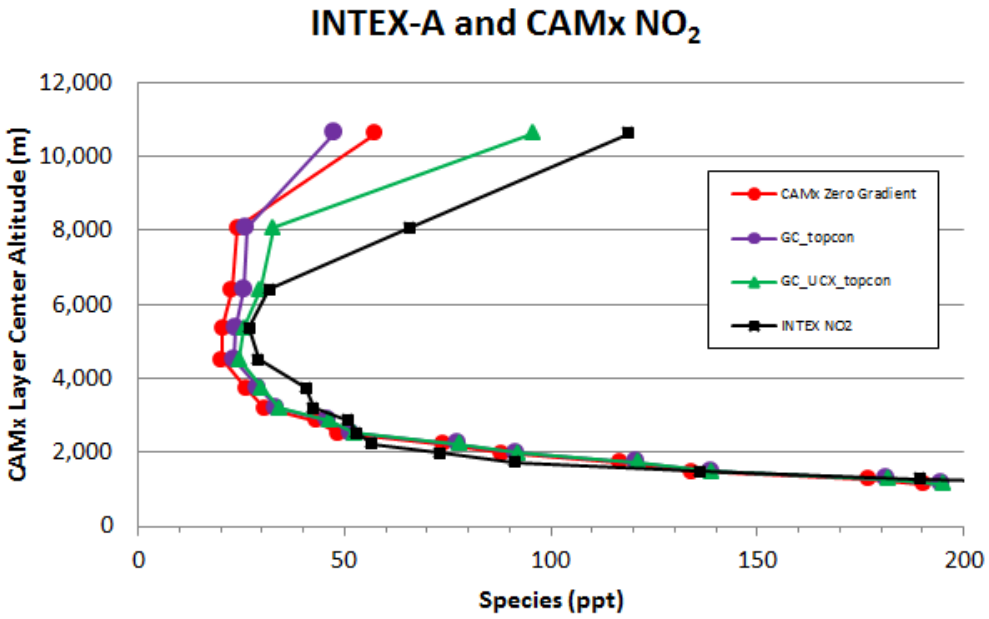

Figure A-23. Comparison of CAMx and INTEX-A domain-average NO_2 vertical profiles.

The modeled profiles for peroxyacetyl nitrate (PAN) all show a pronounced low bias above 2 km, consistent with the low bias seen in the TCEQ's 2006 ozone modeling (Kemball-Cook et al., 2014) (Figure A-24). Agreement between modeled and observed nitric acid (HNO_3; Figure 4-38 A-25) and ozone (Figure A-26) is better, but given that the NOx emission inventory in the upper troposphere was missing two key components, it was not possible to draw conclusions from this comparison.

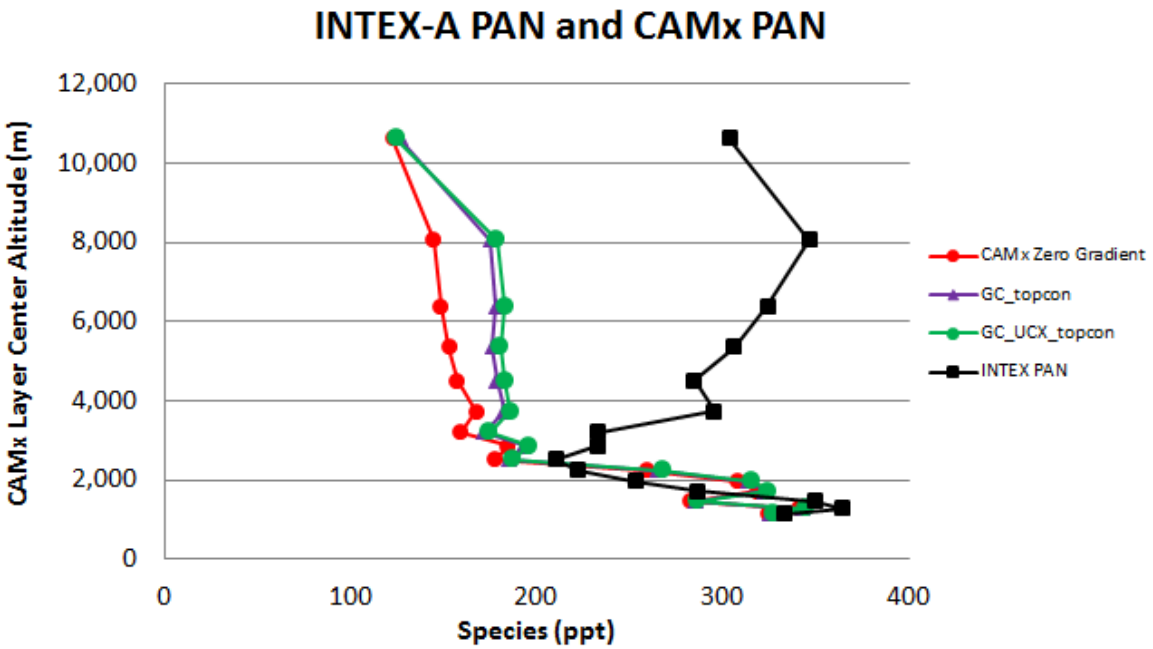

Figure A-24. Comparison of CAMx and INTEX-A domain-average PAN vertical profiles.

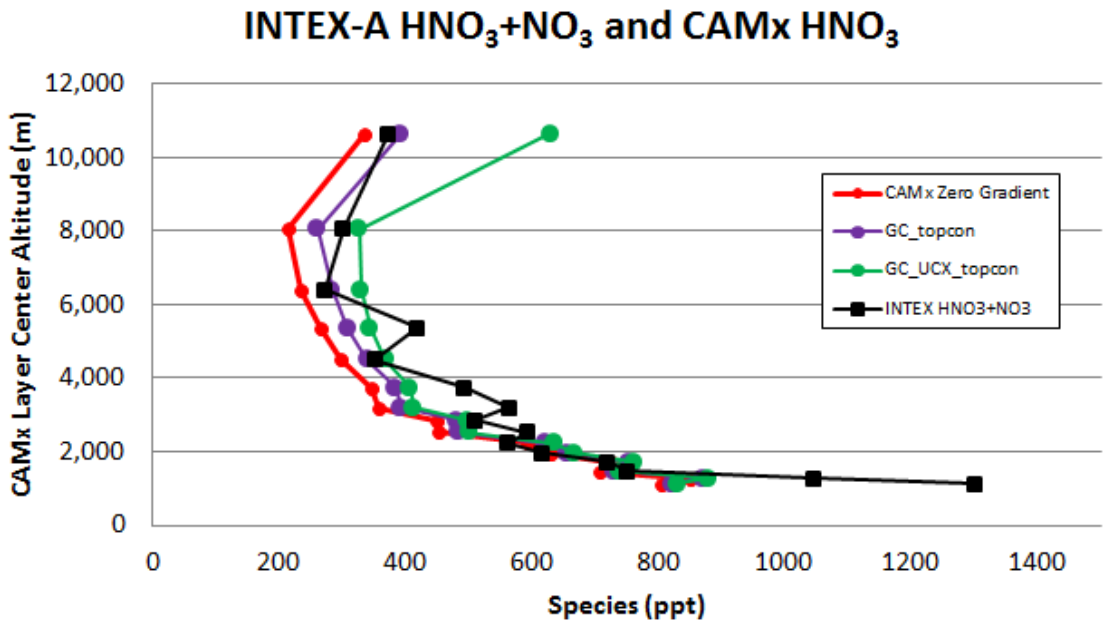

Figure A-25. Comparison of CAMx and INTEX-A domain-average HNO_3 vertical profiles.

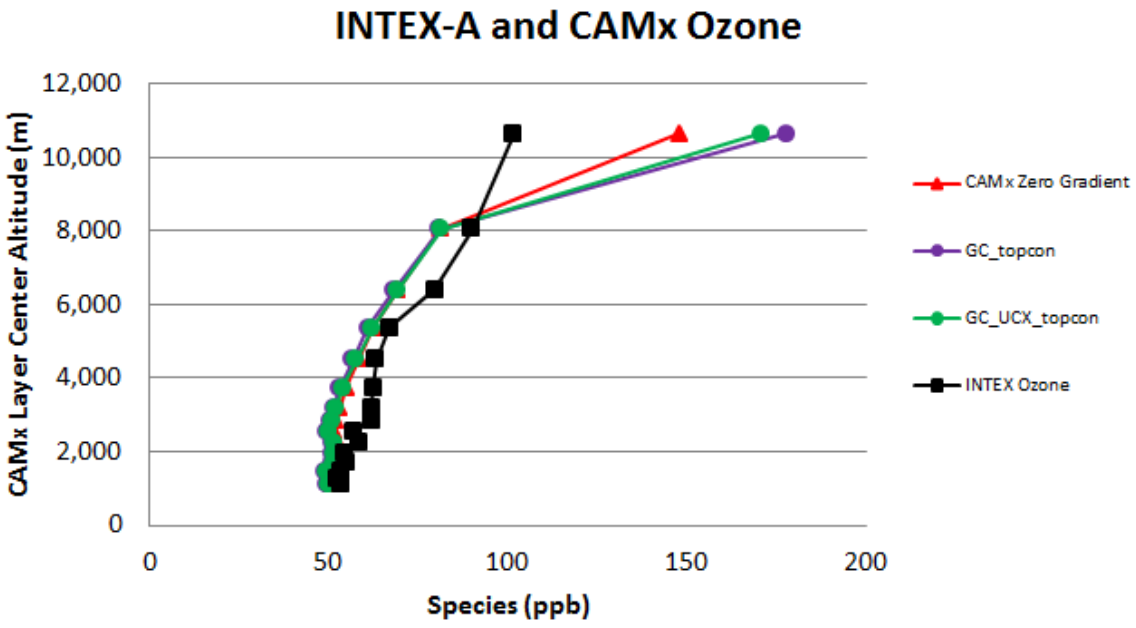

Figure A-26. Comparison of CAMx and INTEX-A domain-average ozone vertical profiles.